

12-2010

Tryptophan Anchored Peptides in Lipid Bilayer Membranes: Control of Peptide Orientation and the Phase Behavior of Cholesterol-Containing Ternary Lipid Mixtures

Johanna Maria Rankenberg
University of Arkansas

Follow this and additional works at: <http://scholarworks.uark.edu/etd>

 Part of the [Biochemistry Commons](#), and the [Biophysics Commons](#)

Recommended Citation

Rankenberg, Johanna Maria, "Tryptophan Anchored Peptides in Lipid Bilayer Membranes: Control of Peptide Orientation and the Phase Behavior of Cholesterol-Containing Ternary Lipid Mixtures" (2010). *Theses and Dissertations*. 196.
<http://scholarworks.uark.edu/etd/196>

This Dissertation is brought to you for free and open access by ScholarWorks@UARK. It has been accepted for inclusion in Theses and Dissertations by an authorized administrator of ScholarWorks@UARK. For more information, please contact scholar@uark.edu, ccmiddle@uark.edu.

TRYPTOPHAN ANCHORED PEPTIDES IN LIPID BILAYER MEMBRANES:
CONTROL OF PEPTIDE ORIENTATION AND THE PHASE BEHAVIOR OF
CHOLESTEROL-CONTAINING TERNARY LIPID MIXTURES

TRYPTOPHAN ANCHORED PEPTIDES IN LIPID BILAYER MEMBRANES:
CONTROL OF PEPTIDE ORIENTATION AND THE PHASE BEHAVIOR OF
CHOLESTEROL-CONTAINING TERNARY LIPID MIXTURES

A dissertation submitted in partial fulfillment
of the requirements for the degree of
Doctor of Philosophy in Cell and Molecular Biology

By

Johanna M. Rankenberg
Hogeschool van Arnhem en Nijmegen
Bachelor of Science in Biochemistry, 2004

December 2010
University of Arkansas

ABSTRACT

Model WALP peptides and “next generation” WALP-derived hydrophobic model peptides were employed to discover principles that govern protein-lipid interactions in biological membranes.

Ternary cholesterol-containing lipid mixtures were examined in the presence of WALP peptides of different lengths (acetyl-GWW(LA)_nLWWA-ethanolamide, with n between 3 and 8). Deuterium NMR spectra from labeled lipids reveal that WALP peptides may stabilize lipid ordered “raft” domains and therefore promote lipid phase separation, albeit to a minor extent. The results depend upon whether dioleoyl- or diphytanoyl-phosphatidylcholine is present as the fluid lipid component.

Several WALP peptides were modified to remove anchoring Trp residues from one end or the other, thereby generating “half-anchored” WALP peptides which have aromatic anchor residues on only one side of the bilayer. The longer “half-anchored” WALP peptides (having 19-21 residues) were found to have small apparent average tilt values in DLPC, DMPC and DOPC lipid bilayer membranes. The results from a combined ¹⁵N PISEMA and ²H GALA analysis—with various analytical treatments of the peptide dynamics—confirmed the small average tilt angle for one of these peptides in DMPC bilayer membranes. Shorter “half-anchored” WALP peptides with a hydrophobic length theoretically capable of spanning only a monolayer leaflet, however, do not adopt well defined membrane orientations and often aggregate.

To a bilayer-spanning “half-anchored” WALP peptide having Trp¹⁷ and Trp¹⁸, we incorporated Trp or Arg as a “third” anchor in position 2 or 6. Incorporation of this third

anchor increases the peptide tilt. When the third anchor is positioned at residue 6, the transmembrane conformation becomes destabilized.

In GWALP23, acetyl-GGALW(LA)₆LWLAGA-ethanolamide, we incorporated Pro-12 (replacing Leu-12) within the transmembrane stretch of the peptide, introducing a distortion in the peptide alpha helix. Based upon combined ²H GALA and ¹⁵N PISEMA solid-state NMR experiments and analysis, the segments N-terminal and C-terminal to the proline are tilted by 34°-40° and 27°-29° (± 6°), respectively, with respect to the lipid bilayer normal, and the proline-induced kink angle is 20-23°.

This dissertation is approved for
Recommendation to the
Graduate Council

Dissertation Director:

Dr. Roger E. Koeppe II

Thesis Committee:

Dr. Kathryn D. Curtin

Dr. Dan J. Davis

Dr. Francis S. Millett

Dr. William Oliver

DISSERTATION DUPLICATION RELEASE

I hereby authorize the University of Arkansas Libraries to duplicate this dissertation when needed for research and/or scholarship.

Agreed _____

Johanna M. Rankenberg

Refused _____

Johanna M. Rankenberg

ACKNOWLEDGEMENTS

First of all I would like to thank my advisor Dr. Koeppe, and colleagues from the university that I had the pleasure of working with at the University of Arkansas. I have gotten to know Dr. Koeppe as an incredibly knowledgeable, modest and patient person. I am truly grateful for all the help and support I have received from him over the years.

Also I would like to thank Dr. Denise Greathouse, who is a wonderful, warm and caring person and is always willing to help out. Furthermore I am grateful to my colleagues from the Koeppe Lab, both past and present, especially my fellow grad students Nick Gleason and Vitaly Vostrikov, for their wonderful company, and useful discussions held over the years.

During my time at the University of Arkansas I have made several good friends, both professionally and personally. My time here would not have been the same without them; therefore I am grateful for their companionship and support. Specifically I would like to mention Deepika Talla and Vitaly Vostrikov, I feel honored to be their friend. In addition to friends and colleagues from recent years, I do not want to forget to mention my friends and former colleagues in the Netherlands who have been often been a great motivation to me.

Of course I would also like to thank all my family both in the Netherlands and in the United States. Eric, my amazing husband, I would like to thank for being the helpful, supportive and inspiring person he is and for sharing his life with me. Furthermore, I would like to thank my parents for their unconditional love and support, my Sister Ellen and her husband Bas for their love and care, my grandparents for their relentless

motivation and all their attention, and Carol, my mother in law, for all the amazing love and care she has given us.

I would like to express my gratitude to the members of my committee for their feedback and support. In addition to my committee members I would like to thank the other University of Arkansas faculty and staff members for sharing their knowledge and for their helpfulness. Specifically Dr. Hinton, and Marv Leister for their help in optimization of NMR experiments.

In addition to colleagues at the University of Arkansas we are grateful for the wonderful collaborations we have with other laboratories. For the work presented in this dissertation I would specifically like to thank Chris Grant and Stan Opella at the national magnet laboratory at UCSD for their help in the PISEMA studies and wonderful hospitality.

During my time at the University of Arkansas my studies have been supported through various grants and teaching assistantships. I am particularly grateful for the opportunity I had to serve as a HHMI Fellow during the first year of the HHMI research for undergraduates program.

TABLE OF CONTENTS

ABSTRACT	ii
DISSERTATION DUPLICATION RELEASE	v
ACKNOWLEDGEMENTS	vi
TABLE OF CONTENTS.....	viii
INTRODUCTION	1
Influence of WALP peptides on the phase behavior of cholesterol-containing ternary lipid mixtures.....	4
Half anchored WALP peptides: Effect of anchor position on peptide orientation	5
Addition of a third anchoring residue to “single” anchor WALP	6
Effects of proline incorporation	6
Table 1	8
Figure 1	9
CHAPTER 1 Influence of WALP peptides on phase behavior of cholesterol-containing ternary lipid mixtures.....	10
1.1 Introduction:	10
1.2 Materials and Methods:	14
1.3 Results	17
1.4 Discussion	21
1.5 Figures	29
CHAPTER 2 Half anchored WALP peptides: Effect of anchor position on peptide orientation	35
2.1 Introduction:	35
2.2 Materials and methods:	38
2.3 Results:	43
2.4 Discussion	49
2.5 Tables	55
2.6 Figures	59

CHAPTER 3 Addition of a third anchoring residue to “single” anchor WALP	74
3.1 Introduction	74
3.2 Materials and Methods	76
3.3 Results:	77
3.4 Discussion:	79
3.5 Tables	83
3.6 Figures	86
CHAPTER 4 Effects of proline incorporation in GWALP23 transmembrane peptides. .	93
4.1 Introduction	93
4.2 Materials and methods	96
4.3 Results	103
4.4 Discussion	107
4.5 Tables	111
4.6 Figures	116
SUMMARY	124
BIBLIOGRAPHY	127
APPENDIX I Abbreviations	136

INTRODUCTION

Biomembranes provide means of compartmentalization for biological bodies, cells and organelles. Also vesicles used in trafficking pathways and signal transduction are examples of biological units defined through encapsulation with a membrane (Singer and Nicolson, 1972). Membranes are not static systems, but rather are dynamic, and their flexibility in both composition and arrangement plays a crucial role for many biological processes. There is still much to understand about the mechanisms and regulation of these systems, and therefore it is crucial to develop comprehensive knowledge of biological membranes. It is of importance therefore to determine the roles that individual membrane components play in the overall system behavior.

Composition, positioning and anchoring of transmembrane (TM) proteins are of great importance. Protein functions, and therefore events on cellular and larger scales, are often regulated by the relative positioning of sections of one or more proteins, or their subunits, with respect to other membrane components or one another (Valiyaveetil et al., 2002). Positioning of proteins is to a great extent rooted in the composition of its transmembrane segments (White and von Heijne, 2008). Therefore, it is crucial to gain a fundamental understanding of amino acid residues that are present within these sections. In addition to a basic understanding of properties associated with a particular amino acid, comprehension of effects associated with its positioning and its interactions with lipids and with adjacent residues is valuable.

Over the past years, transmembrane WALP peptides, acetyl-GWW(LA)_nLWWA-ethanolamide, and their analogues (figure 1) have become established as useful models

for examining protein/lipid interactions, which are a key element in biomembrane function (Davis et al., 1983) (Killian et al., 1996). The focus of the studies presented here concern the behavior of new generations of WALP peptide analogues in well defined lipid model systems. Importantly, lipid mixtures as well as single-component lipid systems will be investigated.

Several well defined lipid systems have been used for the experiments described in this dissertation. In all studies lipid bilayers were employed, albeit in various special conformations. Several of the studies were performed using lipid vesicles, either small unilamellar vesicles (SUV; for circular dichroism and fluorescence studies) or large multilamellar vesicles (MLV; for the lipid raft experiments). Transmembrane peptide orientation was addressed using oriented lipid bilayer membranes, in which the bilayer orientation was regulated either magnetically, in the case of bicelle systems, or mechanically, using stacked glass slides between which the lipid bilayers orient themselves (van der Wel et al., 2002) (Sanders and Schwonek, 1992).

Table 1 lists the various lipid components that comprised the lipid systems examined. Studies to determine peptide orientation used single lipids DLPC, DMPC or DOPC to form mechanically stacked bilayers, or a binary combination of lipids, DMPC (or the ether analogue DM-o-PC) with the short DH-o-PC ether lipid to form bicelles which can be magnetically oriented. MLV systems have been used to study the raft formation behavior of ternary lipid mixtures. These compositions were prepared from either a DOPC/DPPC/Cholesterol, or a DPhPC/DPPC/Cholesterol ternary lipid mixture. These

mixtures exhibit phase separation transition temperatures that are slightly below or somewhat above room temperature, respectively.

As mentioned before, the lipid systems used are model systems. Nevertheless, many of these lipids are indeed found in biological systems, where they are present as part of complex dynamic mixtures of biological molecules forming biomembranes. The usage of the selected lipids is not without biological relevance: by using model systems, one can select lipids based on specific properties, thereby mimicking selected important membrane properties, such as variation in hydrophobic thickness or the tendency of lipids to segregate into domains.

Model transmembrane peptides, such as WALP-derived sequences, allow for analysis of several properties of protein domains that span biological membranes. Aspects that can be studied via model peptides include hydrophobic length of transmembrane segments and the importance of specific preferential anchoring residues, which can provide tethering to the membrane interface and thereby aid in the correct positioning of membrane proteins (Jensen and Mouritsen, 2004) (Killian et al., 1996) (Harzer and Bechinger, 2000) (Ozdirekcan et al., 2005) (Jaud et al., 2009).

Solid-state nuclear magnetic resonance (NMR) techniques in conjunction with isotope labeling of lipid segments or of selected residues in the peptide, enable characterization of structure and dynamic properties of the labeled components. I have successfully employed both deuterium (^2H) and phosphorous (^{31}P) NMR techniques to study lipid phase behavior and dynamics, following established methods (Veatch et al., 2004).

Furthermore, we have used ^2H and ^{15}N based solid-state NMR methods to characterize

the orientation and dynamics of components within lipid bilayer membranes (van der Wel et al., 2002) (Marassi and Opella, 2000) (Wang et al., 2000). By correlating the observed behavior of peptide and lipid model systems to their composition, one can define aspects of importance for the analysis and understanding of biological systems.

The focal points of this dissertation concern peptide effects on and behavior within lipid bilayer membranes; including advancing the understanding of features that are imparted by specific individual amino acid residues within transmembrane peptides or domains of integral proteins. Within this context, I will specifically address the role of anchoring amino acids such as tryptophan, and in some cases comparing arginine, and their positioning within transmembrane sequences. Also, on account of its helix-breaking properties, I will reflect on effects caused by incorporation and positioning of proline within a transmembrane sequence. Below I briefly summarize the experiments to be described in this dissertation.

Influence of WALP peptides on the phase behavior of cholesterol-containing ternary lipid mixtures

These studies address the effects of incorporation of WALP peptides of different lengths on the phase separation propensity in ternary lipid mixtures. This study is significant since it investigates principles concerning the formation of ordered lipid raft domains, which influence a number of biological processes (Simons and Ikonen, 1997).

Dynamic reorganization of biomembrane components can produce structural heterogeneities. These heterogeneities may facilitate formation of functional clusters that

could be vital for the functioning of cells. Among such clusters, lipid rafts are of particular interest since they are believed to play important roles in biologically relevant processes such as signal transduction.

WALP model peptides have potential application as probes to study the formation of lipid rafts. Furthermore, elucidation of the behavior of lipid mixtures with peptides present can provide insights into possible roles of proteins in lipid raft formation.

Half anchored WALP peptides: Effect of anchor position on peptide orientation

WALP and related model peptides provide convenient model systems for studies of the anchoring properties of amino acids, some of which are important for the tethering of proteins to biomembranes by means of interactions at the membrane/water interface.

Traditional WALP peptides consist of two tryptophan residues flanking each side of a hydrophobic leucine-alanine core helix. As part of this work, I have developed “half”-anchored WALP peptides, also referred to as “single” anchor WALP peptides, which contain two tryptophan residues flanking a hydrophobic α -helix on just one side.

Determination of single anchor WALP peptide orientation will help to provide more understanding of the anchoring properties of tryptophan residues (Yau et al., 1998) (van der Wel et al., 2007).

Additionally, the “single” anchored peptides exhibit apparent tilt values that are the smallest yet observed within the WALP family, making them excellent candidates for comparative experiments using other NMR methods. For example, these peptides

provide opportunities to further extend the comparisons between the ^2H -based GALA and ^{15}N -based PISEMA methods.

Addition of a third anchoring residue to “single” anchor WALP

Due to their small tilt and defined sequence composition, the single anchored WALP peptides provide a nice basis for extending the analysis of side chain anchoring properties in lipid bilayers. By incorporating an additional anchoring residue within the “anchor-free” region of the Leu-Ala repeat in a peptide that initially is only N-anchored or only C-anchored, the effect of additional anchoring on the other side of the membrane can be investigated. One will also be able to study the links between the identity as well as location of this third anchor and the effective positioning of the peptide within the lipid bilayer. Better understanding of the variations imposed by the anchoring amino acid identity and positioning could facilitate better prediction of trends concerning the localization of transmembrane sequences based on structural composition (Hessa et al., 2007) (Vostrikov et al., 2010a).

Effects of proline incorporation

Upon incorporation of proline into an α -helical peptide, there are expected changes in the transmembrane positioning of one or both sections flanking the helix discontinuity (Cordes et al., 2002) (Nilsson and von Heijne, 1998). While such changes have been partially characterized for the case of WALP19 (Thomas et al., 2009), GWALP23 offers significant advantages for systematic investigations (Vostrikov et al., 2010a) not to mention future predictions. The effects of proline on transmembrane orientation and

overall peptide positioning will provide important clues regarding the functional importance of including proline within a transmembrane segment. Important new clues are expected from investigations of proline as the central residue in GWALP23.

Table 1
Lipids used

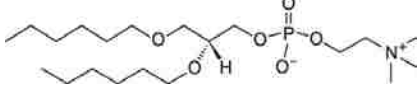
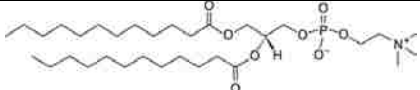
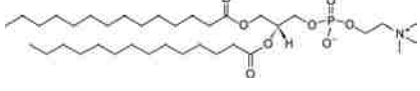
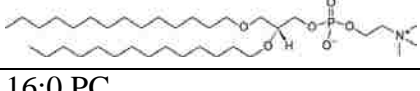
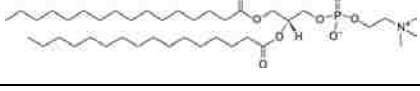
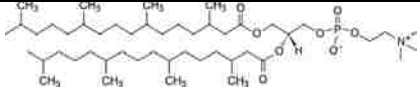
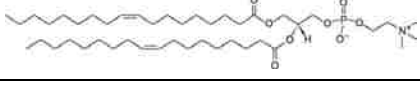
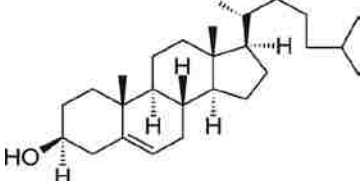
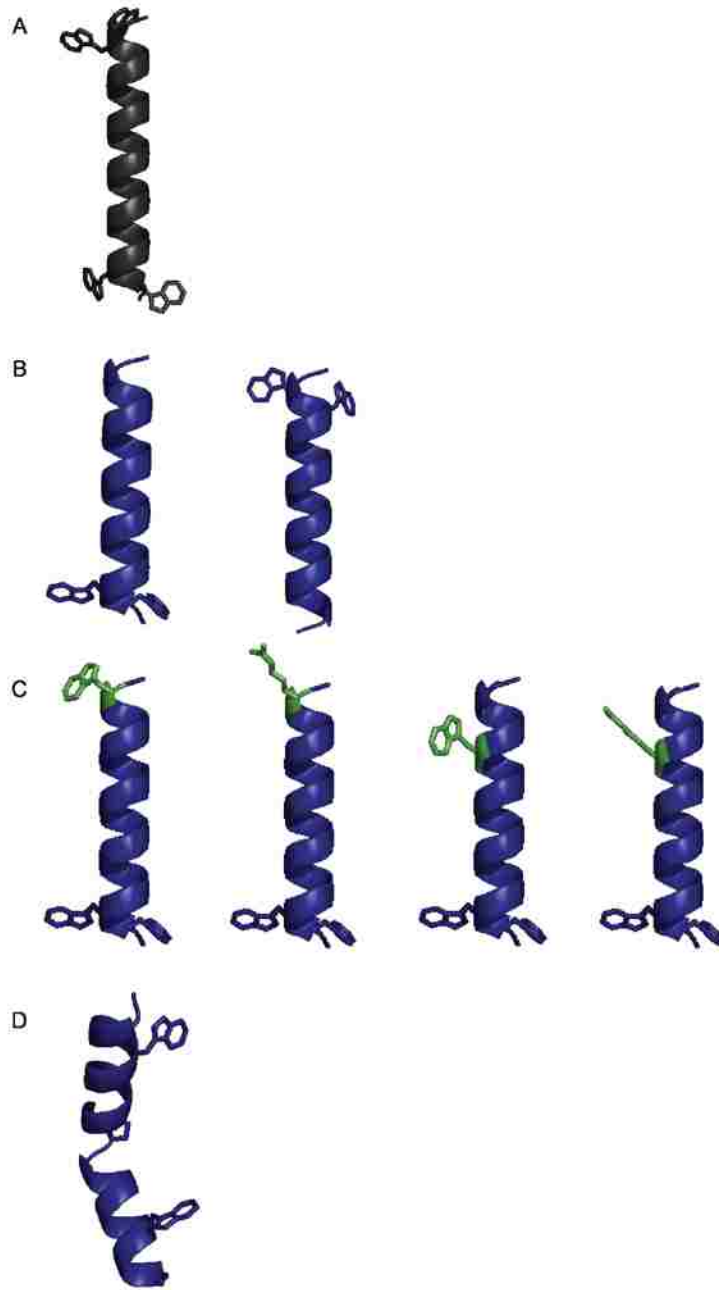
DH-o-PC	06:0 Diether PC 1,2-di-O-hexyl- <i>sn</i> -glycero-3-phosphocholine
	
DLPC	12:0 PC 1,2-dilauroyl- <i>sn</i> -glycero-3-phosphocholine
	
DMPC	14:0 PC 1,2-dimyristoyl- <i>sn</i> -glycero-3-phosphocholine
	
DM-o-PC	14:0 Diether PC 1,2-di-O-tetradecyl- <i>sn</i> -glycero-3-phosphocholine
	
DPPC	16:0 PC 1,2-dipalmitoyl- <i>sn</i> -glycero-3-phosphocholine
	
DPhPC	4ME 16:0 PC 1,2-diphytanoyl- <i>sn</i> -glycero-3-phosphocholine
	
DOPC	18:1 (Δ^9 -Cis) PC 1,2-dioleoyl- <i>sn</i> -glycero-3-phosphocholine
	
cholesterol	
	

Figure 1

Visual representation of WALP model peptide, with a length of 23 residues, (A) and “next generation” WALP-like model peptides used (B-D). Panel B shows C-anchored (left) and N-anchored (right) single anchored WALP peptides. C-terminally tryptophan anchored peptides with a W2, R2, W6 or R6 as third anchoring residue respectively are shown in panel C. GWALP23P12 is shown in panel D.



CHAPTER 1

INFLUENCE OF WALP PEPTIDES ON PHASE BEHAVIOR OF CHOLESTEROL-CONTAINING TERNARY LIPID MIXTURES.

1.1 Introduction:

Biological membranes are comprised of a wide variety of constituents, presenting countless variations of protein and lipid combinations. Membranes do not necessarily comprise a uniform mixture of their components but rather may have a dynamic composition, resulting in transient inhomogeneities in membrane composition. Lateral inhomogeneities of membrane bilayers, along with specific enrichment and clustering of certain components in micro-domains, therefore may be crucial for important biological events.

Biological processes organized within the membrane, such as receptor-mediated signaling, and communication with other membranes, such as immunological interactions, are often mediated through lipid micro domains or rafts (Simonsen, 2008) (Lajoie et al., 2009) (Kabouridis and Jury, 2008) (Jury et al., 2007) (Goebel et al., 2002). Furthermore, secretory and endocytic events, as observed in vesicle transport, and membrane fusion events, including viral fusion, can be mediated through rafts (van Meer and Sprong, 2004) (Luo et al., 2008). Lipid rafts are further expected to play a role in pathology. For example, rafts have been found to be a factor in Alzheimer's disease and systemic lupus erythematosus, and also seem to be significant for cardiovascular diseases (Das and Das, 2009; Vetrivel and Thinakaran) (Jury et al., 2007) (Luo et al., 2008).

When considering lipid raft domains *in vivo*, it has been postulated that proteins may recruit lipids into rafts and not vice versa (Poveda et al., 2008) (Edidin, 2003). This postulate points toward the importance of understanding the effects of proteins or transmembrane peptides on the formation of lipid rafts. There is still a large amount of uncertainty about the formation, structure and organization of micro domains. In studies of complex systems, it is of interest to focus on specific aspects, such as the composition, thickness and curvature of the molecular clusters. Concerning lipid behavior in domain formation, one can generalize that the raft domains contain lipids in a more ordered phase than the more disordered surroundings. For fundamental studies of lipid behavior in rafts, several model systems have been developed (Veatch et al., 2006; Veatch et al., 2004) (de Almeida et al., 2003; Marsh, 2010). Such model systems provide means to address specific questions pertaining to the molecular segregation of membrane components into domains.

It is of interest also to investigate the influence of TM peptide incorporation within raft-forming lipid mixtures. Considering the recruitment of raft components around TM proteins in the cell membrane, one can postulate that addition of TM peptides might stabilize the formation of lipid rafts. There are several scenarios in which TM domain interactions with lipids could modify the system behavior. Upon peptide incorporation into a raft-forming system, the TM peptide could partition into the ordered lipid phase, preferentially occupy the disordered phase, or reside at the domain interface.

Incorporation of peptide might furthermore either promote or inhibit the formation of

lipid rafts, based on preferential interactions with one phase or the other (McIntosh et al., 2003; Vidal and McIntosh, 2005).

To examine basic principles of protein interaction with lipid micro-domains, we have performed a study in which we incorporate WALP model peptides (Killian et al., 1996) in systems capable of lipid segregation. These peptides have the general sequence acetyl-GWW(LA)_nLWWA-ethanolamide, with n ranging from 3 to 8, giving total peptide lengths between 13 and 23 amino acid residues.

To determine if these peptides affect phase separation behavior we measured the phase transition temperature of two raft forming mixtures, with and without various amounts of peptide. The raft forming mixtures used contain lipid with a low gel to liquid crystalline phase transition temperature (low-T_m lipid), lipid with a high gel to liquid crystalline phase transition temperature (high-T_m lipid) and sterol in a 35:35:30 ratio. Cholesterol was chosen as the sterol component and acyl chain deuterated DPPC-d₆₂ was chosen as the high T_m lipid component. As a low T_m lipid we have employed either diphytanoyl phosphatidylcholine, DPhPC (ternary mixture “A”), or DOPC (mixture “B”) (Veatch et al., 2006) (Veatch et al., 2004).

The lipid systems investigated exhibit phase separation into domains as a function of temperature. Compared to *in vivo* rafts (domains smaller than ~10 nm (Edidin, 2003)), the domain size in these model systems is significantly larger (greater than ~150 nm (Veatch et al., 2004)); nonetheless these model systems provide practical means of exploring behavior of lipid raft-forming systems. The miscibility transition temperature varies between the DOPC- the DPhPC-based systems. Below the transition temperature,

the model systems consists of micro-scale raft domains which are clusters of liquid ordered (Lo) lipid components, within a liquid-crystalline (L α) background. The phase separation is associated with segregation of particular lipid components, in which the Lo phase is enriched in low T_m lipid components and sterol, and the L α phase enriched in high T_m lipid components. Above the miscibility transition temperature there is no separation into domains, such that only the L α phase is observed.

Phase separation can be measured in a non-intrusive way by means of deuterium NMR experiments, as described by Veatch *et al.* (Veatch et al., 2004). By monitoring the methyl quadrupolar splittings of ²H-labeled lipids, one can follow the phase separation as a function of temperature. In the studies described here, we address the effect of peptides on the phase behavior of ternary lipid systems. We compared different peptide lengths, different peptide/lipid ratios, and different lipid ternary mixtures (described above). We found qualitatively and quantitatively different behavior for lipid mixtures containing the synthetic DPhPC compared to those containing the natural DOPC.

The phase transition for mixture A takes place at elevated temperatures, while the observation of the phase transition for system B requires cooling of the sample during NMR studies. Incorporation of TM peptide longer than 16 residues distressed lipid system A, resulting in an isotropic phase. Incorporation of shorter peptides did not have a significant effect on phase transition temperatures in mixture A for the peptide concentrations tested. However, system B showed an increase in phase transition temperature upon incorporation of peptide, for all peptides tested. Also, this system did not show indication of further disruption of the system upon peptide incorporation.

1.2 Materials and Methods:

Materials: Wang Resin and Fmoc amino acids were obtained from Advanced Chemtech (Louisville, KY) and Nova Biochem (San Diego, CA). Cholesterol, ethanolamine and trifluoroethanol (TFE) were from Sigma-Aldrich (St. Louis, MO). Deuterium enriched and natural abundance phospholipids were obtained from Avanti polar lipids (Alabaster, AL). Deuterium depleted water was purchased from Cambridge Isotope Laboratories (Andover, MA). Other chemicals were from EMD (Gibbstown, NJ).

Methods: Peptides were synthesized using a Perkin Elmer/Applied Biosystems (Foster City, CA) 433A synthesizer. Peptide synthesis with modified Fmoc-chemistry (extended deprotection and coupling steps) was used to obtain peptides (Table 1), using a 5-fold molar excess of Fmoc amino acids. N-terminal acetylation was accomplished using commercial acetyl-Gly during the synthesis. The C-terminal ethanolamide group was incorporated by using ethanolamine for the cleavage reaction (de Planque et al., 1999). This reaction took place at 295K over 48 hours under constant agitation, using a cleavage cocktail of 80% dichloromethane and 20% ethanolamine, facilitating release of the peptide ethanolamide from resin.

Upon quenching of the cleavage reaction, the peptide was precipitated in deionized water, followed by centrifugation and lyophilization from acetonitrile/water (1:1, v/v). Peptide purity was evaluated using reversed phase (Zorbax-C8) high-performance liquid chromatography (HPLC), in a methanol-water gradient. Peptide identity was confirmed using MALDI mass spectrometry.

MLV samples were prepared based on the method previously described by Veatch *et al.* (Veatch et al., 2006). Samples contained 10 mg deuterium labeled lipid (DPPC-d₆₂) which represented 35% (mole) of the lipid present in the sample. Additionally the samples contained 30% cholesterol as the sterol component, and 35% DPhPC or DOPC as the fluid lipid component. Samples containing peptide were made using peptide:(total lipid) ratios between 1:320 and 1:80. Cholesterol was dissolved in chloroform, and appropriate amounts were mixed with stock solutions of other lipids. For peptide-containing samples, the peptide was dissolved in TFE and added to the sterol/lipid mixture. The resulting solution was dried under a stream of nitrogen gas. Residual traces of solvent were removed by placing the sample under vacuum (10⁻³ torr) for at least 48 hours. The resulting lipid film was hydrated using 400 µl deuterium depleted water. Hydration at 318K was achieved by means of intermittent vortexing steps. Hydrated MLV mixtures were pelleted by centrifugation at 14,600 g. Precipitated MLV mixtures were sealed in glass tubes.

Solid-state NMR spectra were recorded using two Bruker Avance 300 spectrometers, operating at a ¹H detection frequency of 300 MHz. To verify lipid bilayer formation, ³¹P NMR spectra were obtained using a Doty Scientific (Columbia, SC) ³¹P probe with power-gated ¹H decoupling. To probe the lipid phase behavior, deuterium (²H) NMR spectra were recorded. Spectra were obtained using a quadrupolar echo pulse sequence with full phase cycling (Davis et al., 1976), with 80,000 scans being collected at 46.0 MHz (for ²H), using a 3.2 µs 90° pulse time, 120 ms interpulse delay and 125 µs echo delay. Spectra were recorded over a range of temperatures. Temperature calibration was

performed using deuterated methanol (303 to 313 K) and ethylene glycol (308 to 338 K), and extrapolated using linear functions, as previously described (Raiford et al., 1979). NMR spectra below ambient temperature were recorded by cooling the samples via liquid N₂ boil-off, and then reheating.

Deuterium NMR spectra were processed using a 50 Hz line broadening. Lipid methyl quadrupolar splittings were defined based on distances between corresponding peak maxima. The presence of liquid ordered and liquid disordered lipid phases was assessed based on these methyl quadrupolar splittings. Phase behavior as a function of sample temperature was determined in the presence or absence of peptides.

1.3 Results

Using two different ternary lipid mixtures, both having cholesterol and the saturated lipid DPPC, we have investigated the influence of model transmembrane peptides upon the lipid phase behavior. The results were found to vary depending on the identity of the third lipid component, a fluid lipid, which was either DOPC or the synthetic saturated branched lipid DPhPC. For each system, lipid phase separation was monitored as a function of temperature by following the methyl quadrupolar splittings of the deuterium-labeled DPPC-d₆₂ lipid component, which is expected to be present primarily in liquid ordered phase(s) and, to a smaller extent, in a liquid disordered or “raft” phase (Veatch et al., 2004). Deuterium NMR spectra for both system A (with DPhPC) and system B (with DOPC) show phase separation as a function of temperature. We will present first the results for samples having DPhPC as the fluid lipid.

Above a critical phase separation temperature for the lipid system, only quadrupolar splittings of DPPC-d₆₂ terminal methyl group corresponding to L α phase are observed (Figure 1, A). As the temperature is decreased and phase separation takes place, two additional sets of methyl peaks, attributed to the non-equivalent *sn*-1 and *sn*-2 DPPC acyl chains, with respective $\Delta\nu_q$ values of ~ 8 kHz and ~ 9 kHz, denote the formation of a distinct L β phase observed in addition to the peaks for the L α phase (Figure 1, B).

Further decrease in temperature would lead to the poorly resolved spectra characteristic of the L β gel phase. Based on measured methyl quadrupolar splitting values over a range of temperatures, we have established that system A (with DPhPC) shows an apparent phase transition between 321 and 322K when no peptides are present. These phase

transition temperatures are based on set point temperatures corrected via linear temperature calibration. The transition temperature range of 321-322K for 35:35:30 DPhPC:DPPC:cholesterol agrees with earlier results (Veatch et al., 2006).

Incorporation of WALP23 when DPhPC was present led to a large isotropic peak representing DPPC-d₆₂ in the ²H NMR spectra at both low and high temperatures (Figure 1C, D). It is noteworthy that the isotropic phase is induced when only a relatively small amount of WALP23 is present, the molar ratio of WALP23:(total lipid) being 1:160.

This effect was then investigated using other WALP-family peptides of different lengths, with both ³¹P and ²H NMR spectra being recorded. Again with the peptide:lipid ratio being 1:160, the presence of the isotropic phase in lipid system A shows a peptide length dependence (Figure 2). When present, the isotropic phase is evident in both ³¹P and ²H NMR spectra for the systems containing DPhPC and WALP peptides longer than 16 residues (Figure 2). The induction of isotropic phase by longer peptides in system A is observed over a wide range of peptide to lipid ratios, from 1:80 to 1:320 (data not shown). Interestingly, despite the major contribution from a central isotropic peak, the L_α to L_o phase separation can still be distinguished at lower temperatures, as illustrated in both Figure 1 (C, D) and Figure 2 (D, E).

Conversely, shorter WALP peptides, having 16 or fewer residues, do not significantly modify the phase behavior of lipid system A (Figure 2, A-C). Not only is there no isotropic peak discernible upon introduction of WALP16 to the system (Figure 2C), but also the effect on phase transition temperature is minor. Indeed, there is no more than a one degree change in either direction depending on the peptide to lipid ratio. Consistent

results were obtained using a wide range of WALP16:lipid ratios from 1:320 to 1:80. The slight changes in phase transition temperature upon addition of WALP16 do not show a clear concentration dependent trend for the DPhPC-containing lipid system A (Figure 3).

When DOPC replaced DPhPC as the fluid lipid component, the peptide-induced isotropic phase was not seen. Indeed, addition of WALP peptides of varying lengths to lipid system B showed no apparent effects on the integrity of the lipid bilayer; in particular no isotropic peak is observed in any of the samples (Figure 4). With no isotropic phase being present, the temperature-dependent results indicate that peptides from WALP13 through WALP23, at 1:160 peptide:lipid, promote the separation of L_o phases of DOPC:DPPC:cholesterol at somewhat higher temperatures, namely about $5 \pm 5\text{K}$ higher phase transition temperature than when peptide is absent. For the 1:160 peptide to lipid ratio, no evident peptide length dependent trend is measured in system B (Figures 5 and 6). Without peptide, the phase transition for DOPC:DPPC:cholesterol occurs between about 294 and 288K (Figure 5A). When any of the WALP peptides is present, the onset of L_o phase separation seems to begin near 300K (Figure 5). For WALP23, WALP19 or WALP16, the transition occurs between about 300 and 296K. With WALP13 at 1:160, the transition temperature range may be broader—about 27 to 15K—or perhaps just less well defined by the available spectra. These results are summarized in Figure 6.

In addition to the change in phase transition temperature, one can note a slight decrease in the absolute values of DPPC- d_{62} methyl quadrupolar splitting values upon addition of the peptide, which was not the case for systems consisting of a single lipid component (de

Planque et al., 2002) Interestingly, the decrease holds true for both the DOPC and DPhPC-containing lipid systems. Such changes are especially evident for the Δv_q values around the phase transition temperature (Figures 3 and 6).

1.4 Discussion

Lipid phase separation and in particular the formation of ordered or raft phases in cholesterol-containing mixtures have elicited much interest in the past decade. Indeed extensive studies have been performed on domain formation *in vivo* and *in vitro*. The *in vitro* studies often describe model system raft behavior. For example, fluorescence imaging and NMR studies of ternary mixtures have revealed phase transition temperatures of about 294K for DOPC:DPPC:cholesterol (Veatch et al., 2004) and about 316K for DPhPC:DPPC:cholesterol (Veatch et al., 2006). T_m is the temperature below which the bilayer lipids in the $L\alpha$ phase switch to a system in which there is coexistence of L_o phase, rich in DPPC(d_{62}) and cholesterol, and $L\alpha$ phase, rich in the more fluid DOPC or DPhPC.

Similar trends were observed by Bakht *et al.* (Bakht et al., 2007), who found that the diphytanoyl acyl chain structure provides greater thermal stability than dioleoyl acyl chains for ordered domains. As a result, the lipid mixtures with low- T_m diphytanoyl acyl chains are capable of domain formation at higher temperatures than those containing dioleoyl acyl chains with similar headgroups. They note that the stabilization of ordered domains is dependent on two non-additive aspects of the lipid structure: both the acyl chains and the headgroups influence the stabilization of L_o domains. In the studies we have performed, only PC lipids were used together with cholesterol; therefore differences in lipid behavior between the mixtures are due to the changes in the acyl chain structure. Our results in the absence of peptides are in accord with previous work (Bakht et al., 2007; Veatch et al., 2006; Veatch et al., 2004).

The stabilization of ordered domains is affected by the poor miscibility between low- T_m and high- T_m lipids and/or the tight packing in ordered domains enabled by the high- T_m lipid structure. DOPC lipids containing two unsaturated acyl chains pack rather poorly with cholesterol. However, the branched acyl chain structure of DPhPC even more strongly disfavors packing with cholesterol, thereby driving the segregation of cholesterol into domains more strongly (Bakht et al., 2007).

Early experiments revealed that WALP peptides influence the phase behavior of phosphatidyl choline bilayers, composed of a single lipid type, in a manner that depends upon the hydrophobic mismatch (Killian et al., 1996). Importantly, cases of small negative mismatch (when peptide length is shorter than the lipid bilayer thickness) were observed to cause an isotropic phase, which in some instances was equated with a lipid cubic phase (van der Wel et al., 2000). Peptides from the WALP family also were observed to have small effects on lipid chain order in a mismatch-dependent manner (de Planque et al., 1998).

Only a few studies have addressed lipid mixtures capable of phase separation in the presence of transbilayer peptides. Peptide partitioning was assessed mainly using fluorescence techniques such as energy transfer or quenching. Depending on the sequence and therefore the structure of the peptide, and the lipid composition, peptide association has been found for all regions of phase-separated bilayers, namely L_o phase, boundary between L_o and L_α phase, and L_α phase. In the sections below some of these peptide studies will be addressed briefly.

Factors such as hydrophobic mismatch and/or the acylation of peptides may play an important role for the incorporation of peptides into raft domains. However, hydrophobic mismatch and acylation (such as palmitoylation) alone do not provide enough driving force for peptide segregation to Lo domains (McIntosh et al., 2003), (van Duyl et al., 2002). Nevertheless, these mechanisms might, together with other aspects, be important for the formation of or partitioning into Lo domains and could therefore still play a significant role in peptide segregation patterns. Other factors might include specific lipid components of biological raft domains, amino-acid composition of peptide/protein transmembrane domain(s), or regions in proximity to these domains. Furthermore the overall shape of a transmembrane domain may facilitate placement within raft domains.

A “CRAC” domain, Cholesterol Recognition/interaction Amino acid Consensus, consensus sequence is present in some proteins with known raft association, such as the HIV gp41 fusion protein and peripheral-type benzodiazepine receptors (Epanand, 2008). The CRAC sequence motif is located close to the membrane interface and has been shown to favor interaction with cholesterol. Together with other factors, this motif is believed to play a role in the partitioning of peptide and cholesterol into particular domains. A peptide based on the CRAC sequence motif, N-acetyl-LWYIK-amide (Epanand, 2004), has been found to interact preferentially with cholesterol and aid in the formation of cholesterol-rich domains. Charged proteins, such as PtnIns(4,5)P₂, also may promote domain formation of anionic lipids (Epanand, 2008).

While lipids play a major role in the domain segregation process, especially for cholesterol, the presence of proteins or peptides in the bilayer membrane may also play a role. Cholesterol concentrations in raft phases are often, but not always, enriched. (The traditional description of a raft describes enrichment of cholesterol; however some lipid rafts have been found not necessarily containing increased cholesterol content (Epanand, 2004)). Conversely the enrichment of cholesterol in raft phases is expected to be in part due to peptide/protein present in the membrane. This can be through specific interaction or in some cases protein/peptide may cause the presence of cholesterol in the $L\alpha$ lipid phase to be energetically unfavorable. Due to a peptide's affinity for a bilayer devoid of cholesterol, the peptide might aim to eliminate cholesterol from its environment, thereby exhibiting an "apparent" stabilizing effect on rafts by driving the cholesterol to the L_o domain (Epanand, 2004) (Fastenberg et al., 2003).

Levels of cholesterol in a membrane are expected to affect not only the T_m for domain formation but also domain size. Smaller domain size will in turn result in a more gradual thermal melting transition since the process will be less cooperative. The presence of lipids or peptides with preferences to associate with phase boundaries also would promote formation of smaller domains and would be expected similarly to result in a more gradual melting transition.(Bakht et al., 2007).

The partitioning of various WALP peptides, WALP23, WALP27 and WALP31, of different hydrophobic lengths, approximately 25.5 Å, 31.5Å and 37.5Å, respectively, into ternary lipid mixtures consisting of sphingomyelin (SM), DOPC and cholesterol has been addressed (van Duyl et al., 2002). A preferential interaction of WALP peptides to

detergent soluble (DSM) fractions of the membranes, in the $L\alpha$ phase, was noted, without significant partitioning of the peptides to the detergent resistant (DRM) domains, in the L_o phase. In similar studies McIntosh *et al.* address the partitioning of related P23, P29, and P31 peptides, $(\text{KKG}(\text{LA})_4\text{W}(\text{LA})_4\text{KKA})$, $(\text{KKG}(\text{LA})_5\text{LW}(\text{LA})_5\text{LKKA})$, and $(\text{KKG}(\text{LA})_6\text{WA}(\text{LA})_5\text{LKKA})$ respectively, in lipid mixtures of similar composition (McIntosh *et al.*, 2003). They found that these peptides adopt a transmembrane orientation and preferentially partition into the DSM fraction. The latter study does report a relative increase in the amount of longer peptide present in the DRM at a higher temperature, indicating that peptide hydrophobic length has some influence upon partitioning. Nonetheless, both studies conclude that matching of peptide hydrophobic length to that of a particular domain does not necessarily provide enough incentive for the peptide to partition into that lipid domain. The results are likely related to the cohesive ordered structure of the DRM and its low tolerance to structures that might disrupt its packing, the net effect being to expel unfavorable peptides from this environment. Furthermore, palmitoylation of these peptides does not provide a strong preference for peptide association with DRM fractions (van Duyl *et al.*, 2002).

Proteins can be crucial to the stabilization of raft phases by preferentially interacting with raft components. Furthermore the presence of peptides in a raft forming system can give rise to an increased line tension leading to an increase in the domain size to minimize line tension. Third the preferential partitioning of peptide into a liquid disordered phase can drive the segregation of raft associated lipid components by its presence in the disordered phase, since segregation of the raft components may be more energetically favorable than

interaction with protein present in the non-raft phase (Erand, 2004; Erand et al., 2003).

Our studies indeed indicate that peptides can influence the formation of lipid raft domains.

We find experimentally that low concentrations (1/160 peptide/total lipid) of 13-23 residue WALP peptides show a mild promotion of raft formation in

DOPC/DPPC/cholesterol. The results—when DOPC is present in the mixture—are consistent with peptide partitioning to the $L\alpha$ phase, with hydrophobic mismatch between the peptide and $L\alpha$ phase likely contributing to the phase separation.

Our results are somewhat different when DPhPC is present in the mixture. We found that DPhPC containing systems (system A) are not ideal for studies integrating a peptide component. The phase transition of system A takes place above ambient temperature, which is convenient from experimental standpoint. Nevertheless, the incorporation of WALP peptides containing more than 16 residues induces isotropic phase formation. Remarkably, the isotropic phase is induced even at quite low peptide concentrations, although peptides containing less than 16 amino acids seem not to alter the lipid phase behavior. The isotropic phase could result from effects such as the formation of micelles or tubules, or a shift of some lipids to alternate arrangements such as hexagonal or cubic phases to accommodate peptide within the lipid mixture. Interestingly, peptides containing 16 or fewer residues do not show any significant effect on the raft-forming lipid systems or the phase separation temperature, observable by deuterium or phosphorous NMR. Perhaps DPhPC might not be stable with longer WALP peptide due to packing interference. When DPhPC cannot form stable association with either peptide

or cholesterol, the addition of even small amounts of peptide might destabilize the system. It is nevertheless remarkable that in addition to the isotropic peak, phase segregation into L_o and L_α phases is still observed. Due to the significant isotropic peak, we were unable to establish any change in the temperature range over which the additional phase separation took place. Disruption of the lipid bilayer seems a probable cause for the isotropic peak brought about by the longer WALP peptides. Surprisingly in FRET studies using similar lipid mixtures (25% cholesterol 1:1 with DPhPC:DPPC), in the presence of 2 mol% LW peptide and 1 mol % LcTMADPH peptide, used as donor and acceptor respectively, Bakht *et al.* observed no temperature-dependent migration of lipid or peptide components into vesicles of different lipid composition (Bakht et al., 2007).

The system containing DOPC as a low T_m lipid, system B, is amore biologically relevant composition and separates into L_o and L_α phases slightly below ambient temperature. The DOPC system is affected by addition of WALP peptides but does not exhibit the isotropic phase. The primary effect of addition of again low concentrations of WALP peptides of different lengths to system B is an increase of about 5K in the phase transition temperature. The small increase indicates a WALP peptide stabilization of the L_o phase within the L_α lipid surroundings that likely retain more of the peptide. Indeed the effect could result from peptide partitioning into a specific lipid phase, or from stabilization of the phase boundaries, for example by specific positioning of peptides at the raft interface. In the DOPC-containing ternary lipid system, WALP peptides having 13-23 residues are effective at still relatively low concentrations (1/160 peptide/total lipid). Inclination of

the peptide to partition into the $L\alpha$ phase is to be expected if positioning of the peptide in liquid disordered surroundings is energetically more favorable than positioning in liquid ordered surroundings, which could incur a greater energetic cost.

It is also conceivable that the peptides could enhance cross-leaflet stabilization of ordered domains, if the presence of a TM peptide in a specific domain in one leaflet automatically extends across the bilayer to influence the lipid distribution in the other leaflet. Therefore the domain formation on either side of the lipid bilayer could become more strongly coupled upon addition of peptide. This in turn might lead to a greater propensity for domain segregation.

In addition to the change in phase transition temperature, one observes small decreases in the quadrupolar splitting of DPPC- d_{62} when peptide is added. This is an expected result on the lipid packing (de Planque et al., 1998).

In summary, we see different effects of WALP peptides on DOPC- and DPhPC-containing raft-forming lipid mixtures that contain cholesterol and DPPC. WALP peptides longer than 16 residues induce an isotropic phase when DPhPC is present but not in the DOPC system. The shift in phase separation temperature when DOPC is present suggests that WALP peptides having 13-23 residues exhibit a small but measurable stabilizing effect on lipid rafts, at concentrations as low as 0.6 mole per cent peptide. Again one sees that the presence of a transmembrane peptide can influence the distribution of the surrounding lipids and thereby affect the phase behavior.

1.5 Figures

Figure 1

^2H NMR spectra of DPhPC:DPPC- d_{62} :Cholesterol 35:35:30 MLV samples, either without (A, B) or with (C, D) WALP23 peptide. Spectra A and B are indicative of phase separation as a function of temperature. Note the expanded scale for the spectra in the right column of each panel. At 333 K (A) only liquid disordered $L\alpha$ phase is observed. At 300 K (B) liquid ordered phases (L_o) are present in addition to the $L\alpha$ phase. Samples containing WALP23 (1:160; peptide:total lipid) indicate presence of a significant amount of isotropic lipid phase, both at 333 K (C) and at 300 K (D).

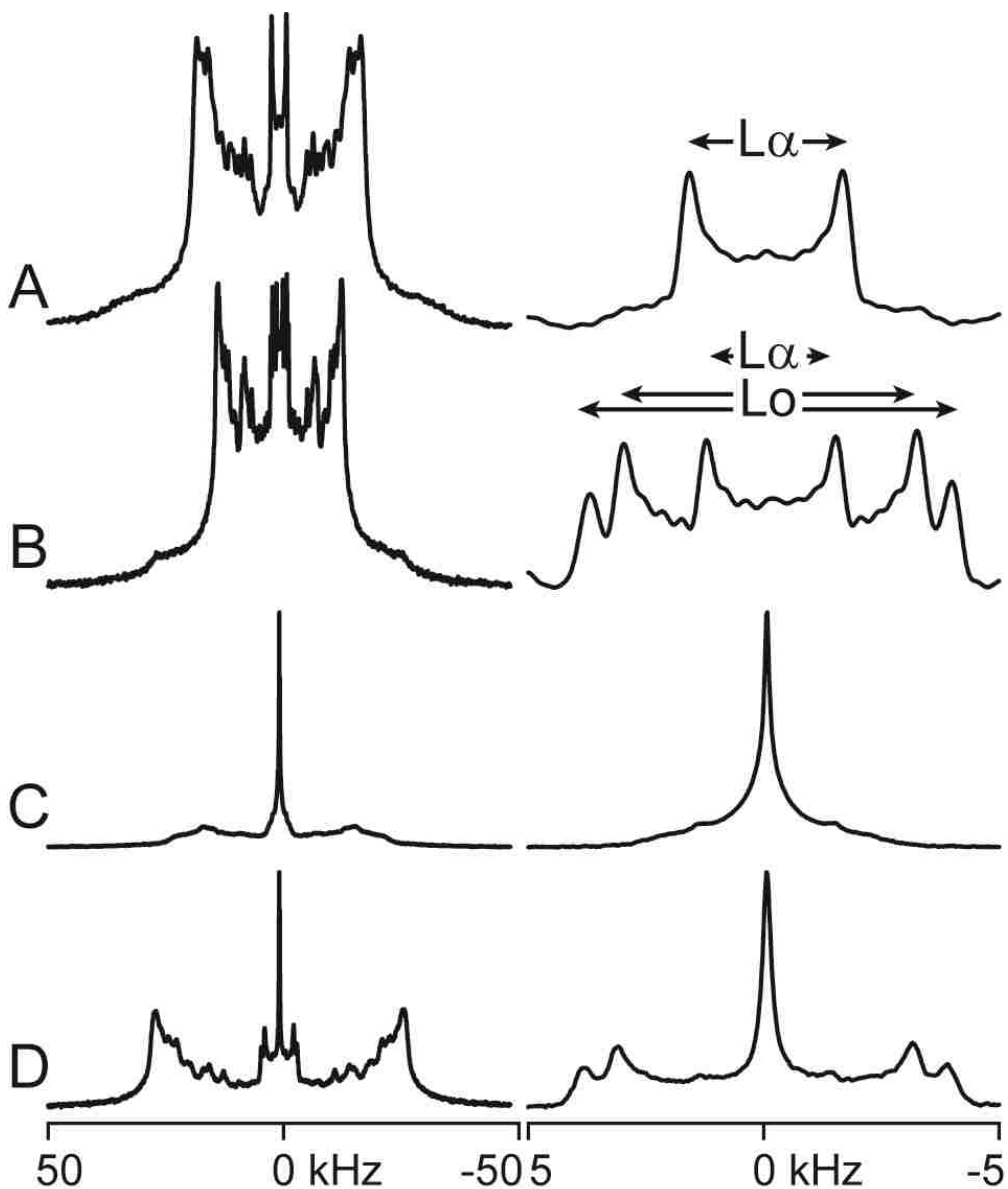


Figure 2

^2H and ^{31}P NMR spectra of DPhPC:DPPC- d_{62} :Cholesterol 35:35:30 MLV samples in the absence or presence of WALP peptides of different lengths: no peptide (A), WALP13 (B), WALP16 (C), WALP19 (D) or WALP23 (E). Sample temperatures were 302 K for ^2H spectra and 323 K for ^{31}P NMR spectra. The peptide/lipid ratio is 1:160.

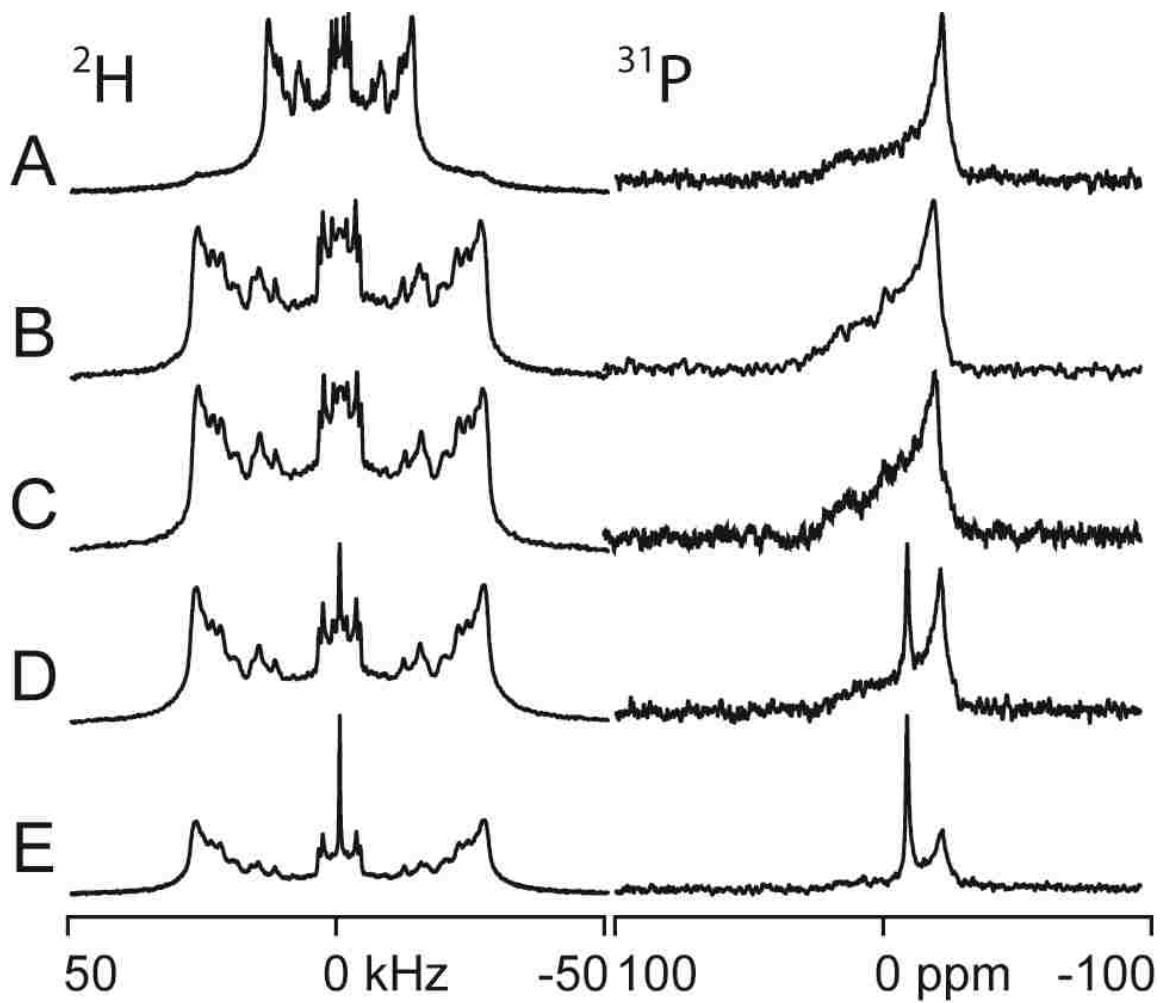


Figure 3

Observed methyl quadrupolar splittings as a function of temperature in DPhPC:DPPC-d62:Cholesterol 35:35:30 samples with no peptide (black squares) and with WALP16 at a range of peptide to total lipid ratios: 1:80 (red inverse triangles), 1:120 (orange triangles), 1:160 (green circles), 1:320 (blue squares). Corresponding lipid phases are indicated on the plot.

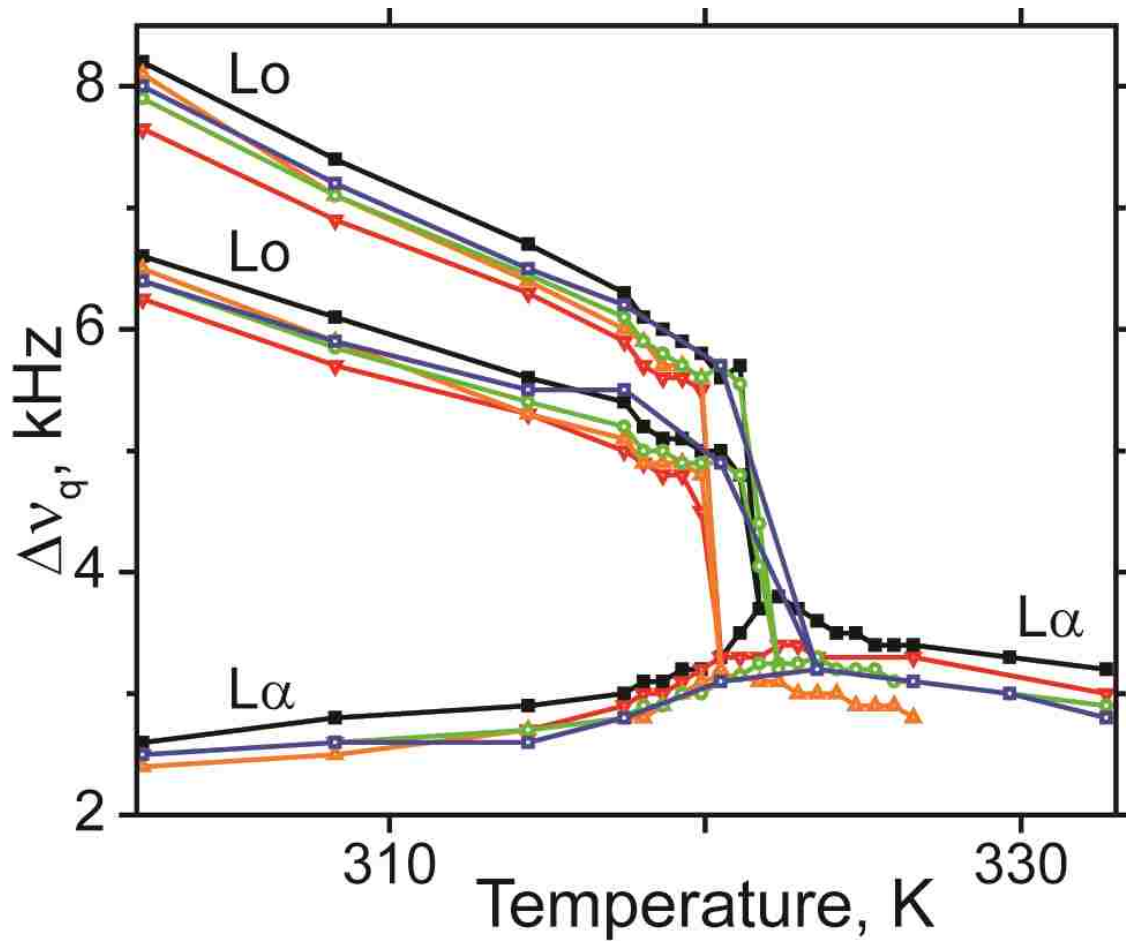


Figure 4

^2H and ^{31}P NMR spectra of DOPC:DPPC- d_{62} :Cholesterol 35:35:30 with no peptide (A), or with WALP13 (B), WALP16 (C), WALP19 (D) or WALP23 (E) in a 1:160 peptide:lipid ratio. Sample temperatures were 281K for ^2H and 323K for ^{31}P NMR spectra. With DOPC replacing DPhPC in the lipid mixture, no isotropic phase is observed.

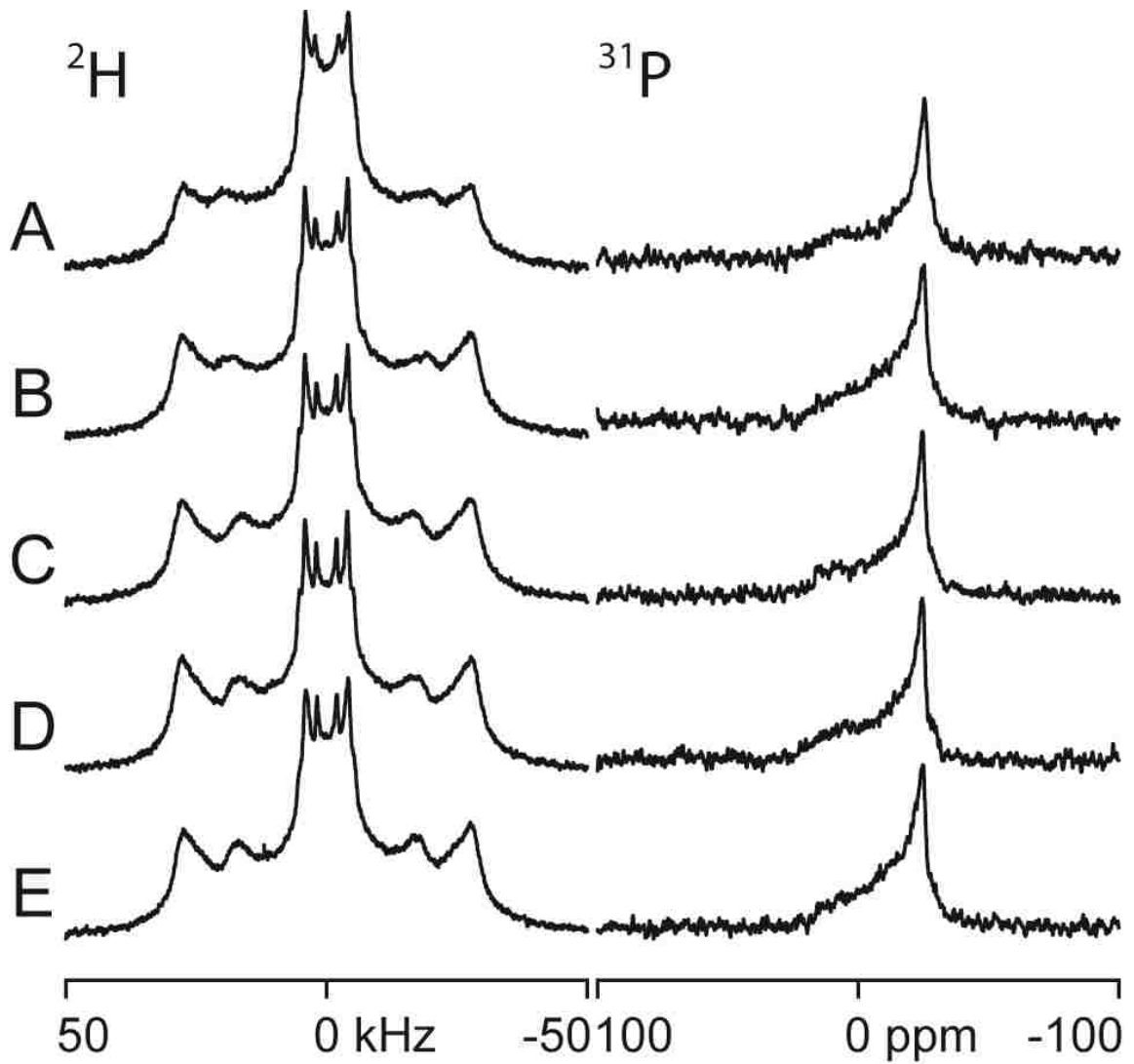


Figure 5

^2H NMR spectra of DOPC:DPPC-d62:Cholesterol 35:35:30 near the phase transition temperature. Samples contained either no peptide (A), or WALP13 (B), WALP16 (C), WALP19 (D), WALP23 (E) at a 1:160 P:L ratio.

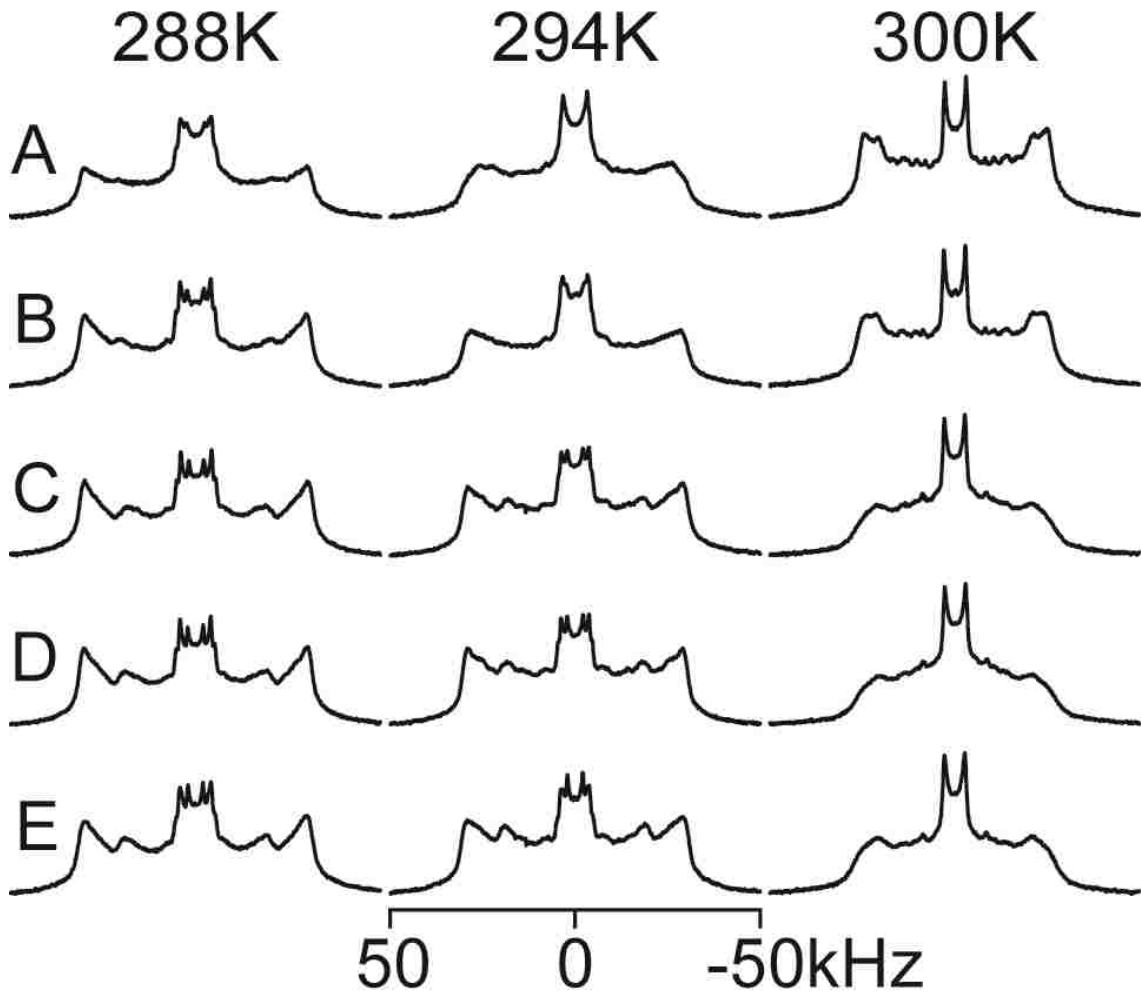
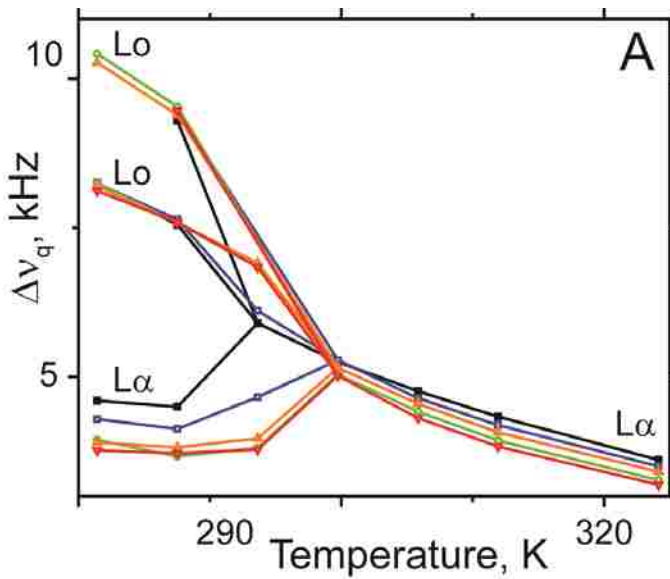
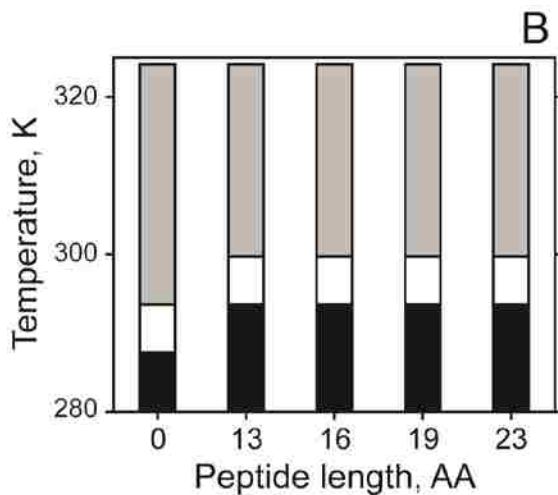


Figure 6

A. Observed methyl quadrupolar splittings as a function of temperature in DOPC:DPPC-d62:Cholesterol 35:35:30 samples with no peptide (black squares), or with WALP13 (blue squares), WALP16 (green circles), WALP19 (orange triangles), or WALP23 (red inverse triangles) at a 1:160 P:L ratio.



B. Observed phase transitions in DOPC:DPPC-d62:Cholesterol 35:35:30 with and without WALP peptide at a 1:160 peptide to lipid ratio. Colors indicate phase separation into L α and Lo phases (black), presence of L α phase only (grey), or phase transition region (white).



CHAPTER 2

HALF ANCHORED WALP PEPTIDES: EFFECT OF ANCHOR POSITION ON PEPTIDE ORIENTATION

2.1 Introduction:

Model systems of peptides have proven useful for understanding protein/lipid interactions in biological lipid bilayer membranes. In particular, WALP and related peptides have been extensively studied to determine their behavior and positioning in lipid bilayers of differing thickness. WALP peptides, originally developed using gramicidin A channels as inspiration, traditionally contain two tryptophan residues on either side of a hydrophobic, helical core composed of alternating Leu and Ala residues (Killian et al., 1996). In proteins associated with biological membranes, such as photosynthetic reaction center and potassium channels (KCSA) (Doyle et al., 1998; Schiffer et al., 1992), aromatic amino acids are often found at the membrane/water interface. These interfacial amino acid residues play a role in anchoring the proteins in particular orientations within the membrane. It follows that the aromatic Trp residues are key constituents of WALP model peptides, since they perform the important function of anchoring these peptides within the membrane, restricting trans-bilayer movement, and determining the peptide tilt (van der Wel et al., 2002).

Previous studies have addressed the concept of hydrophobic mismatch between WALP (or related peptides) and lipid bilayer membranes (de Planque et al., 2002; van der Wel et al., 2002). The lipid bilayer thickness and the peptide hydrophobic length, defined as the distance between the Trp anchors on either side of the Leu-Ala core, affect the lipid phase

behavior and may influence the peptide orientation in cases where the bilayer phase is maintained. Various methodologies have been employed to address WALP peptide orientation within hydrated, oriented model lipid bilayer membranes. These measurements have included circular dichroism and infrared spectroscopy (de Planque et al., 2001; Killian et al., 1996; Ozdirekcan et al., 2007; van der Wel et al., 2002; Vostrikov et al., 2008) as well as solid-state NMR spectra (van der Wel et al., 2002) (Ozdirekcan et al., 2007) (Vostrikov et al., 2008), fluorescence quenching (de Planque et al., 2001; Holt et al., 2010; Killian et al., 1996; Ozdirekcan et al., 2007; van der Wel et al., 2002; Vostrikov et al., 2008), and molecular modeling (Esteban-Martin and Salgado, 2007; Lee and Im, 2008; Ozdirekcan et al., 2007; Strandberg et al., 2009). The solid-state NMR methods have included the ^2H -based Geometric Analysis of Labeled Alanines (“GALA”) (Strandberg et al., 2004; van der Wel et al., 2002) and the ^{15}N -based Polarization Inversion with Spin Exchange at Magic Angle (“PISEMA”) (Marassi and Opella, 2000; Wang et al., 2000). In several direct comparisons, the two methods have shown remarkable agreement (Vostrikov et al., 2010a; Vostrikov et al., 2008). More recently, dynamic considerations involving multiple parameters have been incorporated into the analysis (Esteban-Martin and Salgado, 2007; Ozdirekcan et al., 2007; Strandberg et al., 2009; Vostrikov et al., 2010a).

Here we discuss further experiments to investigate the independent anchoring properties of Trp residues when present on only one but not both sides of a lipid bilayer membrane. The presence or absence of Trp residues in particular interfacial anchoring positions could affect peptide orientation, namely both the direction and the apparent magnitude of

peptide tilt with respect to the lipid bilayer normal. Trp residues on (only) one side of the membrane, without potential opposition from Trp residues on the other side of the membrane, provide a means to investigate the properties of peptides that are “held” on only one end. Therefore we have developed “single-end” anchored WALP peptides. Our C-anchored $(AL)_n$ WWG and N-anchored GGWW $(LA)_n$ peptides each retain two Trp residues near one end. The peptide termini are blocked with acetyl and ethanolamide groups, respectively, so that charged ends are avoided.

In this study we address the apparent tilt and rotation of the “single-end” anchored WALP-like peptides of different lengths in DLPC, DMPC and DOPC bilayer membranes. In all cases, oriented peptide/lipid samples were characterized by means of ^2H NMR spectra from labeled alanines. In some cases, the ^2H NMR data were supplemented with two-dimensional $^{15}\text{N}/^{15}\text{N}$ - ^1H spectra (Nevzorov and Opella, 2003). The combined use of ^2H and ^{15}N methods enables us to estimate the dynamics of the bilayer-incorporated peptides. The results provide a comparison with characterizations of other membrane-spanning peptides that seem to be anchored on only one side of the bilayer (Percot et al., 1999). We find generally that the N- or C-anchored peptides of sufficient length tend to span the bilayer with quite small tilt angles along with rather extensive dynamics, and that shorter peptides may tend to aggregate.

2.2 Materials and methods:

Materials. Isotope enriched amino acids (^2H and ^{15}N) and ^2H -depleted water were from Cambridge Isotope Laboratories (Andover, MA). Commercial L-alanine- d_4 was Fmoc-protected using Fmoc-ON-Succinimide as described (ten Kortenaar et al., 1986).

Unlabeled Fmoc-amino acids and preloaded Wang resin were obtained from Nova Biochem (San Diego, CA) and Advanced Chemtech (Louisville, KY). Ethanolamine and trifluoroethanol (TFE) were from Sigma-Aldrich (St. Louis, MO). Lipids (DOPC, di-C18:1 Δ 9c; DMPC, di-C14:0 and DLPC, di-C12:0) were obtained from Avanti polar lipids (Alabaster, AL). Other chemicals were from EMD (Gibbstown, NJ).

Peptides (Table 1) were synthesized on a Perkin Elmer/Applied Biosystems (Foster City, CA) 433A synthesizer, using modified Fmoc chemistry with extended times for the coupling and deprotection steps. Deuterium labeled alanine- d_4 was incorporated at specific residues, namely in 100% abundance at a single residue, or at lower 50-75% abundance at a second sequence position, by combining appropriate amounts of Fmoc-Ala- d_4 and Fmoc-Ala in one vial. During peptide synthesis a five-fold excess of Fmoc-amino acid was used for unlabeled residues. Labeled residues were incorporated using two-fold excess, followed by a second “chase” coupling using five-fold excess of unlabeled Fmoc-amino acid for chemical completeness (de Planque et al., 1999).

Terminal groups were incorporated during synthesis (N-terminal acetyl), and ethanolamine cleavage (C-terminal ethanolamide).

Ethanolamine was used to release peptides from Wang resin. The reaction took place in 80% dichloromethane, 20% ethanolamine under constant agitation. After 48 hours at 22 °C, the reaction was quenched and the peptide precipitated using deionized water. Precipitated peptide was lyophilized from one mL of acetonitrile/water (1:1, v/v). Peptide purity was evaluated using reversed phase HPLC (Zorbax-C8 column eluted with a methanol-water gradient). Additionally, the peptide identity was confirmed using MALDI mass spectrometry.

Spectroscopy. To provide information on the peptide secondary structure, circular dichroism (CD) spectra were obtained (190-250 nm range scanned at 20 nm/min, using a 1 mm path length, 0.2 nm step resolution, and 1 nm bandwidth, with five scans averaged). To gain insight into the hydrophobicity of the local environment of the tryptophan residues, intrinsic tryptophan fluorescence emission spectra were recorded over a range of 300-500 nm, using an excitation wavelength of 284 nm. Slits were set at 7.5 nm for both excitation and emission. Ten scans were recorded at a rate of 200 nm/min and averaged.

NMR samples were prepared using two μmol peptide from TFE stock solution, and 80 μmol lipid in chloroform. The peptide-lipid mixture was dried to a film under N_2 , followed by drying under vacuum (10^{-3} torr) for at least 24 hr. The film was redissolved in 95% methanol, 5% water and evenly distributed over 40 glass slides (4.8 x 23 x 0.07 mm, Marienfeld, Lauda-Königshofen, Germany). After a brief period of air drying, the slides were placed under vacuum for at least 48 hr. The peptide-lipid films were hydrated 45% (w/w) using deuterium depleted water. Upon hydration the slides were stacked and

sealed in a glass cuvette, which was incubated for >48 hr at 45°C to allow spontaneous formation and alignment of lipid bilayers.

Solid-state NMR spectra of oriented samples were recorded at 50 °C using a Bruker Avance 300 Spectrometer (Bruker Instruments, Billerica, MA). To verify the formation of lipid bilayers, ³¹P NMR spectra were recorded using a probe from Doty Scientific (Columbia, SC). To obtain quadrupolar splittings from ²H-labeled alanines incorporated in the peptides, ²H NMR spectra were recorded at 46 MHz, using a quadrupolar echo sequence with full phase cycling (Davis et al., 1976), 4.5 μs 90° pulse time, 90 ms interpulse delay and 125 μs echo delay. The spectra for ²H were processed using a line broadening of 200 Hz. Quadrupolar splittings for labeled alanines were defined based on the distances between corresponding peak maxima and were assigned to particular alanine residues based on the relative intensities in relation to the isotopic abundances employed during peptide synthesis (see above).

Following assignment of the quadrupolar splittings, the apparent average peptide orientation in each lipid bilayer membrane was estimated using GALA analysis as previously described (Strandberg et al., 2004; van der Wel et al., 2002). The analysis considers the quadrupolar splittings observed for alanine residues arranged in an α-helix. Helix tilt τ and rotation ρ are considered with respect to C_α of the first amino acid of the peptide. Using equations [1] and [2], predicted quadrupolar splittings, based upon τ , ρ and S_{zz} as variable parameters, were compared to the experimental observations.

$$\Delta\nu_q = \frac{3}{2} S_{zz} \frac{e^2 q Q}{h} \left(\frac{1}{2} [3 \cos^2 \theta - 1] \right) \left(\frac{1}{2} [3 \cos^2 \beta - 1] \right)$$

[Equation 1]

$$\theta = f(\tau, \rho, \varepsilon_{//})$$

[Equation 2]

In equation [1], the quadrupolar splitting ($\Delta\nu_q$) depends upon the static coupling constant

$\frac{e^2 q Q}{h}$ (168 kHz for aliphatic deuterons, or 56 kHz for C-D₃ groups due to fast averaging

around a tetrahedral γ angle of methyl moiety), a static order parameter (S_{zz}) of ~0.87

(Strandberg et al., 2002; Thomas et al., 2009), the orientation angle θ of the bond vector

in question with respect to the applied magnetic field, and the macroscopic sample

orientation angle β for the bilayer normal relative to the external magnetic field direction.

The peptide geometry is reflected in angle $\varepsilon_{//}$ between the C _{α} -C _{β} bond vector and the

peptide helix axis. The angle θ between the C _{α} -C _{β} bond vector and the applied magnetic

field depends on the peptide geometry ($\varepsilon_{//}$) peptide orientation (τ and ρ) and dynamic

properties of the system reflected in the order parameter (S_{zz}). Using these parameters,

the peptide orientation was calculated by considering the best fit (lowest RMSD value

between calculated and observed quadrupolar splittings) for a range of peptide

orientations.

PISEMA spectra were recorded by our collaborators using a Varian Inova 500 (¹⁵N-¹H)

spectrometers using established pulse sequences (Cook and Opella, 2010; Marassi and

Opella, 2000). A combined solid-state NMR analysis was achieved using software provided by Vitaly Vostrikov, based upon published methods for Gaussian evaluation of ^2H quadrupolar splittings and ^{15}N - ^1H dipolar couplings (Holt et al., 2010; Strandberg et al., 2009).

2.3 Results:

Peptide analysis. After peptide synthesis (see Table 1 for peptide sequences) and cleavage from the resin, the peptide identity was confirmed by matching the peptide isotopic mass to the expected value. For deuterium labeled peptides, isotopic distribution of the peptide was also considered. HPLC analysis of peptides indicated approximately 95% peptide purity, as can be seen in figure 1 and 2.

Spectroscopy. Circular dichroism (CD) spectra indicate that single anchored n=8 peptides adopt an α -helical conformation in small unilamellar vesicles of lipids with acyl-chain lengths of 12, 14 or 18 carbons (Figure 3). It is evident from these CD spectra that shorter lipids cause the peptides to adopt a larger extent of α -helical conformation. Half WALP peptides with a short Leu-Ala repeat segment (n=3) show spectra similar to that for β -sheets indicating no significant α -helix formation.

Intrinsic tryptophan fluorescence studies indicate a 5 nm shift in the maximum emission wavelength for n=8 single anchored peptides when comparing the N- and C-anchored peptide emission spectra to one another, Figure 4. The emission maxima found via tryptophan fluorescence is 340 nm for the N-anchored and 345nm for the C-anchored peptides, in relation to 351nm emission maximum for an entirely aqueous environment. No change in the emission maximum based on the length of lipids used in the SUV preparations was found for either of the peptides. Since these peptides are anchored on a single side of the membrane, the fluorescence spectra of the N-anchored n=8 peptide, exhibiting a blue shifted emission maximum with respect to the C-anchored peptide,

indicate positioning in an overall more buried hydrophobic membrane environment for the tryptophan residues on that side. Although these peptides allow us to look at the hydrophobic environment of the anchoring tryptophan residues one side of the membrane at a time, these studies do not however differentiate between whether one or both of the anchoring tryptophan residues on one side of the membrane being positioned in a more buried environment, since the fluorescence spectra represent a sum of the fluorescence of both of the residues.

Oriented samples. For all oriented samples prepared ^{31}P NMR spectra were recorded. These spectra demonstrated that the lipid phase present is predominantly oriented lipid bilayer. However, a small amount of residual unoriented lipid bilayer is commonly observed in the samples. Examples of ^{31}P NMR spectra can be found in Figure 5.

Half WALP. The design of the half WALP peptide with n about 3 or 4 is such that the peptide hydrophobic length should match that of a DMPC monolayer or a single leaflet of a lipid bilayer. Although the peptide might in theory position itself in DMPC lipid bilayers where it could insert across a single leaflet of the bilayer we have found that this is not the case. Deuterium NMR spectra from hydrated, oriented DMPC bilayers with half WALP peptides show a distinct Pake powder pattern, recognized by a full range of quadrupolar splitting that reaches a maximum at 37 kHz, as can be seen in Figure 6. The spectra are nearly identical for the $\beta=90^\circ$ and $\beta=0^\circ$ sample orientations, indicating slow motion of the peptide on the ^2H NMR timescale. The observed Pake patterns are likely a result of peptide aggregation. Possibly, unsatisfied terminal hydrogen bonds may play a role in preventing membrane insertion of the peptide into the lipid bilayer. To address

this issue we have synthesized a complementary N-anchored half WALP. When the two peptides were incorporated together into a DMPC oriented bilayer sample, in a 1:1 ratio (1:40 total peptide to lipid ratio), the resulting ^2H spectra also remain as Pake patterns, figure 6. The preservation of Pake pattern indicates that the presence of N-anchored half WALP peptides as a possible partner for formation of hydrogen bonds does not result in membrane insertion of C-anchored half WALP peptides

Single anchored WALP. Longer single anchored WALP peptides, with a hydrophobic length capable of spanning the hydrophobic length of lipid bilayer membranes, do adopt transmembrane configurations in oriented DLPC, DMPC and DOPC lipid bilayers.

Quadrupolar splittings (Table 2) for these peptides have been determined from recorded deuterium NMR spectra (Figures 7-11). Splittings were assigned based on the measured distance between corresponding peaks for each labeled alanine residue in the oriented samples. For each sample the quadrupolar splittings were obtained at both the $\beta=0^\circ$ and the $\beta=90^\circ$ orientation, as shown in Figures 8 and 9. As one can observe in the spectra, rapid reorientation around the membrane normal results in 0.5 fold reduction of $\Delta\nu_q$ values obtained at $\beta=90^\circ$ as compared to the $\beta=0^\circ$ orientation. Due to a small amount of the sample that adopted a non-oriented configuration, residual signal can sometimes be observed for which the $\Delta\nu_q$ values are 0.5 times those of the main peaks present in the $\beta=0^\circ$ spectra. The quadrupolar splittings for the $\beta=0^\circ$ sample orientation, with an uncertainty of $\pm 0.5\text{kHz}$, were used to calculate peptide average apparent tilt value and rotation with respect to the C- α atom of the initial residue (the latter also specifies the direction of the tilt) (van der Wel et al., 2002). Due to limitation on the number of data

points obtainable for these ^2H -Ala labeled peptides; molecular motion was in most cases treated using a single order parameter (Strandberg et al., 2002). When additional ^{15}N data were available (see below), we were able to apply two-parameter Gaussian dynamics (Strandberg et al., 2009) in selected cases. Using the “semistatic” GALA analysis with principal order parameter S_{zz} we have been able to obtain the average apparent tilt and rotation of the peptides in lipid bilayer membranes with RMSD values no more than 1.3 kHz. These calculations converged to a principal order parameters (S_{zz}) between 0.72 and 0.79, which account for some motional properties of the peptide. Values determined for each peptide in the different lipids investigated are indicated in table 3. An $\varepsilon_{//}$ value of 59.4° has been used for the alanine side chains.

Helical wave plots containing the observed and the calculated quadrupolar splittings for N- and C- anchored WALP peptides are shown in Figure 12. These figures nicely demonstrate that the apparent tilt for both the N- and C-anchored peptides exhibits a dependence on the hydrophobic length of the lipid bilayer. Slight increases in the tilt magnitudes are observed as the bilayer gets thinner. This bilayer thickness dependence of tilt is slightly more pronounced in N-anchored WALP peptides than in their C-anchored counterparts. The calculated average apparent tilt values are 1.7° and 2.0° in DOPC, 3.0° and 0.7° in DMPC and 7.3° and 4.3° in DLPC bilayer systems for the N-anchored and the C-anchored peptides, respectively, Table 3. As the tilt becomes small, the direction of tilt becomes essentially undefined. The tilt direction is more adequately represented by a range of acceptable rotational directions. In the RMSD plots shown in Figure 13 one can observe that as the tilt decreases, as a function of bilayer thickness, the

well defined rotational direction becomes much more obscure and an acceptable fit can be obtained for these small tilt values for a larger range of tilt directions.

The helical wheel plots, Figure 12, give a nice indication of the relation between the observed quadrupolar splittings and the predicted values which are based on calculated tilt and rotation values. Additionally these plots somewhat illustrate the magnitude of tilt angles, as a function of lipid bilayer thickness. As the peptide tilt angle decreases, the amplitude of the helical wheel also decreases. The quality of the fits can be further observed in the RMSD plots shown in Figure 13 and 14. Here the RMSD values are plotted as a function of the peptide tilt and rotation. In addition to the relationship between tilt, rotation and bilayer thickness, here one can as mentioned notice the relationship between a small tilt angle and consequently less well defined peptide rotation, indicated by the RMSD contour levels of 0.5, 1 and 1.5 kHz.

For one particular peptide, C-anchored WALP n=8, we incorporated ^{15}N labels in residues 11-15 in one sample and residues 5-15 in another sample. These labels enabled us to record PISEMA spectra for bicelle-incorporated peptides at the national magnetic laboratory at the University of California, San Diego. In the PISEMA spectra (Figure 15) one can observe the ^{15}N - ^1H dipolar couplings and ^{15}N chemical shift values. The rather small sizes of the “PISA” wheels in the spectra already indicates only a small tilt of the peptide helix axis with respect to the lipid bilayer normal (Wang et al., 2000), in agreement with the conclusions from the ^2H NMR experiments (above). Assignment of the resonance peaks 11-15 in the spectrum with 5 labels was accomplished in part by comparison with GALA fit to the ^2H NMR data (Figure 12). These assignments in turn

enabled us to determine the peptide rotation with respect to the corresponding ^{15}N - ^1H dipolar coupling values. Based on the dipolar coupling values we have been able to fit a PISA wheel with a specific peptide tilt to the ^{15}N - ^1H dipolar couplings and ^{15}N chemical shift resonances in the obtained spectra (Vostrikov et al., 2008). The PISA wheel fit is consistent with a tilt of 6° . The peptide orientation in magnetically aligned bicelle samples was determined using deuterated alanine quadrupolar splitting values alone, by considering the PISA wheel fit to the ^{15}N - ^1H dipolar couplings and ^{15}N chemical shift values, and in a combined analysis of ^2H quadrupolar splittings in conjunction with the assigned ^{15}N - ^1H dipolar coupling values. Using solely ^2H data obtained for bicelle samples a tilt of 3.7° with a rotation of 54° was found. The PISA wheel fit alone does not specifically define the rotation but gives a tilt value of 3 - 6° , depending on the exact value of S_{zz} and precise values of ^{15}N chemical shift tensor components. When combining the ^2H and ^1H - ^{15}N data the peptide tilt was determined to be 4° with a 52° rotation

2.4 Discussion

Traditional WALP peptides contain two tryptophan residues on either side of a leucine alanine helical repeat of variable length, $(LA)_n$. Because the motional behavior of the N- and C-terminal tryptophan (W) residues is different (van der Wel et al., 2007), we have developed peptides with two tryptophan residues on only one side of a poly- $(LA)_n$ sequence, to investigate their respective influences on the average peptide orientation. To further explore the properties of these peptides having only one pair of anchoring tryptophans at either the amino or carboxy terminus we have performed both deuterium NMR and ^{15}N studies.

We have synthesized “half-anchored” WALP peptides of different lengths. Half WALP peptides with a hydrophobic length similar to a bilayer leaflet will be discussed below. The longer half-anchored WALP peptides have hydrophobic lengths similar to those of WALP19 or WALP23, but are anchored to the lipid bilayer membrane on only one side. We find that the longer half-anchored WALP peptides incorporate into lipid bilayers and assume transmembrane orientations. Unlike shorter half-anchored analogs (below), these longer peptides with eight Leu-Ala pairs show no signs of aggregation and therefore allow investigation of the peptide/lipid interactions.

Circular dichroism spectra indicate that the N-anchored and C-anchored half anchored WALP peptides with eight Leu-Ala pairs retain alpha-helical conformations, whereas the shorter half WALP peptides show a decrease in helicity. It is likely that the relatively short length of the peptides is not sufficient to create a stable hydrogen bonding pattern,

prohibiting the α -helix formation throughout the sequence (Joh et al., 2008). Isotope labeling of selected residues in the Leu-Ala peptide core facilitates determination of the average peptide orientation within lipid bilayer membranes using solid-state NMR techniques.

Via deuterium labeling of specific alanine residues we have calculated the average apparent peptide orientation within lipid bilayers that are mechanically and in some cases magnetically aligned. The methods have involved solid-state deuterium NMR spectroscopy in conjunction with GALA analysis. The bilayer length-dependent tilt of these half-anchored peptides, in DOPC, DMPC and DLPC lipid bilayer membranes, appears to be similar yet slightly smaller than for WALP23 (Strandberg et al., 2004). The observed average tilts range between about 1 and 7 degrees from the bilayer normal for the N-anchored and C-anchored peptides, compared to 4-8 degrees for WALP23. The intrinsically small values found for the apparent average tilt of half-anchored WALP peptides, with a single anchoring region, using semi static GALA analysis indicate that these peptides are tilted less and/or experience more motional averaging since they do not have anchoring residues on both sides of the lipid membrane. The largest tilt angles found for these peptides using semi static analysis do not exceed $\sim 4^\circ$ for the C-anchored and $\sim 7^\circ$ for the N-anchored peptide, while the tilt magnitudes in longer lipids are smaller. In spite of the small apparent tilt values, they do show systematic variation with the lipid bilayer hydrophobic thickness. The largest tilt values for these peptides are found in DLPC lipid bilayers where there is a significant positive hydrophobic mismatch. When considering the various mechanically oriented samples, there is not however a clear

mismatch dependent trend in the peptide tilt observed for the C-anchored sequence in DMPC and DOPC lipid bilayer systems. Since we observe small apparent tilt values both for the C- anchored and the N- anchored peptide, we would like to point out that neither the N- nor the C-terminal anchoring is likely to have a significantly more pronounced effect than the other in determining the magnitude of the peptide tilt within the lipid bilayer. That said, there seems to be a slightly larger tilt for the N-anchored peptides, especially in DLPC. For the DLPC systems, where the most pronounced peptide tilt is found, the direction of the peptide tilt (with respect to residue 1) is roughly opposite for the C- and N-anchored peptides. Since the tilt value observed for the DMPC and DOPC lipid systems is so small, the tilt direction is also much less well defined in these systems. We note that as the tilt magnitude approaches zero, the tilt direction becomes undefined.

The exceptionally small average apparent tilt values make the single anchored peptides excellent candidates for comparative experiments using other NMR methods. These peptides therefore provide an opportunity to extend the comparisons between the ^2H -based GALA and ^{15}N -based PISEMA methods. Previous studies using GWALP23 peptides showed good agreement of peptide orientation determined by ^2H and ^{15}N NMR based methods (Vostrikov et al., 2008). For α -helical peptides such as single anchored WALP these methodologies are able to determine peptide alignment within a lipid bilayer using NMR signals and constraints originating from peptide geometry. When comparing the results found for the C-anchored WALP peptides GALA and PISEMA analysis, again we find good agreement for the peptide orientation.

In the C-14 lipid, a similar tilt is calculated from the ^2H studies using DMPC bilayer samples and the ^{15}N studies using bicelle samples, containing DM-o-PC. For these samples, therefore, a small difference in peptide orientation is observed between mechanically and magnetically oriented bilayers. For this reason we have prepared a set of magnetically oriented samples for the acquisition of both the ^2H and ^{15}N data, thereby enabling a reliable comparison of sample alignment methods. The direction of tilt matches remarkably well for all of the analysis methods and sample alignment methods. Upon assignment of resonance peaks in the PISEMA spectrum with five ^{15}N labels, in concordance with data from ^2H bicelle studies for this peptide, we were able to assign a rotation value of 52° for the C-anchored peptide.

When addressing specific peptide dynamics using calculations allowing for variable $\sigma\tau$ and $\sigma\rho$ values in a Gaussian analysis (Strandberg et al., 2009), we still find small tilt values for these peptides. In some cases the peptides do seem to have slightly larger average tilt magnitudes when approached as a dynamic model; however the changes are small. Even with a two-fold increase in average tilt, these peptides would still have very low tilts, especially compared to other peptides with similar hydrophobic lengths (Strandberg et al., 2009).

In addition to resolving issues of tryptophan anchoring, single anchored WALP peptides are valuable for addressing other questions. For example, such WALP peptides provide an interesting means to investigate potential insertion of a model peptide capable of crossing only a single bilayer leaflet, and investigating its positioning with respect to the bilayer. The short single anchored half WALP peptides that we developed have the

hydrophobic length of one leaflet of the lipid bilayer and therefore have the theoretical capability of spanning a monolayer or bilayer leaflet. Insertion of a half WALP peptide might be influenced by interaction with a peptide counterpart positioned in the opposite bilayer leaflet, perhaps to enable formation of otherwise potentially unsatisfied H-bonds at the peptide termini. For this purpose we have investigated short C-anchored half WALP peptides both with and without an N-anchored counterpart.

Based on our deuterium NMR results we conclude that, rather than inserting into the lipid bilayer in a position spanning one leaflet of the bilayer, these short half WALP peptides behave as short peptides with a large negative hydrophobic mismatch. It appears that the mismatch is relieved by oligomerization of the peptides (de Planque and Killian, 2003). Although non-lamellar phase formation has been previously described for negative hydrophobic mismatch, this does not seem to be the case for half WALP peptides based on our ^{31}P spectra. The oligomerization process described for short peptides is further supported by molecular dynamics studies (Sparr et al., 2005),(Schmidt et al., 2008). Based on their studies, Schmidt et al. conclude that negative hydrophobic mismatch strongly supports dimerization and sequential peptide clustering (Schmidt et al., 2008). Such protein aggregation has been previously predicted (Mouritsen and Bloom, 1984). For half WALP peptides we indeed observe a large amount of peptide aggregation, denoted by Pake pattern observed in the solid state ^2H NMR studies, at both $\beta = 90^\circ$ and $\beta = 0^\circ$ sample orientations. This aggregation is likely due to the severe amount of hydrophobic mismatch that peptides experience when trying to associate themselves in a transmembrane conformation or might simply be a result of unfavorable peptide lipid

interactions for half WALP peptide positioning spanning just one leaflet of the bilayer. In addition to the peptide aggregation as a result to hydrophobic mismatch CD studies indicate a certain amount of unwinding of the short Leu-Ala repeat, indicated by the decrease of α -helicity, indicating possible deformation of the peptide backbone, likely in an attempt to compensate for some of the hydrophobic mismatch. It is notable that in contrast with a poly-alanine peptide, which is not hydrophobic enough to incorporate in a lipid bilayer, even short half WALP peptides are not water soluble (Lewis et al., 2001).

In conclusion; single anchored WALP peptides provide some new insight into the anchoring behavior of Trp residues and the importance of peptide hydrophobic length. Both ^2H and ^{15}N studies indicate small apparent average tilt angles and extensive dynamics for single anchored peptides with a hydrophobic length capable of spanning across a lipid bilayer. Both N- and C- anchored peptides show these small tilt values. As expected, the direction of the peptide tilt becomes less well defined as the tilt magnitude becomes very small. Because the shorter half-WALP peptides tend to aggregate, we deduce that they are unable to find stable positions as individual molecular entities spanning only one-half of a lipid bilayer membrane.

2.5 Tables

Table 1

Peptides with acetyl (Ac) and ethanolamide (EA) terminal protecting groups.

C-anchored WALP	n=4	Ac- ALALALALWWG -EA
C-anchored WALP	n=8	Ac- ALALALALALALALALWWG -EA
N-anchored WALP	n=8	Ac- GGWWLALALALALALALALA -EA

Table 2

²H NMR average quadrupolar splitting values, in kHz, for N-anchored n=8 and C-anchored n=8 single anchored WALP peptides in oriented DLPC, DMPC, DMPC/DH-o-PC bicelles and DOPC lipid bilayers at an orientation of $\beta=0^\circ$ with respect to the magnetic field.

N-anchored WALP

Ala #	DLPC	DMPC	DOPC
6	15.1	12.4	10.0
8	3.4	1.8	5.1
10	16.0	10.2	9.3
12	2.4	6.8	4.9
14	12.6	7.4	8.3
16	6.8	7.4	8.3
18	4.4	5.5	6.8

C-anchored WALP

Ala #	DLPC	DMPC	Bicelle	DOPC
3	0.0	5.1	0.0	9.6
5	10.8	8.1	10.6	5.1
7	4.2	6.8	4.0	9.5
9	7.9	7.7	7.4	3.0
11	7.9	7.7	7.4	9.0
13	5.2	7.4	6.2	5.9
15	11.3	7.4	8.8	7.4

¹H-¹⁵N NMR dipolar coupling values, in kHz, for C-anchored n=8 WALP in DMPC/DH-o-PC bicelles q3.2

Ala #	DM-o-PC
11	3.55
12	3.35
13	3.85
14	3.70
15	3.30

Table 3

Calculated peptide orientations of the C- and N-anchored WALP peptides in various lipids using a semi static and dynamic (Gaussian) calculation model, ^2H quadrupolar splitting values and ^1H - ^{15}N dipolar coupling values (^{15}N) were used for analysis as indicated.**

C-anchored WALP

	^2H DLPC	^2H DMPC	^2H Bicelle	^{15}N Bicelle	$^2\text{H}, ^{15}\text{N}$ Bicelle	^2H DOPC
Szz						
Tau	4.3	0.7	3.7	6	4	2.0
Rho	46	60	54	86	52	284
RMSD	0.66	0.54	0.96	0.66	0.753	0.62
Szz	0.72	0.77	0.69	0.71	0.68	0.74
Gaussian						
Tau0	7	1	6		6	4
Rho0	46	48	54		54	284
RMSD	0.511	0.334	0.956		0.743	0.612
sTau	20	19	20		20	19
sRho	55	50	60		55	65
Szz*	0.88	0.88	0.88		0.88	0.88

N-anchored WALP

	^2H DLPC	^2H DMPC	^2H DOPC
Szz			
Tau	7.3	3.0	1.7
Rho	202	180	193
RMSD	0.88	0.94	0.51
Szz	0.73	0.78	0.79
Gaussian			
Tau0	12	7	3
Rho0	201	180	193
RMSD	0.889	0.935	0.487
sTau	18	16	15
sRho	55	75	60
Szz*	0.88	0.88	0.88

**Dynamic analysis using a fixed internal order parameter*, accounting for intra molecular motion, allowed for determination of τ , ρ and whole body dynamics $\sigma\tau$ and

$\sigma\rho$. Semi-static analysis determines the best fit, lowest RMSD, for peptide orientation including variable τ and ρ in addition to a variable order parameter, S_{zz} , accounting for whole body dynamics and internal peptide motion. Analysis of ^{15}N data were based on ^1H - ^{15}N dipolar coupling values obtained for residues 11-15. Calculations based on both ^1H - ^{15}N dipolar ^2H quadrupolar splitting values used weighting factors of 1 for the deuterium data and 0.5 for the ^1H - ^{15}N dipolar couplings.

2.6 Figures

Figure 1

MALDI Mass spectra representative of single anchored WALP peptides after peptide cleavage.

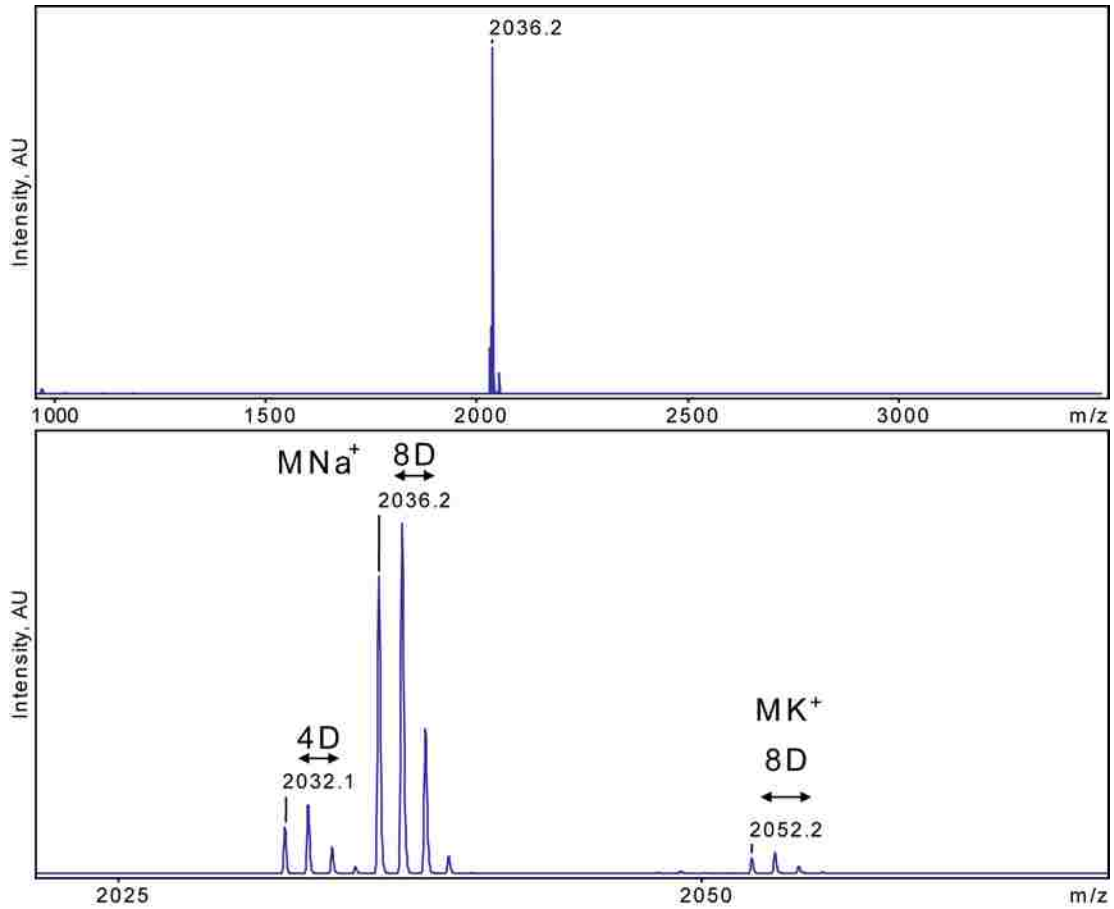


Figure 2
HPLC spectra representative of single anchored WALP peptides

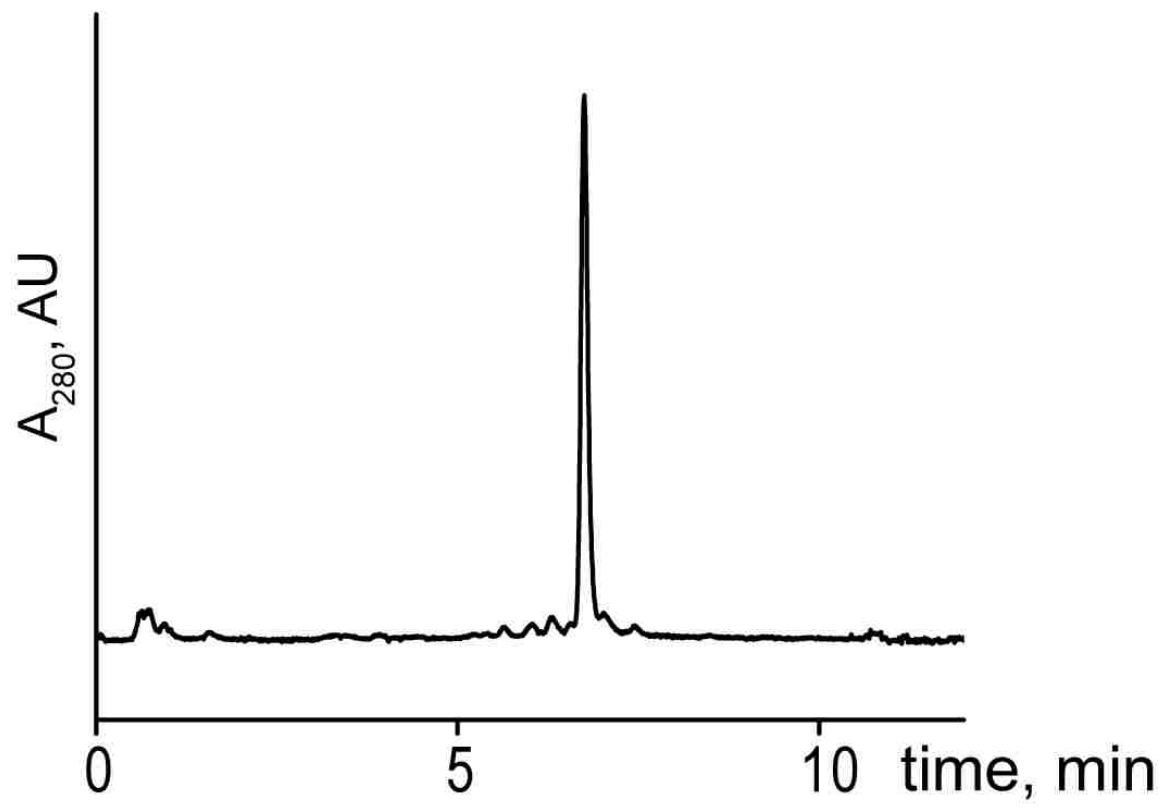


Figure 3

Circular dichroism spectra of N-anchored n=8 (A), C-anchored n=8 (B) and C-anchored n=4 (C) in DLPC (black), DMPC (grey) and DOPC (light gray) vesicles.

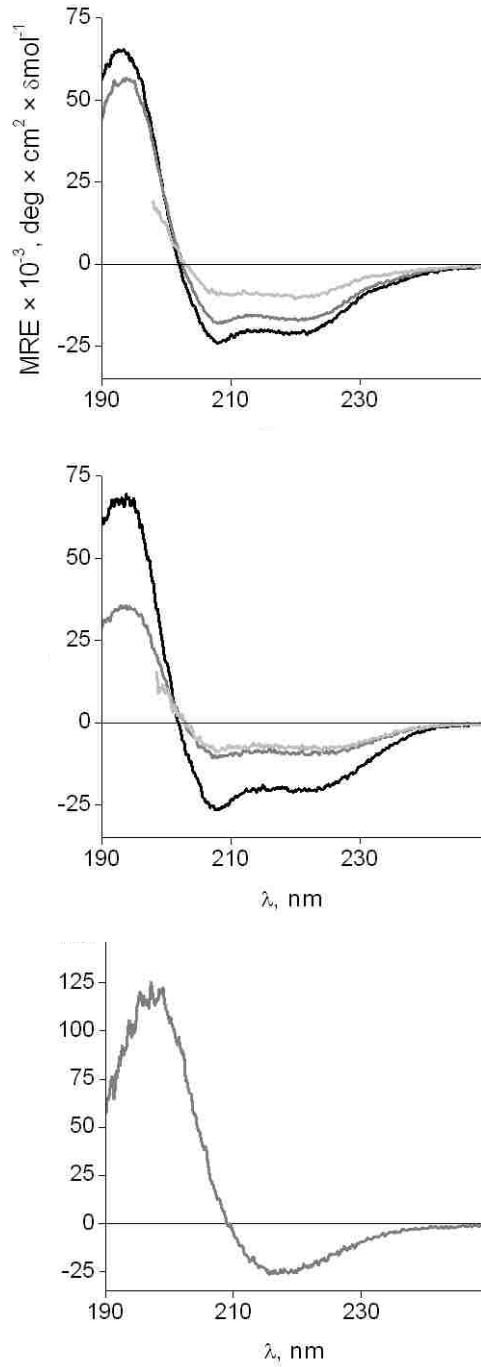


Figure 4

Intrinsic tryptophan fluorescence spectra of N-anchored n=8 (A), C-anchored n=8 (B) in DLPC (black), DMPC (blue) and DOPC (red) small unilamellar vesicles.

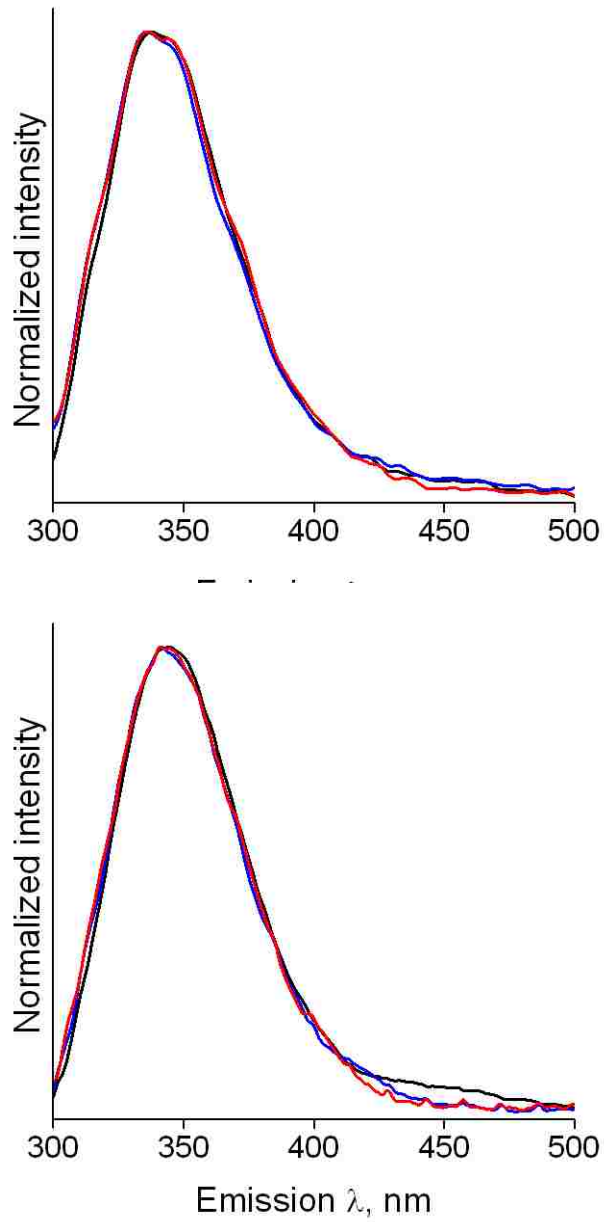


Figure 5

Representative ^{31}P NMR spectra, C-anchored n=8 WALP in DMPC at $\beta=0^\circ$ and $\beta=90^\circ$ orientation with respect to the magnetic field.



Figure 6

^2H NMR spectra of C-anchored n=4 WALP peptides (A-F) and combined C-anchored n=4 WALP : N-anchored n=4 WALP in a 1:1 mixture, in oriented bilayers of DLPC, DMPC and DOPC at orientation of $\beta=0^\circ$ (A-C, G) and $\beta=90^\circ$ (D-F, H) with respect to the magnetic field. Alanine d-4 labeled residues 7^{100%} 5^{50%} 3^{75%} on the C-anchored peptide.

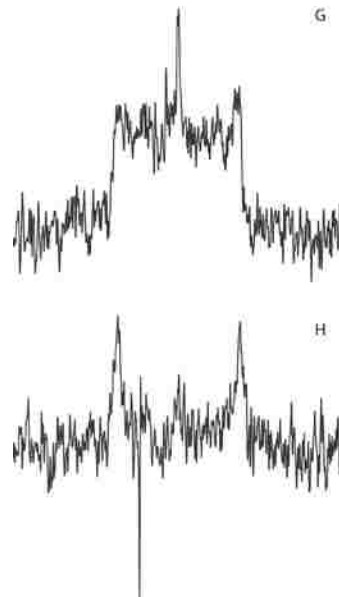
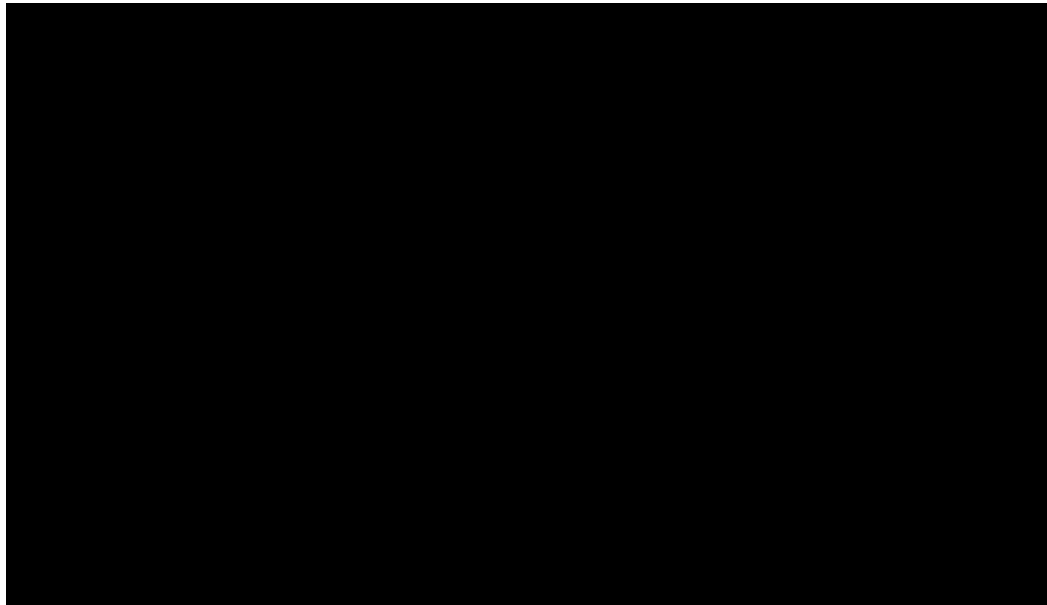


Figure 7

^2H NMR spectra of N-anchored $n=8$ (A,B), C-anchored $n=8$ (C,D) and C-anchored $n=4$ (E,F) single anchor WALP peptides in oriented DMPC bilayers at $\beta=0^\circ$ (A,C,F) and $\beta=90^\circ$ (B,D,E).

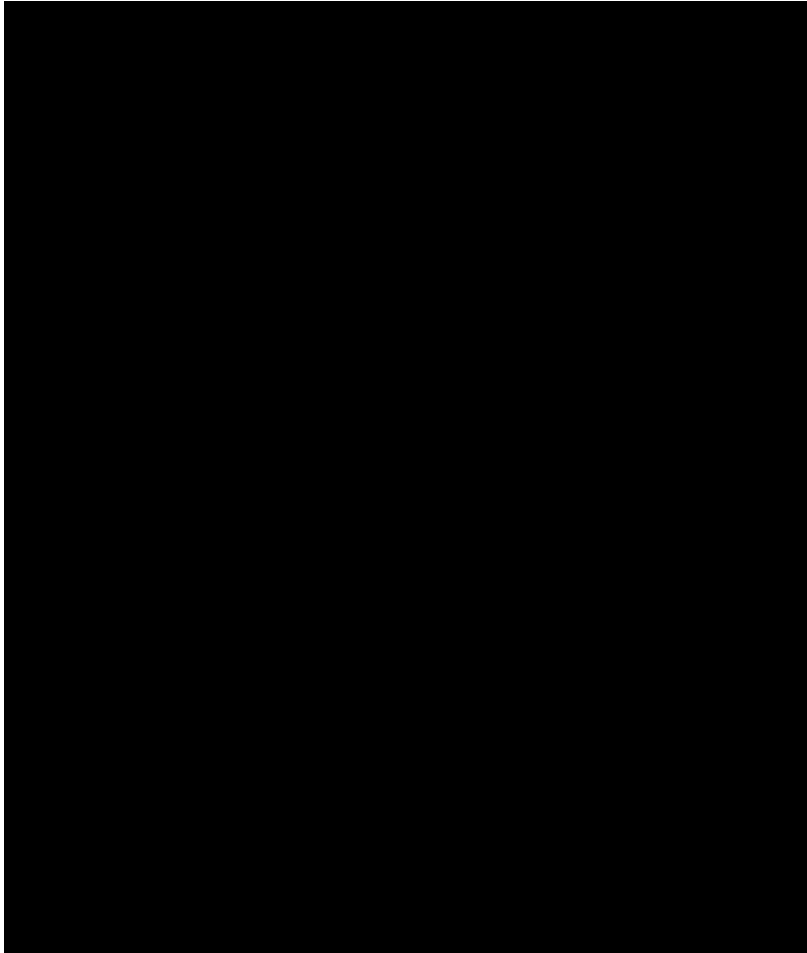


Figure 8

^2H NMR spectra of N-anchored n=8 WALP peptides in oriented bilayers of DLPC, DMPC and DOPC at orientation of $\beta=0^\circ$ with respect to the magnetic field. Alanine d-4 labeling of residues is indicated on the left.

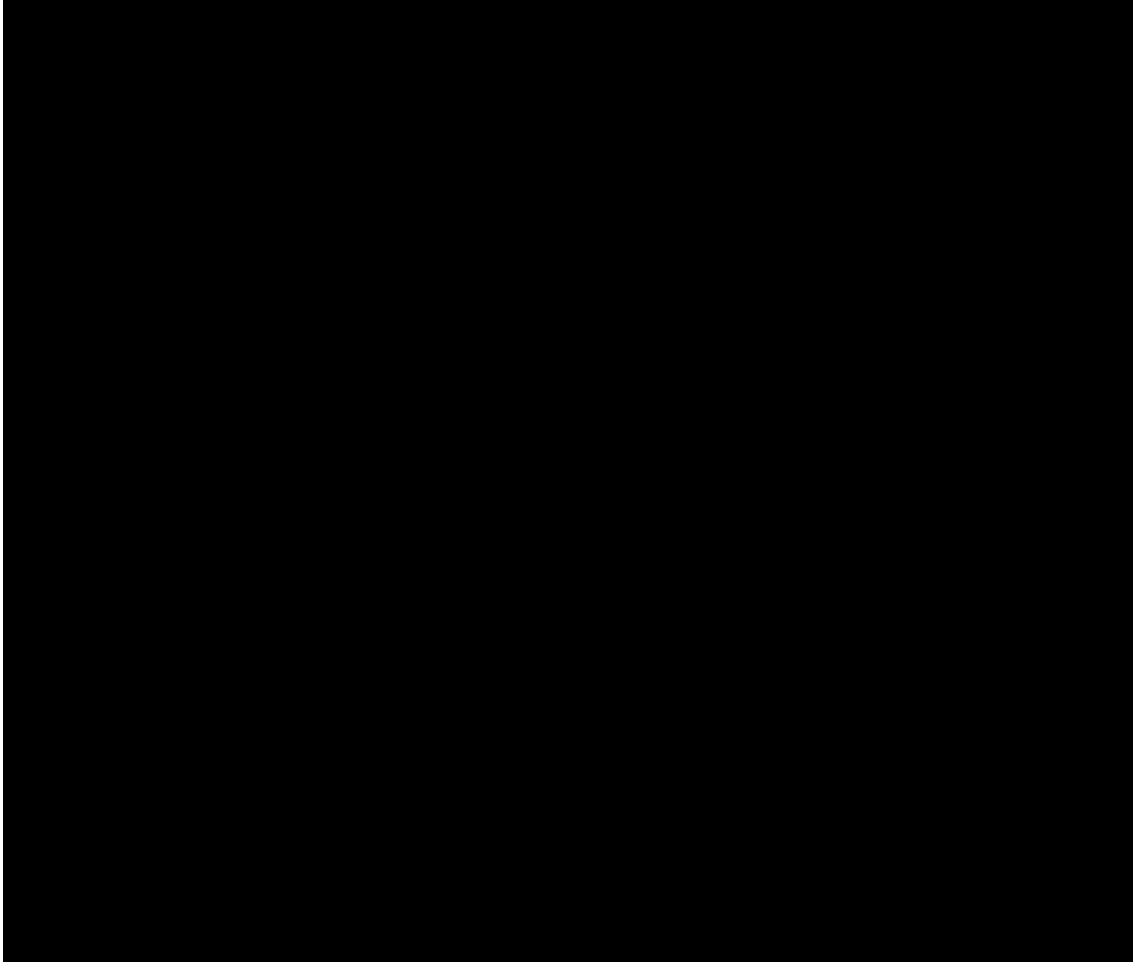


Figure 9

^2H NMR spectra of N-anchored n=8 and WALP peptides in oriented bilayers of DLPC, DMPC and DOPC at orientation of $\beta=90^\circ$ with respect to the magnetic field. Alanine d-4 labeling of residues is indicated on the left.

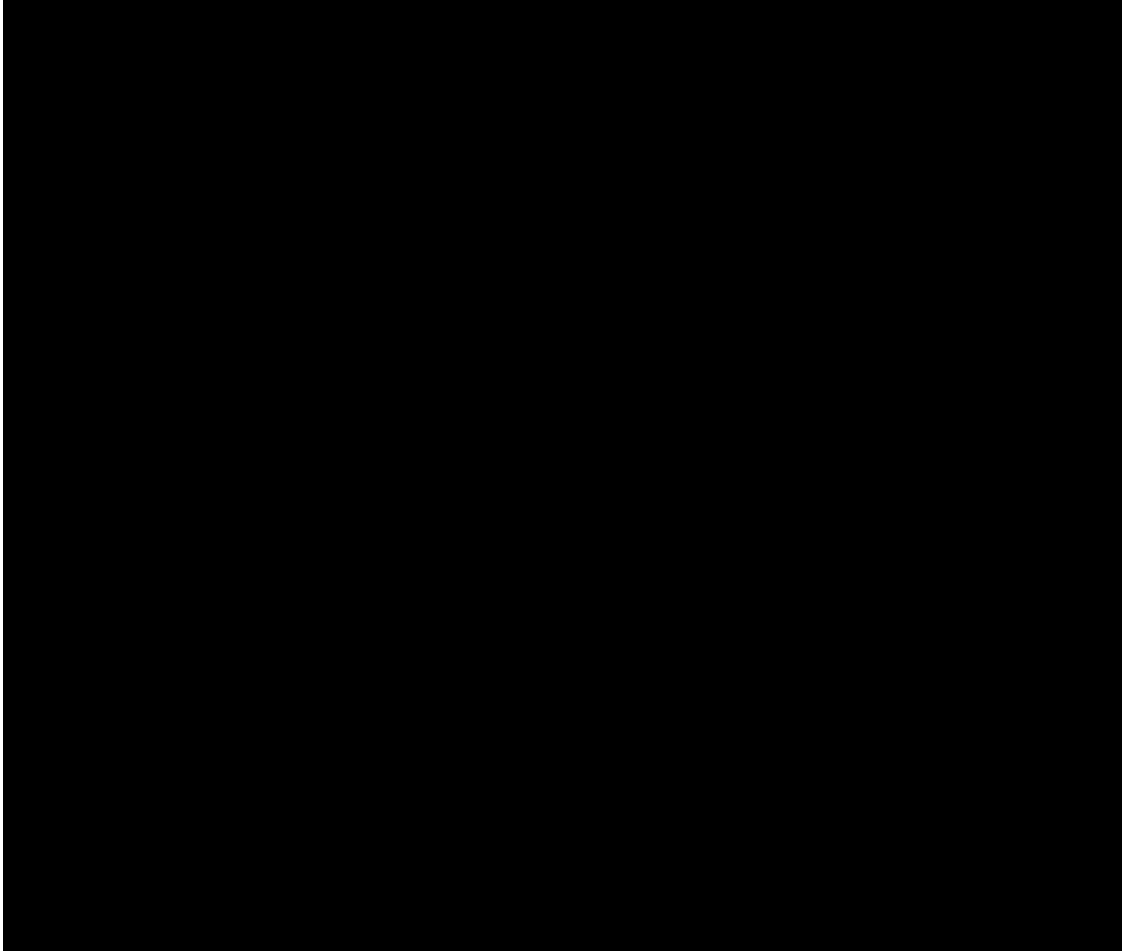


Figure 10

^2H NMR spectra of C-anchored n=8 WALP peptides in oriented bilayers of DLPC, DMPC and DOPC at orientation of $\beta=0^\circ$ with respect to the magnetic field. Alanine d-4 labeling of residues is indicated on the left.

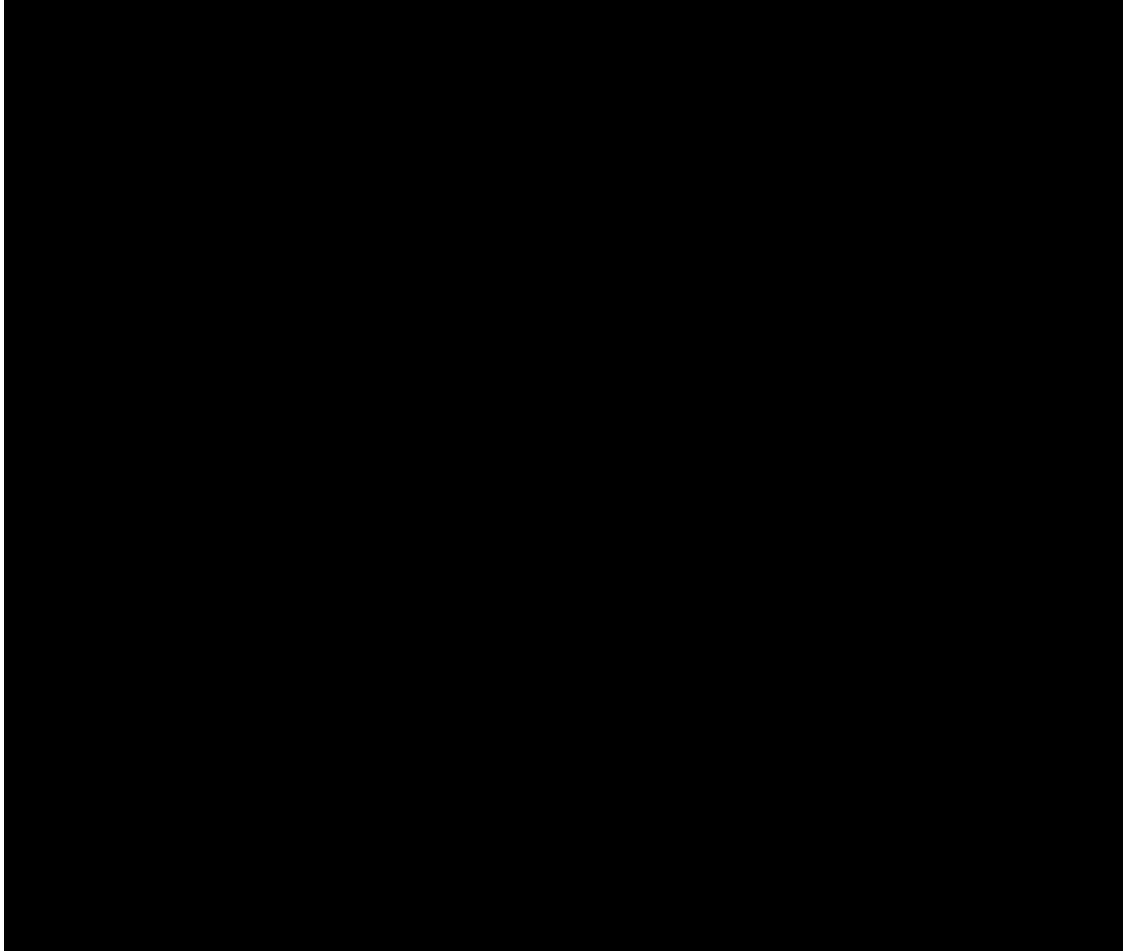


Figure 11

^2H NMR spectra of C-anchored n=8 WALP peptides in oriented bilayers of DLPC, DMPC and DOPC at orientation of $\beta=90^\circ$ with respect to the magnetic field. Alanine d-4 labeling of residues is indicated on the left.

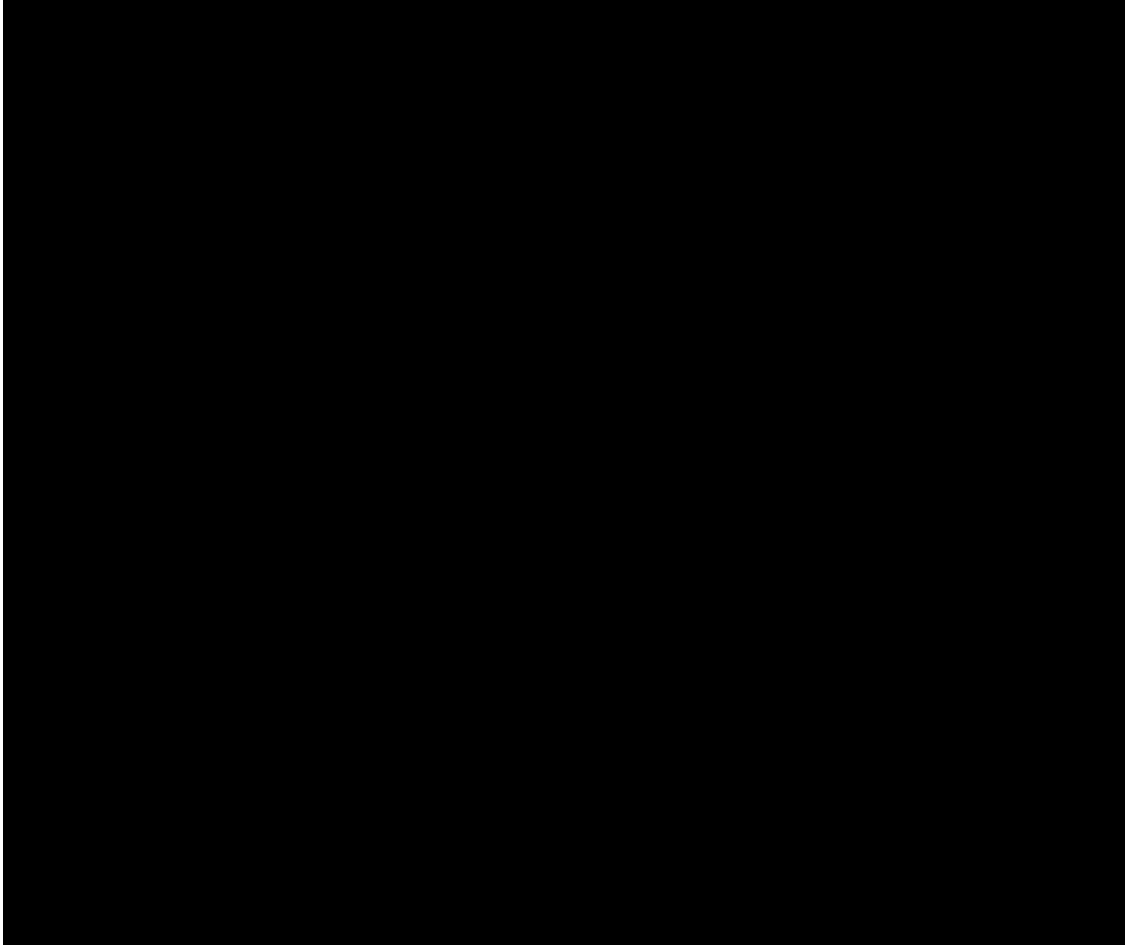


Figure 12

Helical wheel plots with observed quadrupolar splittings for N-anchored n=8 (triangles, gray) and C-anchored n=8 (circles, black) single anchored WALP peptide in oriented DLPC (A), DMPC (B, D) and DOPC (C) bilayers. In figure D one can observe comparison between mechanically oriented bilayers (black), bicelle (gray) and bicelle analysis using combined ^2H and ^{15}N data (red). Figure E shows the calculated helical wave plots for C-anchored n=8 in bicelle analysis using combined ^2H and ^{15}N data. Semi static calculations are represented by solid lines, whereas Gaussian analysis are represented by dashed lines.

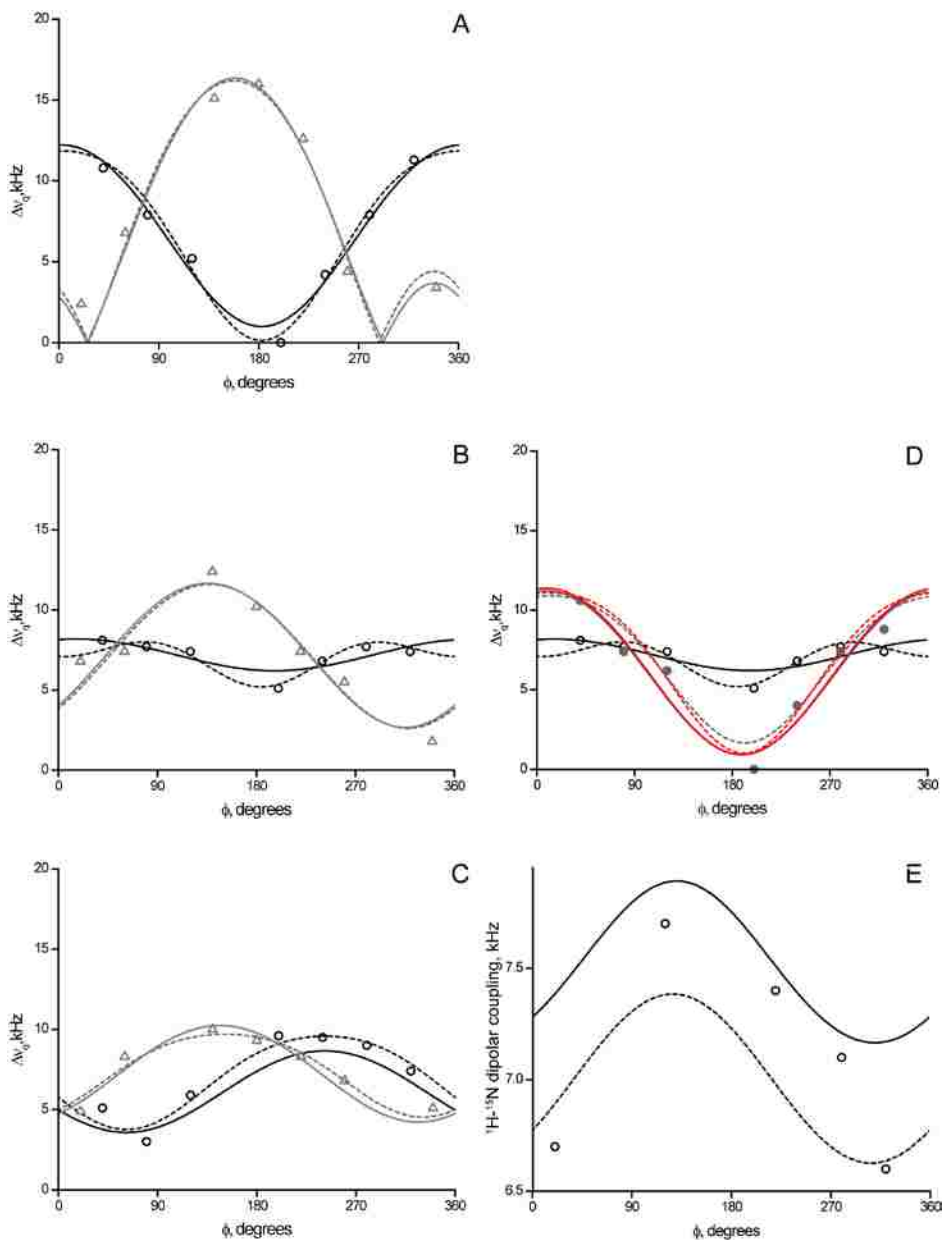


Figure 13

RMSD plots showing contour levels of 0.5, 1 and 1.5 kHz, based on S_{zz} based (solid lines) and Gaussian (dashed lines) analysis of N-anchored $n=8$ (gray) and C-anchored $n=8$ (black) single anchored WALP peptide in oriented DLPC (A), DMPC (B) and DOPC (C) bilayers. See (D) for comparison of C-anchored peptide in DM(-O-)PC bilayers as analyzed by different techniques, ^2H mechanically oriented bilayers (black) ^2H bicelle studies (grey) and a combined ^2H ^1H - ^{15}N analysis.

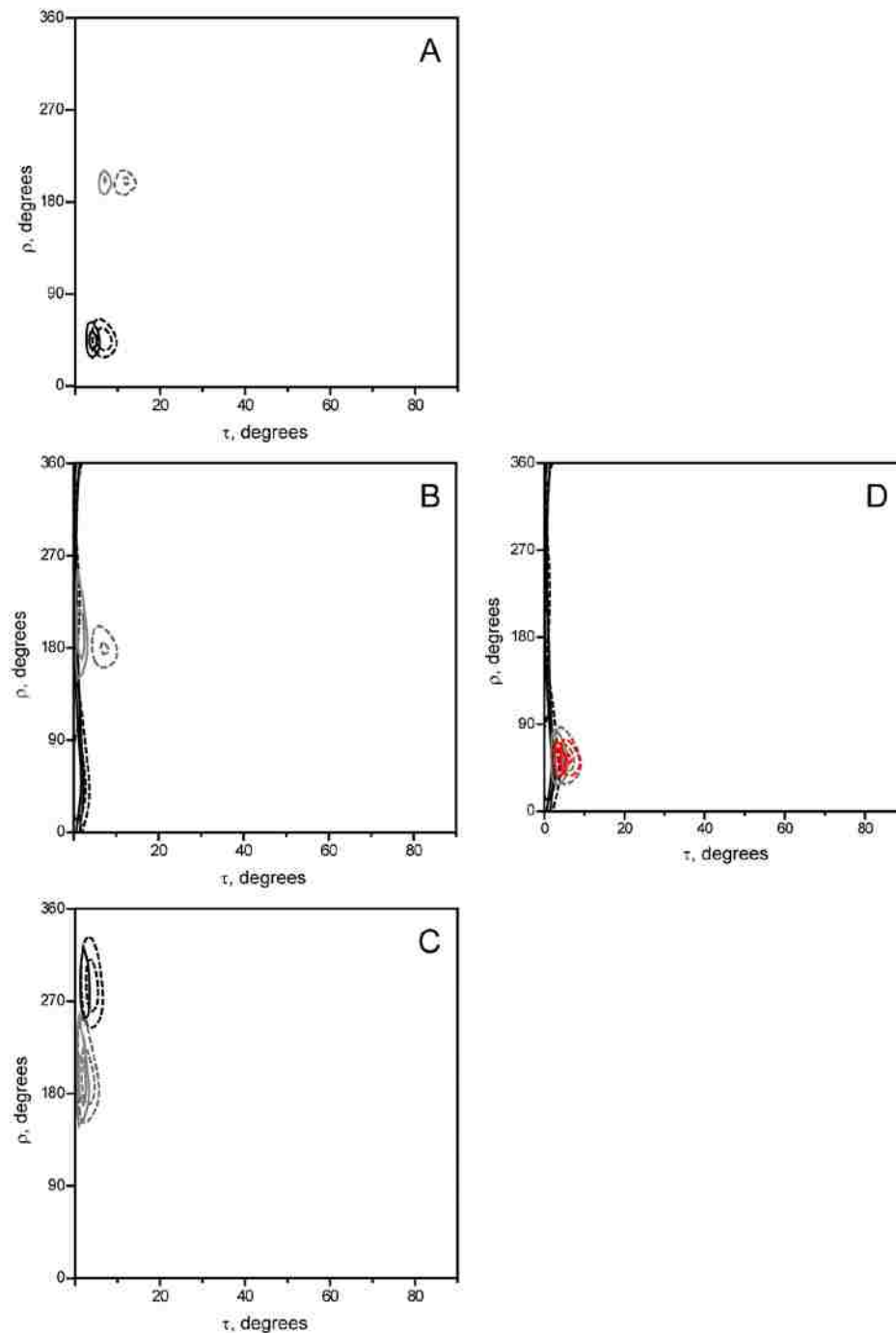


Figure 14

RMSD plot as a function of $\sigma\tau$ and $\sigma\rho$ for the Gaussian analysis of C-anchored n=8 WALP peptide in DMPC bilayers (A) and in DM(-O-)PC bilayers (B, C). Analyzed by different techniques, ^2H mechanically oriented bilayers (A) ^2H bicelle studies (B) and a combined ^2H ^1H - ^{15}N analysis (C) showing contour levels of 0.5 to 1 with 0.1 kHz intervals.

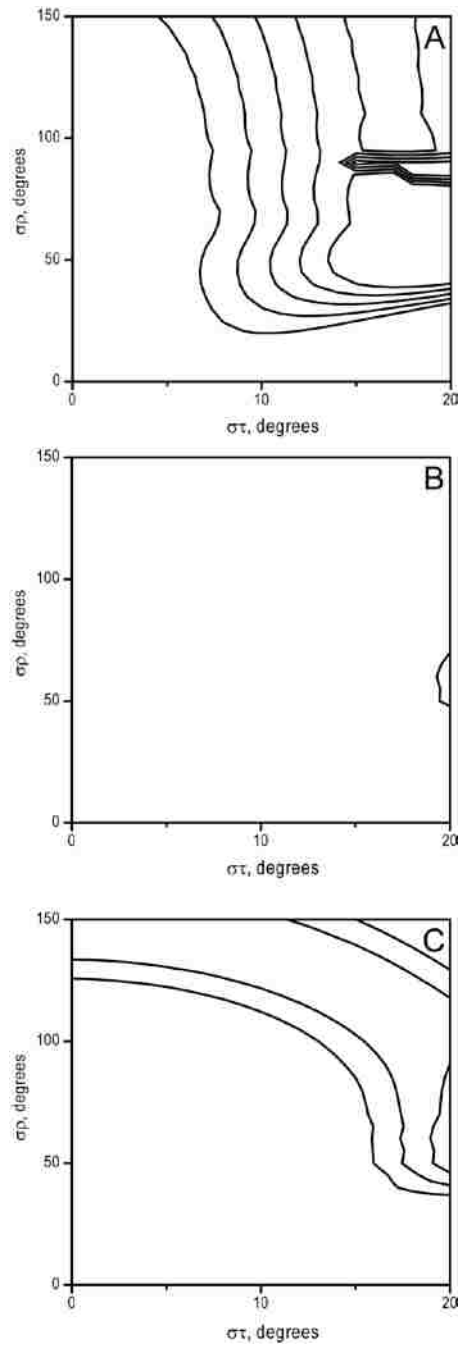
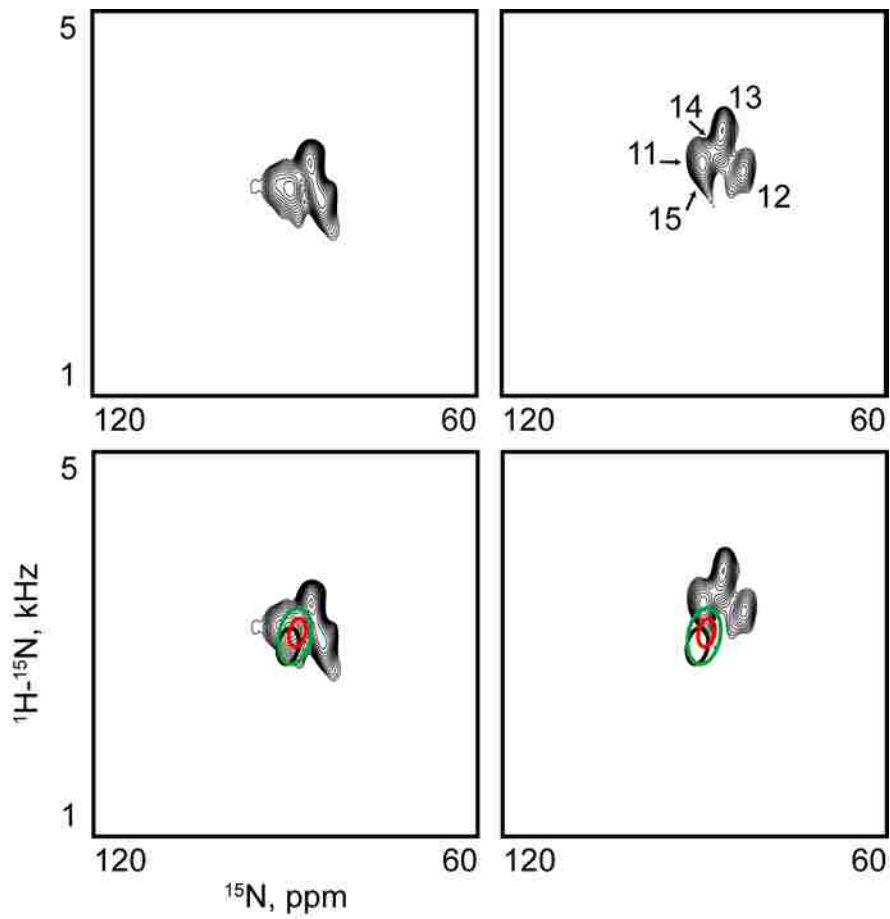


Figure 15

Pisema spectrum with fits for C-anchored WALP with 11 labels (A, C) and 5 Labels (B, D). Helical wheel patterns are indicated based on analysis of ^{15}N data (green) and a combination of ^2H and ^{15}N data are indicated (Black weighing 1 and 0.5, and red equal weighing). Tilt and S_{zz} values for the respective fits are 6° 0.71, 4° 0.68 and 3° 0.71)



CHAPTER 3

ADDITION OF A THIRD ANCHORING RESIDUE TO “SINGLE” ANCHOR WALP

3.1 Introduction

In the studies of general principles pertaining to structure and function of bilayer associated proteins, model peptides can play a valuable role. By aiding data accumulation concerning interactions of protein components with their surroundings, model peptides can support in developing a greater understanding of the properties and roles of proteins in biomembranes. Well known examples are the much studied model peptides of the WALP family (Killian et al., 1996). Traditional WALP peptides contain two tryptophan residues on either side of a leucine alanine helical repeat of variable length, $(LA)_n$. Because the motional behavior of the N- and C-terminal tryptophan (W) residues is different (van der Wel et al., 2007), it is of interest to investigate how the positions of the anchoring tryptophans will influence the average peptide orientation. As discussed in the half anchored WALP peptides chapter, to explore further the properties of these anchoring residues, we have developed peptides with two tryptophan residues on only one side of a poly- $(LA)_n$ sequence.

Having only one pair of anchoring tryptophans at either the amino or carboxy terminus, the peptides were designated as N-anchored WALP and C-anchored WALP (acetyl-GGWW $(LA)_8$ -ethanolamide and acetyl- $(AL)_8$ WWG-ethanolamide, respectively). These “half-anchored” WALP peptides have hydrophobic lengths similar to that of WALP23, yet unlike WALP23 they are anchored to the lipid bilayer membrane on only one side. We find that the half-anchored WALP peptides incorporate into lipid bilayers and assume

defined orientations. Unlike shorter half-anchored analogs that contain only three or four Leu-Ala pairs, these longer peptides with eight Leu-Ala pairs show no signs of aggregation and therefore allow further investigation of the peptide/lipid interactions.

Here we describe studies in which we extend the investigations of the anchoring behavior in WALP-like peptides. Based on the C-anchored WALP peptides, we now add an additional third anchor that is separated from the two tryptophan residues by a variable number of pairs of leucine and alanine residues. Addition of a third anchoring residue (either W or R) to C-anchored WALP peptides (acetyl-(AL)₈WWG-ethanolamide) results in changes in the peptide orientation. Half anchored peptides provide a wonderfully suitable basis for such studies due to their remarkably small intrinsic peptide tilts, observed over a range of lipid bilayer hydrophobic thicknesses.

Via deuterium labeling of specific alanine residues, one can determine the average apparent peptide orientation within mechanically aligned lipid bilayers, using solid-state deuterium NMR spectroscopy in conjunction with GALA analysis (van der Wel et al., 2002) (Strandberg et al., 2002). The magnitude of the change in peptide tilt and rotation is dependent on both the type and position of the additional anchor residue, as well as the hydrophobic length of the lipid bilayer in which the peptide is incorporated.

3.2 Materials and Methods

For materials and methods used please refer to the previous chapter; “Half anchored WALP peptides: Effect of anchor position on peptide orientation”. Peptide sequences of the peptides that were synthesized can be found in Table 1.

3.3 Results:

Prior to the ^2H NMR experiments, ^{31}P NMR spectra were recorded. Typical ^{31}P NMR spectra were similar to spectra that can be seen in figure S4 in the previous chapter concerning single anchored WALP peptides. In all cases, the ^{31}P NMR spectra indicated the predominance of aligned and fluid (hydrated) lipid bilayers in the samples.

In order to determine the orientations of the peptides in DLPC, DOPC and DMPC lipid bilayer membranes, samples incorporating the peptides in mechanically aligned oriented bilayers have been prepared. See Table 1 for the peptide sequences. Assignment of the corresponding quadrupolar splitting values from the spectra was based on the relative abundance for each labeled alanine residue and the relative intensities of the two pairs of corresponding peaks; assignments are shown in Table 2. Deuterium NMR spectra were recorded at sample orientations $\beta = 0^\circ$ and $\beta = 90^\circ$, in which the lipid bilayers were aligned perpendicular and parallel to the magnetic field, respectively. Spectra corresponding to the $\beta = 0^\circ$ sample orientation are shown in figures 1-4. For the analysis of data, the quadrupolar splitting values found for $\beta = 0^\circ$ and $(\beta = 90^\circ) \times 2$ were averaged. We were not able to obtain quadrupolar splitting values for the R6 peptide in DOPC, likely due to the lack of a well defined peptide conformation or orientation in this lipid.

For each of the peptides, the average apparent tilt and rotation values were calculated with respect to the C- α atom of the initial Ala¹ residue. These calculations were performed using traditional GALA analysis based on the quadrupolar splittings assigned for the recorded ^2H spectra. Using the traditional semi static GALA analysis with a set

principal order parameter, S_{zz} (0.875), we have been able to obtain the average apparent tilt and rotation of the peptides in lipid bilayer membranes. These calculations converged to $\varepsilon_{//}$ values between 56.5° and 60.2° for the alanine side chains in the different peptides, as indicated in Table 3. The obtained RMSD values for these calculations were no more than 0.7 kHz.

To illustrate the effects of incorporation of a third anchoring residue, we show helical wheel plots of each of the peptides in the various lipid systems (Figure 5). Additionally, polar plots and RMSD plots (Figure 6 and 7) nicely represent the change in peptide tilt and rotation as a function of both bilayer thickness and the third anchoring residue position and identity. As a means of comparison, C-anchored WALP is depicted in this figure in addition to the peptides with a third anchor.

3.4 Discussion:

We have been able to calculate average apparent tilt and rotation values for several of the peptides containing three anchoring residues using semi-static calculation methods. The results depend upon the position of the single Arg or Trp anchor that is inserted near the N-terminal end of a C-anchored peptide that has dual Trp anchors already. Each of these peptides contains tryptophan anchoring residues in positions 17 and 18 of the sequence, as does the previously described C-anchored WALP peptide. To assess the contribution of a third anchoring residue near the other end of the peptide, aromatic tryptophan or charged arginine residues have been incorporated into the sequence at position 2 or 6 (replacing Leu). Each of these substitutions affects peptide positioning in the each of the lipids. We will now address in detail the effects of incorporation of the third anchor residue.

When looking at general effects of the third anchor in the different lipid mixtures, we conclude that the apparent peptide tilt increases. Comparison of the tilt values found for the various peptides with three anchors (see table 3) with the results for the C-anchored peptide anchored by just two tryptophan residues reveals several features. For DLPC we find that the magnitudes of the tilt values show the trend: $W2 \approx \text{C-anchored (only)} < W6 < R2 \approx R6$. For the longer lipid DMPC the trend for the tilt magnitudes is somewhat different: $(\text{C-anchored peptide}) < W2 < W6 < R2 < R6$. In the DOPC lipid system it is striking that we are unable to determine a well defined peptide tilt for the R6 peptide. The trend for the tilt values found for the other peptides is as follows: $\text{C-anchored} < W2$

< R2 < W6. From the data obtained, no clear trend is evident for the different directions of tilt.

The orientation of the W2 peptide shows a little dependence on the thickness of the lipid bilayer, with the apparent tilt values ranging from only about 3° to 4.3° in the DLPC, DMPC and DOPC lipid bilayers. The rather small apparent tilt values for the W2 peptide likely reflect rather extensive peptide dynamics (Holt et al., 2010; Strandberg et al., 2009). The R2 peptide on the other hand shows an expected decrease of apparent tilt values, from about 11.7° to 8.7° to 6.3° as the bilayer thickness progressively increases. The results for R2 match theoretical expectations quite well, as the decrease in the positive hydrophobic mismatch is expected to decrease also the magnitude of the apparent tilt. The different effects of the Arg and Trp residues are likely related to their different anchoring properties, the aromatic Trp should interact preferentially with the interfacial glycerol moieties of the lipid headgroups, while the long flexible polar Arg should prefer a more hydrophilic environment.

The behavior of the peptides containing the added anchoring residue in position six, whether R6 or W6, show much less well defined peptide orientation. This is to be expected due to the short hydrophobic length of the remaining core sequence. The less well defined peptide orientation is reflected in poor fits with RMSD values in the range of 2-3 kHz. The fits are poor when all seven data points are included. Even analysis of just the alanine residues between position 6 and the tryptophans at positions 17-18 does not in most cases significantly improve the fit. One might have expected improvement by exclusion of alanine data points prior to the W6 residue; as such alanines might no longer

fit an ideal α -helix. Interestingly, the largest improvement to the fit by exclusion of the three N-terminal data points is found in DOPC. The less well defined orientation of the R6 peptide is represented by the small order parameters (S_{zz}) found for the best fits in DLPC and DMPC, as well as the lack of a well defined peptide orientation in DOPC (reflected in the extra resonances found in the deuterium NMR spectra, which prevented assignment of the resonances altogether).

Previous studies in our lab have investigated the effects on peptide orientation of incorporating an arginine residue in the center of GWALP23 in DOPC bilayers (Vostrikov et al., 2010b). Indeed for GWALP23-R12, no clearly defined peptide orientation could be assigned. Rather, molecular dynamics simulations as well as NMR spectra indicate that there are several specific stable conformations that interconvert slowly. GWALP23 with R14, on the other hand, does exhibit a defined transmembrane orientation with a tilt of about 17° in DOPC. Perhaps as in GWALP23-R12 a series of conformations might be responsible for lack of a well defined peptide orientation with R as a third anchor in position 6 of acetyl-ALALAR(AL)₅WWG-ethanolamide.

Several previous studies employed arginines as anchoring residues, either in combination with tryptophan anchors in RWALP23 (Vostrikov et al., 2010a) or as sole anchoring residues in RALP23 (de Planque et al., 2002). Like the peptide with a third anchoring R at position 2, RALP23 and RWALP23 both adopt stable transmembrane positions in the lipid bilayer. Moreover the R2 and R6 versions investigated here, as well as RWALP23, all show mismatch dependent tilt of the transmembrane orientation. Indeed for each of these peptides the largest tilt is found in the short DLPC lipid and the smallest tilt is

observed in the long DOPC lipid. Also, when comparing arginine and tryptophan anchored peptides to peptides containing just tryptophan anchors in the same positions, larger tilt values are consistently observed for peptides containing arginine anchors. As arginine can be found in or around transmembrane regions of essential biological proteins. It is important to understand the effects on transmembrane orientation that result from arginine positioning in transmembrane peptide regions (MacKinnon, 2004) (Glukhov et al., 2007). Based on the studies presented here, we conclude that the incorporation of a third anchoring residue in position 2 leads to a smaller apparent peptide tilt value than when the third anchoring residue is placed in position 6, in all of the lipids tested. Furthermore, peptides containing the third anchor in position 2 as opposed to position 6 show a more stable transmembrane conformation. This result is to be expected based on the difference in hydrophobic length. Furthermore it is important to note that there is a significant change in the magnitude of tilt for the peptide based on the anchoring residue used, in that peptides with Arg tilt to a greater extent than those with Trp as a third anchor. These findings are fundamentally important since they provide insights concerning the structural and functional properties of transmembrane associated arginine peptides.

3.5 Tables

Table 1

Peptide sequences of studied analogues.

W2	acetyl- A <u>W</u> ALALAL <u>AL</u> ALAL <u>AL</u> AL <u>W</u> WG-ethanolamide
W6	acetyl-ALAL <u>A</u> W <u>A</u> AL <u>A</u> AL <u>A</u> AL <u>W</u> WG-ethanolamide
R2	acetyl- A <u>R</u> ALALAL <u>AL</u> ALAL <u>AL</u> AL <u>W</u> WG-amide
R6	acetyl-ALAL <u>A</u> R <u>A</u> AL <u>A</u> AL <u>A</u> AL <u>W</u> WG-amide
C-anchored	acetyl-ALALALALALALALAL <u>W</u> WG-ethanolamide

Table 2

Quadrupolar splitting values in kHz observed for the corresponding isotope enriched alanine residues

W2:

ac-AWALALALALALALALWWG-ea

Ala #	DLPC	DMPC	DOPC
9	11.7	10.6	8.8
11	2.7	3.6	4.6
13	10.8	12.9	12.3
15	5.1	1	1

W6:

ac-ALALAWALALALALALWWG-ea

Ala #	DLPC	DMPC	DOPC
3	15.25	15.45	15.9
5	1.8	1.3	15.9
7	15.55	11.65	14.95
9	2.3	0	0
9	2.2	0	0.7
11	16	13.8	12
13	13.6	9.85	1.3
15	0	2.7	6.55

R2:

ac-ARALALALALALALALWWG-a

Ala #	DLPC	DMPC	DOPC
9	2.5	0.7	0
11	15.1	14.5	13.1
13	13	9.9	6.5
15	0	3.1	6.5

R6:

ac-ALALARALALALALALWWG-a

Ala #	DLPC	DMPC	DOPC
9	6	5.9	-
11	13.2	13.6	-
13	8.3	7.8	-
15	12.7	12.5	-

Table 3

Calculated peptide orientations of the three residue anchored WALP peptides in various lipids calculated using a semi static calculation model. *Where indicated ²H quadrupolar splitting values used are 3, 5, 7, 9, 11, 13 and 15 or 7, 9, 11, 13 and 15 respectively.

	W2 DLPC	W2 DMPC	W2 DOPC
S_{zz}	0.78	0.82	0.81
τ	3.0	4	4.3
ρ	125	190	206
RMSD	0.13	0.28	0.15

*Ala 3-15	W6 DLPC	W6 DMPC	W6 DOPC
S_{zz}	0.90	0.77	0.50
τ	6.3	6.0	15.0
ρ	243	252	264
RMSD	2.94	2.09	3.33

*Ala 7-15	W6 DLPC	W6 DMPC	W6 DOPC
S_{zz}	0.39	0.31	0.67
τ	55.7	58.0	6.3
ρ	245	242	280
RMSD	2.23	1.83	1.05

	R2 DLPC	R2 DMPC	R2 DOPC
S_{zz}	0.98	0.95	0.85
τ	11.7	8.7	6.3
ρ	247	252	263
RMSD	0.08	0.26	0.08

	R6 DLPC	R6 DMPC	R6 DOPC
S_{zz}	0.42	0.44	
τ	14.0	13.0	
ρ	337	334	
RMSD	0.05	0.16	

3.6 Figures

Figure 1

Deuterium spectra at the $\beta=0^\circ$ sample orientation with respect to the magnetic field. Peptide with third anchor W2, deuterium labelled alanine residues positioned at 13^(70%) and 15^(100%) (A,C,E) and 9^(50%) and 11^(100%) (B,D,F) in DLPC (A,B) DMPC (C,D) and DOPC (E,F) oriented lipid bilayers

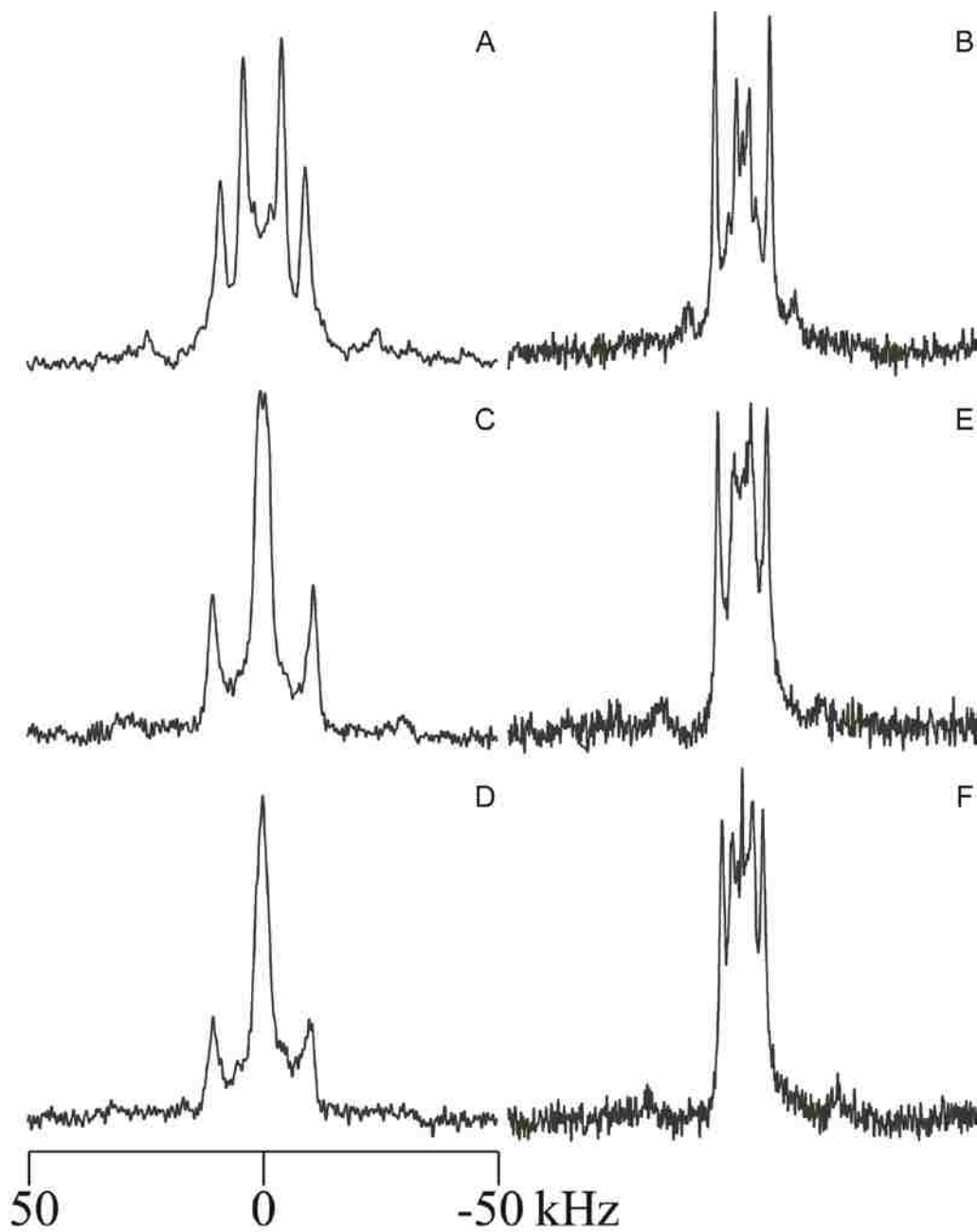


Figure 2

Deuterium spectra at the $\beta=0^\circ$ sample orientation with respect to the magnetic field. Peptide with third anchor W6, deuterium labelled alanine residues positioned at 13^(70%) and 15^(100%) (A,E,I), 9^(50%) and 11^(100%) (B,F,J), 3^(50%) and 5^(100%) (C,G,K) and 7^(100%) and 9^(50%) (D,H,L) in DLPC (A-D) DMPC (E-H) and DOPC (I-K) oriented lipid bilayers

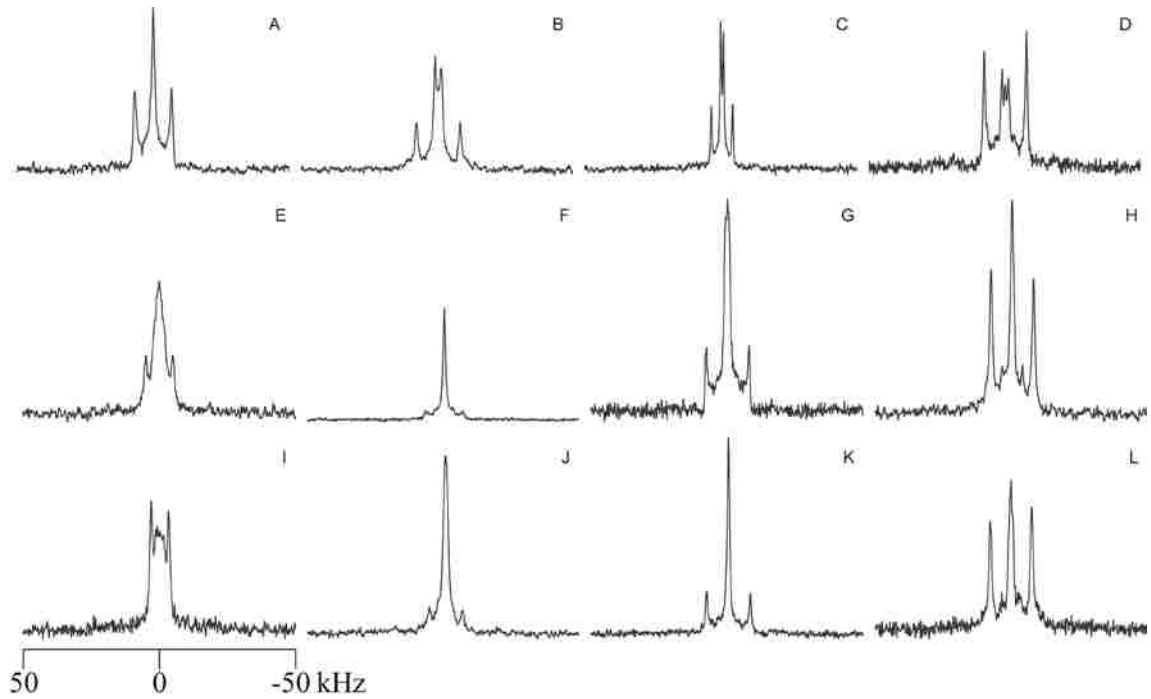


Figure 3

Deuterium spectra at the $\beta=0^\circ$ sample orientation with respect to the magnetic field. Peptide with third anchor R2, deuterium labelled alanine residues positioned at 13^(70%) and 15^(100%) (A,C,E) and 9^(50%) and 11^(100%) (B,D,F) in DLPC (A,B) DMPC (C,D) and DOPC (E,F) oriented lipid bilayers.

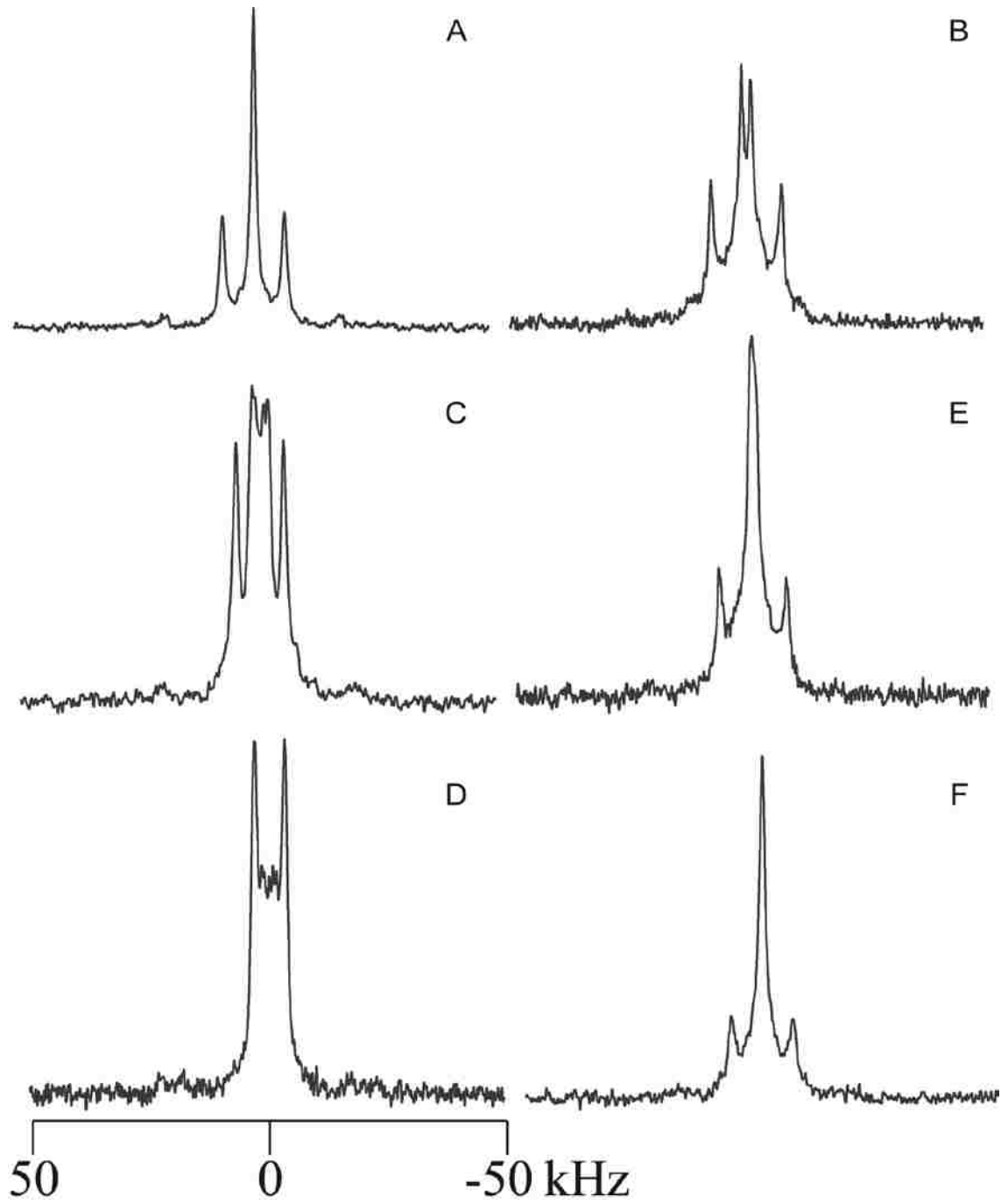


Figure 4

Deuterium spectra at the $\beta=0^\circ$ sample orientation with respect to the magnetic field. Peptide with third anchor W2, deuterium labelled alanine residues positioned at 13^(70%) and 15^(100%) (A,C,E) and 9^(50%) and 11^(100%) (B,D,F) in DLPC (A,B) DMPC (C,D) and DOPC (E,F) oriented lipid bilayers

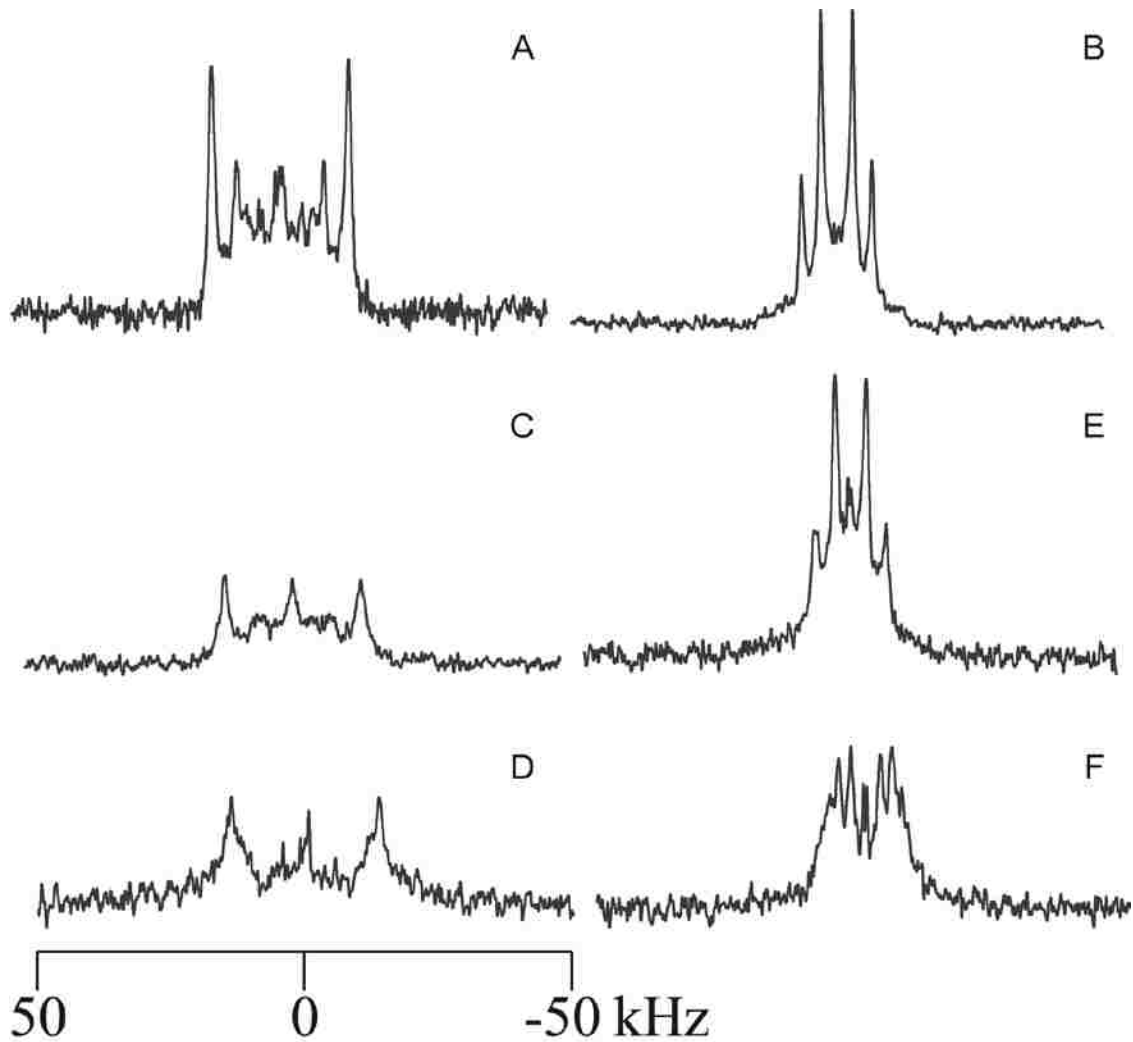


Figure 5

Helical wave plots for DLPC (A) DMPC (B) and DOPC (C) in which the waves corresponding to the various peptides are colored as follows: W2, black; W6, red; R2, green and R6 blue.

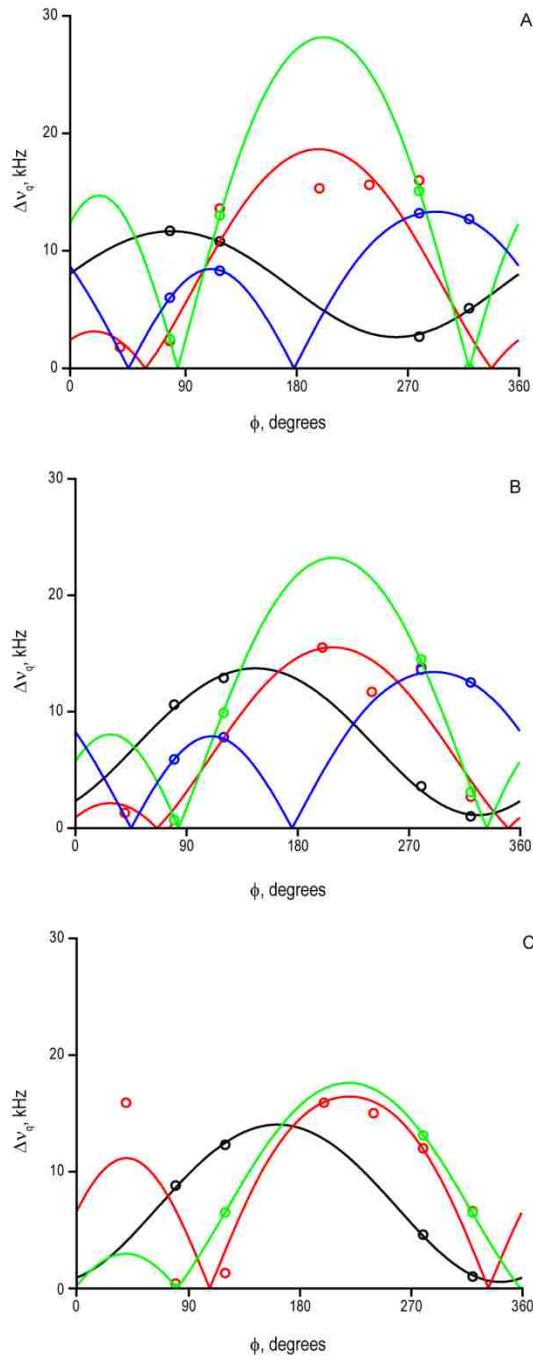


Figure 6

Tilt and rotational values obtained for C-anchored WALP and peptides with additional 3rd anchor. The different lipid systems are indicated as follows: DLPC (squares) DMPC (circles) DOPC (triangles) where as the different peptides are color coded according to the following scheme W2, black; W6, red; R2, green; R6, blue; and for reference C-anchored WALP, gray.

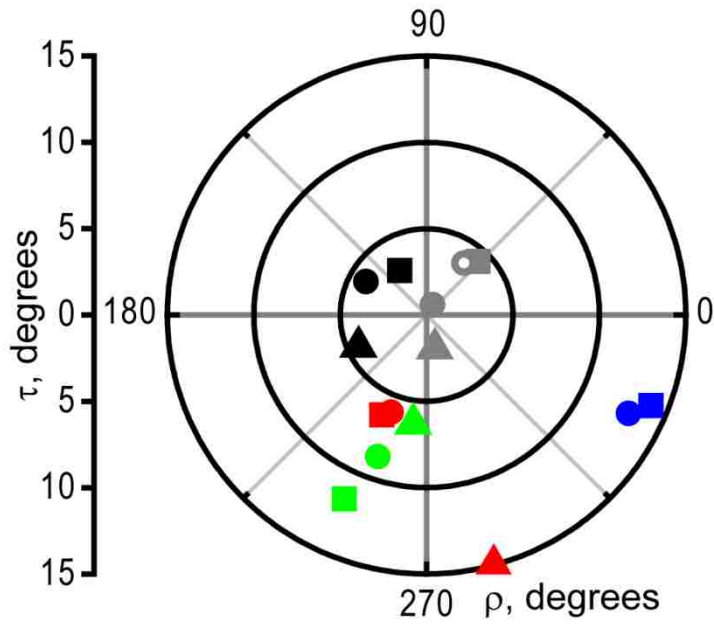
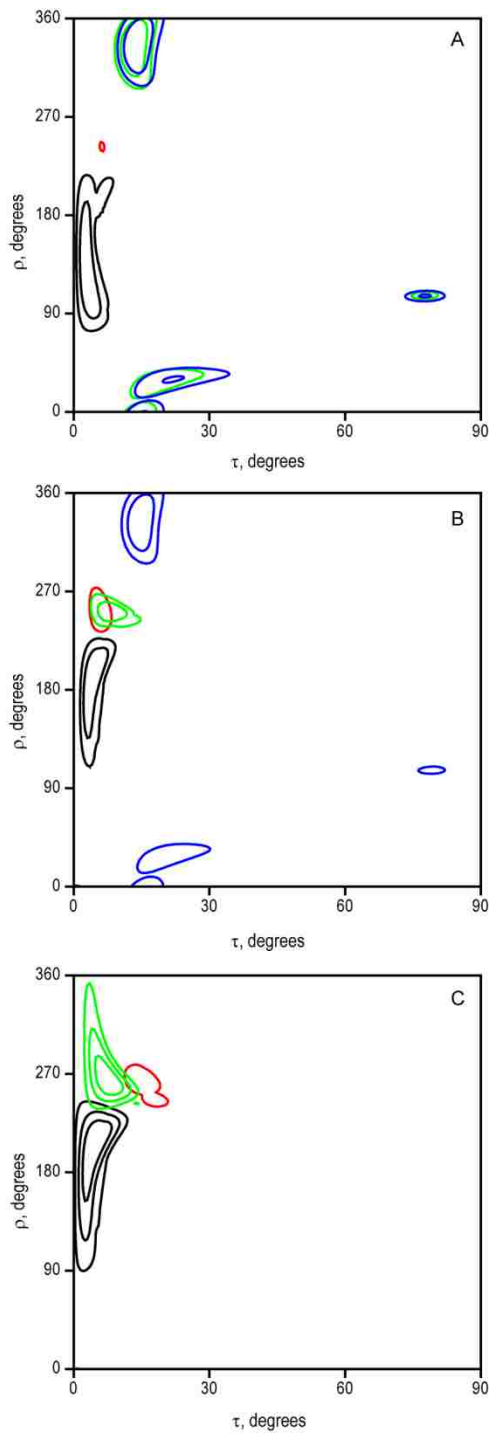


Figure 7

RMSD plots for DLPC (A) DMPC (B) and DOPC (C) in which the contour levels corresponding to the various peptides are colored as follows: W2, black; W6, red; R2, green and R6 blue. Contour levels shown are 1, 2, 3 kHz for A and B and 1, 2, 3 and 4 kHz for C.



CHAPTER 4

EFFECTS OF PROLINE INCORPORATION IN GWALP23

TRANSMEMBRANE PEPTIDES.

4.1 Introduction

When considering membrane proteins one often finds proline residues within transmembrane sequences of these proteins (Page et al., 2007). Important processes carried out by these proteins are, in part, reliant on the presence and positioning of particular transmembrane proline residues (Cordes et al., 2002; Decaffmeyer et al., 2008; Glukhov et al., 2007; Ulmschneider and Sansom, 2001; von Heijne, 1991). To further examine the structural consequences and functional properties resulting from proline positioning in TM sequences, it is of interest to study the effects of proline on model transmembrane sequences. For this purpose we have incorporated proline in GWALP peptides, resulting in GWALP23 L12P (acetyl-GGALWLALALAP¹²ALALALWLAGA-ethanolamide), and GWALP23 L14P (acetyl-GGALWLALALALAP¹⁴ALALWLAGA-ethanolamide). The GWALP series of peptides offers the significant advantage of having only one tryptophan anchor near each end of the TM sequence (Vostrikov et al., 2008). While proline has been characterized when two Trp anchors flank the TM sequence of the WALP19 model peptide (Thomas et al., 2009), the behavior of peptides having only single Trp anchors near each end often is more predictable and systematic with respect to the tilt angle and the lipid bilayer thickness (Vostrikov et al., 2010a; Vostrikov et al., 2010b).

The behavior of the native GWALP23 peptide, containing a leucine residue at position 12, in lipid bilayers is well defined (Vostrikov et al., 2010a; Vostrikov et al., 2008). To study the effects of proline incorporation on the behavior of GWALP23, we have specifically incorporated deuterium labeled alanine residues within the C terminal part of the peptide sequence, following the proline. Additionally, we incorporated ^{15}N labels throughout the central core (with the exception of Pro12), defined as the inter-tryptophan residues. When considering the helix breaking properties of proline, the N-terminal domain is expected to be the most affected, because the proline residue lacks an amino hydrogen and is incapable therefore to form a hydrogen bond with a carbonyl group of an amino acid four residues earlier. A solid-state NMR study of a related transmembrane peptide demonstrated this indeed to be the case (Thomas et al., 2009). The distortion introduced into the transmembrane helix by the proline, which effectively divides the continuous α -helix into two sections, is of interest to characterize, in terms of not only the helix kink angle but also the individual tilt magnitudes and directions for the N- and C-terminal domains. If sufficient data can be obtained, aspects of the segment dynamics also can be characterized, as one can expect the whole body motions of two segments to be coupled. For this reason, deuterium NMR data, obtained from the deuterated alanine residues in conjunction with the Geometric Analysis of Labeled Alanine (GALA) method, will be used together with ^{15}N - ^1H dipolar coupling values, from the ^{15}N labeled residues and the PISEMA experiment, to provide a combined analysis of the properties of the GWALP23-L12P helical segments.

When using a single NMR technique to obtain restraints for determination of peptide orientation, one of the more challenging aspects is acquisition of a sufficient number of data points for accurate sampling of the orientation of particular helical segments. The combined use of the ^{15}N and ^2H based solid-state NMR techniques enables a robust determination of the peptide behavior. Advantages are offered by both the complementary nature of these NMR techniques and the significant increase in number of data points obtainable per peptide segment as well as different sensitivity toward distinct motions (Holt et al., 2010). Considering that GWALP23 has a relatively long alpha-helical domain with only one anchoring residue on each side, this peptide is an apt candidate for such studies. The insertion of a proline residue into the transmembrane segment of GWALP23 is expected to preserve sufficiently long α -helical segments for determination of their orientations.

Previous work within our lab has shown that introduction of a proline residue in WALP19 (L10P) interrupts the helix and results in two segments with distinct orientations and a kink angle of about 20 degrees between them (Thomas et al., 2009). The presence of only single Trp anchors and the availability of ^{15}N data will enable us to obtain considerably more information for GWALP23-L12P. Small comparisons also will be made with regard to preliminary data for a second peptide, GWALP23-L14P.

4.2 Materials and methods

Materials Fmoc-amino acids and resin were obtained from and Advanced Chemtech (Louisville, KY). Isotope enriched ^{15}N Fmoc-amino acids, deuterium labeled alanine and ^2H -depleted water were from Cambridge Isotope Laboratories (Andover, MA) and Isotec (St. Louis, MO). Commercial L-alanine- d_4 was Fmoc-protected using Fmoc-ON-Succinimide, Nova Biochem (San Diego, CA), as described by ten Kortenaar *et al.* (ten Kortenaar et al., 1986). Ethanolamine and trifluoroethanol (TFE) were obtained from Sigma-Aldrich (St. Louis, MO). All Lipids (DH-o-PC, DLPC, DMPC, DM-o-PC and DOPC) were acquired from Avanti polar lipids (Alabaster, AL). Other solvents used were from EMD (Gibbstown, NJ).

Peptide synthesis was performed on a Perkin Elmer/Applied Biosystems (Foster City, CA) 433A synthesizer, using modified Fmoc-chemistry with extended coupling times and additional deprotection steps. Backbone- and side chain deuterated Ala or ^{15}N -amino acids were incorporated at specific residues during peptide synthesis. Using our dual labeling strategy, ^2H -labeled alanine was incorporated at 100% abundance at one residue and at a lower 50% abundance at another position in the sequence, in the same peptide (Vostrikov et al., 2008). Partial labeling, resulting in a lower percent labeling at the second selected position, was achieved by combining appropriate amounts of Fmoc-Ala- d_4 and Fmoc-Ala for a specific coupling step. During peptide synthesis a five-fold excess of Fmoc-amino acid was used for unlabeled and ^{15}N -labeled residues. Two-fold excess followed by a double coupling with five-fold excess Fmoc-amino acid was used for ^2H -labeled amino acids. Uncharged protecting groups were incorporated during synthesis

and after peptide synthesis: N-terminal acetylation to conclude the peptide synthesis, and C-terminal ethanolamide during subsequent ethanolamine cleavage. Cleavage cocktail consisting of ethanolamine, 20% in dichloromethane was used to introduce the C-terminal protecting group in concert with the release of peptide from the Wang resin. The reaction took place for 48 hours under constant agitation at 22 °C. The reaction was quenched using deionized water upon which the peptide precipitated. Precipitated peptide was centrifuged to form a pellet, which was lyophilized twice from 1 ml of acetonitrile/water (1:1, v/v). The purity of the peptide was evaluated via HPLC using a reversed phase Zorbax-C8 column, with a methanol-water gradient. The peptide identity was confirmed using MALDI mass spectrometry.

NMR samples were prepared using peptides denoted in Table 1. Mechanically oriented samples for deuterium NMR spectroscopy were prepared with a 1:40 peptide to lipid ratio using one of various lipids, DLPC, DMPC or DOPC. Magnetically oriented samples for both ^2H and ^{15}N NMR studies were prepared using a ratio of 1:80 peptide to long chain lipid (DMPC for deuterium studies or DM-o-PC for ^{15}N based studies; 61 μmol), in addition to short chain lipid DH-o-PC (19 μmol , $q=3.2$) present to enable bicelle formation. Peptide in TFE solution and lipids, in chloroform, were mixed together in appropriate amounts. Solvents were removed via evaporation under nitrogen flow and subsequent drying under vacuum (10^{-3} torr) for at least 36 hr. Formed lipid films were hydrated using 175 μl deuterium-depleted water at 45°C for 3 hours. To promote bicelle formation, the sample was subjected to cooling on ice followed by reheating to 45 °C several times until desired sample characteristics were obtained,

namely, a slightly opalescent solution with low viscosity at low temperature ($\sim 4^{\circ}\text{C}$) in which increase of temperature results in an increased sample viscosity. Samples were transferred to a sample vial and sealed in preparation for NMR studies. The procedures were the same for ^2H - and ^{15}N -labeled peptides in bicelle samples. The, more costly, behaviorally similar, ether lipids DM-o-PC and DH-o-PC were chosen for ^{15}N based studies based on their superior chemical stability, allowing for shipment to the national magnet lab located at the university of San Diego, California, where spectra for these samples were recorded.

For preparation of mechanically oriented samples a peptide-lipid mixture was prepared from 2 μmol peptide and 80 μmol lipid. Solvent was evaporated followed by drying under high vacuum (10^{-3} torr) for at least 24 hr. The peptide-lipid mixture was evenly distributed over 40 glass slides (4.8 x 23 x 0.07 mm, Marienfeld, Lauda-Königshofen, Germany) after dissolving in 95% methanol, 5% water. The slides with the peptide-lipid mixture were placed under vacuum for at least 48 hr after which the peptide-lipid films were hydrated using deuterium depleted water to a hydration level of 45% (w/w). The hydrated slides were stacked and sealed in a glass cuvette. To allow for formation and alignment of peptide containing lipid bilayers the samples were incubated for >48 hr at 45°C .

Solid-state ^{31}P NMR spectra of oriented samples were recorded at 50°C on a Bruker Avance 300 Spectrometer (Bruker Instruments, Billerica, MA) using a probe from Doty Scientific (Columbia, SC), to verify the formation of oriented lipid bilayers or bicelles.

To obtain quadrupolar splittings from ^2H -labeled alanines incorporated in the peptides, ^2H NMR spectra were recorded. For the acquisition of ^2H spectra a Bruker Avance 300 Spectrometer and Bruker Deuterium probe were used (Bruker Instruments, Billerica, MA). The spectra were recorded at 46.0 MHz, using a full phase cycling quadrupolar echo sequence (Davis et al., 1976), with a $4.5\ \mu\text{s}$ 90° pulse time, 90 ms interpulse delay and $125\ \mu\text{s}$ echo delay. The ^2H spectra were processed using exponential weighing function with a line broadening of 200 Hz. Alanine quadrupolar splitting values were assigned to the labeled alanine residues based on the distances between corresponding peak maxima and relative intensities associated with the isotopic abundances used in peptide synthesis.

For ^{15}N enriched residues, ^{15}N chemical shift - ^{15}N - ^1H dipolar coupling correlation spectra were recorded at a national magnet lab at University of California, San Diego. These PISEMA experiments were obtained using a Varian Inova 500 (^{15}N - ^1H) spectrometer and established pulse sequences (Cook and Opella, 2010; Marassi and Opella, 2000).

Following assignment of the quadrupolar splittings and subsequent assignment of PISEMA resonances, orientation of the peptide segments was determined. Using a combination of ^2H quadrupolar splitting values and ^{15}N - ^1H dipolar coupling values obtained for specific labeled residues and by considering peptide geometry restrains, we were able to calculate the orientations of the different peptide segments. We have performed these calculations both with a semi-static model and with explicit dynamic model that considers Gaussian distributions in tilt and direction of tilt.

The analysis using semi-static peptide dynamics involves a principle order parameter S_{zz} to estimate the overall peptide motion and resolve the apparent average peptide orientation. These calculations are based on the GALA analysis, equations [1], [3] and [5], as previously described (Strandberg et al., 2004; van der Wel et al., 2002). We now also incorporate ^{15}N - ^1H dipolar coupling values obtained from PISEMA spectra, equations [2], [4] and [5], to determine the best fit to the experimental data (Nevzorov et al., 2004). These calculations are performed using τ , ρ and S_{zz} as variable parameters. The analysis considers the ^2H quadrupolar splittings and/or ^{15}N - ^1H dipolar coupling values for the isotope labeled residues based on ideal α -helix geometry.

$$\Delta v_q = \frac{3}{2} QCC \cdot S_{zz} \left(\frac{1}{2} [3 \cos^2 \theta - 1] \right) \left(\frac{1}{2} [3 \cos^2 \beta - 1] \right) \left\langle \frac{1}{2} [3 \cos^2 \gamma - 1] \right\rangle$$

[Equation 1]

$$\Delta v_{HN} = DCC \cdot S_{zz} \left(\frac{1}{2} [3 \cos^2 \theta - 1] \right) \left(\frac{1}{2} [3 \cos^2 \beta - 1] \right)$$

[Equation 2]

$$QCC = \frac{3}{2} \frac{e^2 q Q}{h}$$

[Equation 3]

$$DCC = \frac{\mu_0 \gamma_N \gamma_H \hbar}{4 \pi r_{N-H}^3}$$

[Equation 4]

$$\theta = f(\tau, \rho, \varepsilon_{//})$$

[Equation 5]

The quadrupolar splitting, equation [1], depends upon the static coupling constant, equation [3], and is 168 kHz, which is reduced further by 1/3 to 56 kHz for C-D₃ groups (γ term in equation [1]), (Thomas et al., 2009; van der Wel et al., 2002), the orientation angle θ for the alanine C $_{\alpha}$ -C $_{\beta}$ bond with respect to the bilayer normal, and the macroscopic sample orientation angle β for the bilayer normal with respect to the external magnetic field. The peptide geometry is reflected in angle $\varepsilon_{//}$, 59.4°, the angle between peptide helix axis and the C $_{\alpha}$ -C $_{\beta}$ bond vector for deuterium labeled alanine residues. The angle θ between the bond vector and the bilayer normal depends on the peptide geometry ($\varepsilon_{//}$) and the orientation of the peptide's helix axis (τ and ρ). While earlier analysis (van der Wel et al., 2002) involved searching for appropriate values of $\varepsilon_{//}$, current procedures fix $\varepsilon_{//}$ at the known value of 59.4° and vary S_{zz} to obtain a best fit.

The dipolar coupling values are dependent on the dipolar coupling constant, equation 4 (11.335 kHz) (Ketchum et al., 1996), and the angle θ between N-H bond and the applied magnetic field, which is dependent on the peptide orientation with respect to the bilayer normal, τ and ρ , and the $\varepsilon_{//}$ value. The $\varepsilon_{//}$ angle is in this case 14°, the angle between the peptide helix axis and the N-H bond vector for ¹⁵N labeled residues.

Using these equations and parameters, the peptide orientation was calculated by considering the best fit (lowest RMSD value between calculated and observed quadrupolar splittings) for a range of peptide orientations. Helix tilt τ and rotation ρ are determined in relation to C_α of the first amino acid (Gly¹) of the peptide. To calculate a kink angle (κ) introduced between two α -helical segments upon proline incorporation, we determine the difference in rotation between the N and C terminal segments and account for the difference in tilt found for each of these segments, Equation 6 (Daily et al., 2008).

$$\cos(\kappa) = \sin(\tau_N) \sin(\tau_C) \cos(\Delta\rho) + \cos(\tau_N) \cos(\tau_C)$$

[Equation 6]

In addition to the semi-static model we have also performed calculations considering more peptide extensive dynamics, accounting for Gaussian distributions in peptide tilt and rotation ($\sigma\tau$, $\sigma\rho$). In this analysis a principle order parameter is set to 0.88 to account for internal peptide dynamics, and a best fit (RMSD) for peptide tilt and rotation, accounting for fluctuations in both tilt angle and direction (rotation) with a Gaussian distribution, is modeled to the experimentally observed data. These analyses were performed in similar manner to those described by Strandberg et al. (Strandberg et al., 2009).

4.3 Results

After peptide synthesis, reaffirmation of peptide molecular weight and isotope enrichment via mass spectrometry (Figure 1) and determination of sufficient peptide purity (>95%), Figure 2, peptides were incorporated into mechanically or magnetically aligned lipid bilayers.

Oriented samples were prepared using peptides containing specific deuterated alanine residues in the C-terminal segment. To confirm alignment of the bilayers ^{31}P NMR spectra have been recorded prior to ^2H measurements; representative spectra are displayed in Figure 3A. Using the ^2H NMR spectra (Figure 3B-C), quadrupolar splitting values were assigned to the corresponding alanine residues based on relative signal intensity, bearing in mind the isotope abundance used for the particular labeled residues; see Table 2.

Bicelle samples were prepared using ^{15}N enriched leucine and alanine in positions 13 to 17 C-terminal to the proline, or in positions 5 to 11 and 13 to 18 on either side of the proline residue. PISEMA spectra were recorded at the national magnetic laboratory at the University of California, San Diego for the ^{15}N samples. Resonance peaks were assigned (Figure 4) based on peptide geometry, which indicates the relative distribution of resonances from labeled residues on a helical wheel, and correlation to assignments made during the deuterium studies. Dipolar coupling values were recorded (Table 3) for the labeled residues and used in subsequent analysis of the orientation of peptide segments.

For peptides in DMPC bilayers with small amount of DH-o-PC to ensure bicelle formation, the orientations of the two segments of the peptide were determined using a combined analysis in which both ^2H quadrupolar and ^1H - ^{15}N dipolar coupling values were used. The analysis is based on calculation models in which the theoretical quadrupolar and dipolar waves together most closely approximate the values found experimentally, as determined by a root mean squared deviation. We have determined the average apparent peptide orientations using both semi-static and Gaussian dynamic analysis (see materials and methods section). Those results are listed in Table 4. Our results indicate a tilt of the N-terminal segment of about 34° for the semi-static model, or a closely similar value of 40° for the Gaussian analysis, with a corresponding $\sigma\tau$ of only 2° . The tilt observed for the C-terminal segment is 27° for the semi-static model, or a similar value of about 29° with a $\sigma\tau$ of 12° for the converged Gaussian analysis. The direction of the peptide tilt of each of these segments is the same for both analyses, namely 269° for the N terminal segment and 307° for the C-terminal segment (relative to $\text{Gly}^1 \text{C}_\alpha$). The Gaussian analysis indicates substantial $\sigma\rho$ values of about 50° for the N-terminal segment and about 24° for the C-terminal segment. For comparison, RMSD plots for have been provided for both the semi-static and Gaussian methods (Figure 5), as well as a plot for $\sigma\tau$ and $\sigma\rho$ values (Figure 6).

Using the orientations determined for the segments on each side of the proline residue, we were able to calculate a kink (κ) angle introduced into the peptide as described in equation [6]. The κ value determined for this peptide based on the semi-static analysis is $\sim 20^\circ$ whereas the κ determined for the Gaussian analysis is $\sim 24^\circ$.

Based on peptide geometry around incorporated proline residues, in which distortion is more prominent N-terminal to the proline, we have adopted a deuterium labeling strategy starting within the C-terminal segment. Analysis of the C-terminal segment in lipids other than DMPC is somewhat less straightforward because ^{15}N data are not (yet) available (Table 5). For analysis of the peptide positioning in DLPC and DOPC, we do not yet have well characterized bicelles representing these lipids. To increase somewhat the size of the ^2H data set, we have included a peptide variation in which a substitution (L16A) provides an additional data point. We have shown previously that this type of substitution often has only a small effect on the helical properties of the peptide segment and therefore should fit into the helical wave and provide valuable additional quadrupolar splitting values (Thomas et al., 2009). As previously, also in this study we have incorporated a control label on another previously labeled residue to check for possible changes in conformation as a result of the substitution that was made. The control residue 15 changed little (Table 2) when the L16A substitution was introduced.

We also tested whether the C-terminal segment remained helical through a deuterated Ala²¹ residue. In parallel studies within our lab it has been determined that residues falling outside the region between the anchoring Trp residues do not extend the helical conformation found within the transmembrane part (Vostrikov et al., 2010a). We find a similar result here. As a consequence we must discard the data point obtained for Ala 21 since it will not be representative of the conformation of the C-terminal helical segment. For illustration purposes, we show data points for residue A²¹ on the helical wheel plots (Figure 5); however they have not been incorporated in the analysis. To further illustrate

that incorporation of data obtained from Ala 21 is not feasible, one should note the significant increase in RMSD obtained when this data point is included in the analysis (Table 5). With the small number of data points, a dynamic analysis is not feasible at this time. The semi static analysis suggests that the C-terminal segment exhibits a rather large tilt angle with respect to the membrane normal in both DLPC and DOPC (table 5). The analysis remains somewhat uncertain, as analysis using only three data points suggests a C-terminal tilt of about 77° in DLPC and 76° in DOPC. When the L16A substitution is included as a fourth data point, the apparent tilt for the C-terminal segment drops to about 24° in DLPC and 50° in DOPC.

Since we have not yet obtained the orientation of the N-terminal segment of GWALP23-P12 in DOPC or DLPC, we cannot determine the magnitude of the proline-induced kink in these lipid bilayers.

Finally, we have initiated work with a P^{14} peptide and have determined the quadrupolar splittings for the two of the C-terminal Ala residues within GWALP-P14. The number of data points is not yet sufficient to define a segment tilt. The quadrupolar splitting values nevertheless do indicate a deviation in orientation of the C-terminal segment as compared to GWALP23-P12 in the same lipids. The changes are especially evident in the shorter lipids.

4.4 Discussion

Using $^{15}\text{N}/^{15}\text{N}-^1\text{H}$ PISEMA and ^2H based solid-state NMR methodology we have been able to calculate a kink angle and the average apparent orientations of both ends of a proline containing GWALP peptide in lipid bilayers of DM-o-PC and DMPC, respectively. Using assignments made for the resonance peaks in the PISA helical wheel and assignment of the quadrupolar splittings to particular deuterium labeled residues, we were able to obtain sufficient number of data points, $^1\text{H}-^{15}\text{N}$ dipolar coupling and ^2H quadrupolar splitting values, to determine the orientations of both the N-terminal and the C-terminal segments, on either side of the proline in the GWALP23-P12 sequence. Based on the orientations of these segments, one can determine their positions relative to one another, that is to say the kink, κ , formed in the peptide backbone by the proline residue. In addition to the difference in tilt magnitude $\Delta\tau$ between the segments it is also crucial to know the rotation difference $\Delta\rho$ between the segments on either side of the proline, since these values together determine κ .

In addition to calculation of the peptide tilt and rotation, simple visual observation of helical wheel representations with respect to the obtained PISEMA spectra provide a striking confirmation of the kink introduced by the proline. This can be recognized as there are two distinct sets of continuous resonances that fit to separate helical wheel patterns, Figure 4.

As discussed before, the calculated tilt and rotation of the segments have been determined using both a semi-static model with a principal order parameter and a dynamic model that

incorporates two motion parameters ($\sigma\tau$ and $\sigma\rho$). Considering the semi-static model, the peptide orientation consists of a 34° tilted N-terminal segment connected to the 27° tilted C-terminal segment via a 20° kink angle. The kink angle between the segments also reflects the $\sim 40^\circ$ difference in rotation for the two segments, 269° and 307° respectively. Considering the dynamic Gaussian model, we calculate a 40° tilted N-terminus connected to the 29° tilted C-terminus via a 24° kink angle. Overall, the agreement is quite good between the two models for the analysis, with both of them giving a kink angle of about 20° - 24° and a swivel angle of about 38° - 40° . The magnitude of the kink angle also is similar to the value of 19° determined previously for WALP19 in DOPC (Thomas et al., 2009).

In addressing the dynamic model one should note, nevertheless, that the peptide dynamics have been calculated independently for each of the individual segments. We have currently not addressed the inter-segment dynamics, $\sigma\kappa$, or the effect that a connection to another segment could impose, e.g. restriction of movement for one terminus because it is connected to the other. We can speculate that restriction of one of the termini might result in a decrease of each segment's preferred range of motion. However, when considering the whole body dynamic motion (that of the two segments combined) there might be a net increase in motion, perhaps due to the introduction of $\sigma\kappa$, variation in the swivel angle.

In comparison to previous studies on the proline-containing WALP19-P10 in DOPC lipid bilayers, we find a similar κ angle, 20 - 23° versus 19° , but significantly larger τ angles for each of the proline flanking segments, namely 34 - 40° and 27 - 29° versus 7° and 11.9° ,

respectfully (Thomas et al., 2009). The greater hydrophobic length of GWALP23-P12 probably accounts for the larger segmental tilt values, compare to WALP19-P10, while the proline-induced kink angle remains remarkably similar.

Concerning the biological relevance, we would like to note that an array of biologically occurring proline-containing transmembrane helices display a wide range of proline-induced kink angles of 0-70° (Cordes et al., 2002). Here we demonstrate a prime example of how the use of PISEMA studies in conjunction with solid state deuterium NMR provides an elegant means to determine the relative orientations of transmembrane helical segments on either side of a localized distortion. The method should prove relevant for investigating such distorted α -helical biologically relevant peptide sequences containing a helix breaking residue such as the here investigated proline and also glycine, also known for its helix breaking properties.

In addition to the studies of GWALP23-P12 in bilayers with myristoyl acyl chains in which we combine ^2H and ^1H - ^{15}N solid state NMR techniques, we have performed preliminary ^2H studies using shorter and longer lipid systems. The preliminary results indicate that the C-terminal segment of the peptide also is tilted by a relatively large amount in these lipid systems. Future studies will be needed to address the orientation of the N-terminal segment. Complementary studies using PISEMA methodology and solution NMR experiments in SDS micelles could provide additional insights.

The experiments with GWALP23-P14 are at an early stage. Based on the currently available data, we can state that the tilt of the C-terminal segment of this peptide, as expected, has changed its orientation upon the shift of the proline residue in the sequence

by two positions. Additional analysis using studies that are either ^2H based, ^{15}N based, or both, will be needed to reveal the orientation of the N-terminal segment, the C-terminal segment and the magnitude of the proline induced kink.

The studies presented here attest to the fact that resourceful application of various solid state NMR techniques provides means for a robust analysis of structures with biological relevance. The combined analysis of ^2H and ^{15}N NMR spectra enabled determination of a proline-induced kink angle in a designed model peptide. The biological occurrence of transmembrane proline-containing peptides is sufficiently common that is important to understand the implications of presence of a proline residue on the structure, dynamics and positioning of a transmembrane sequence. We find that upon introduction of proline in to a previously “ideal” α -helix of GWALP23 a moderately large kink is introduced, and the peptide segments on either side of the proline both adopt a significant tilt with respect to the membrane normal, whereas the peptide originally had a moderately small tilt of only about 9° in DMPC (Vostrikov et al., 2010a). For biologically relevant protein domains, such effects on peptide orientation could have severe consequences, especially considering that structure and function are tightly intertwined. As a result, supported by our studies, we note that serious effects on transmembrane protein properties and therefore even cellular functions could result from the introduction or elimination of specific transmembrane proline residues.

4.5 Tables

Table 1

Sequence of peptides used in this work.

A

GWALP23	L12P	acetyl-GGALWLALALAP <u>P</u> ALALALWLAGA-ethanolamide
GWALP23	L12P L16A	acetyl-GGALWLALALAP <u>P</u> ALAAALWLAGA-ethanolamide
GWALP23	L12P	acetyl-GGALWLALALAP <u>P</u> ALALALWLAGA-ethanolamide
GWALP23	L14P	acetyl-GGALWLALALALAP <u>P</u> ALALWLAGA-ethanolamide

B

GWALP23	L12P	acetyl-GGALWLALALAP <u>P</u> ALALALWLAGA-ethanolamide
GWALP23	L12P	acetyl-GGALWLALALAP <u>P</u> ALALALWLAGA-ethanolamide

Table 2

Observed quadrupolar splitting values in kHz obtained from ^2H MNR spectra (see figure 3 B-C)

GWALP23 L12P (and L16A) peptides

Ala#	DLPC	DMPC	DOPC
13	28.5	26	14.3
15* ^a	28.3	27.8	25.5
15* ¹³	28.5	27.5	25.0
15* ¹⁶	28.0	28.0	25.9
16	12.3	0.0	8.1
17	8.2	12.7	10.2
21	7.2	2.2	6.0

GWALP23 L14P

Ala#	DLPC	DMPC	DOPC
15	13.5	11.7	8.3
17	20.7	16.3	15.5

*^a Average quadrupolar splitting values for residue 15

*¹³ Quadrupolar splitting for residue 15 obtained from peptide with residue 13 also is labeled

*¹⁶ Quadrupolar splitting for residue 15 obtained from peptide with residue 16, a L16A substitution, is also labeled

Table 3

Dipolar coupling and ^{15}N chemical shift values obtained corresponding to resonance peaks in the PISEMA spectrum (see figure 4).

Residue #	^1H - ^{15}N dipolar coupling, kHz	^{15}N chemical shift, ppm
6	0.8	111.0
7	1.5	89.8
8	2.9	95.6
9	1.6	118.5
10	0.4	103.0
11	1.2	96.2
13	2.6	107.5
14	1.5	98.5
15	2.5	85.5
16	3.5	94.0
17	2.3	109.3
18	1.9	88.5

Table 4

Calculated peptide orientation of the N- and C-terminal segments flanking the central Proline 12 residue using a dynamic (Gaussian) and semi static calculation model.*

GWALP23-P12, N-terminus in DMPC

Model		Gauss	Szz
Tau0	°	40	34
Rho0	°	269	269
RMSD	KHz	0.227	0.255
σ Tau	°	2	-
σ Rho	°	50	-
S_{zz}		0.88*	0.63

GWALP23-P12, C-terminus in DMPC, and apparent kink.

Model		Gauss	Szz
Tau0	°	29	27
Rho0	°	307	307
RMSD	KHz	0.388	0.385
σ Tau	°	12	-
σ Rho	°	24	-
S_{zz}		0.88*	0.78
Kappa		23.7	20.2

Dynamic analysis using a fixed internal order parameter, accounting for intra molecular motion, allowed for determination of τ , ρ and whole body dynamics $\sigma\tau$ and $\sigma\rho$. Semi-static analysis determines the best fit, lowest RMSD, for peptide orientation including variable τ and ρ in addition to a variable order parameter, S_{zz} , accounting for whole body dynamics and internal peptide motion. N-terminal analysis was based on ^1H - ^{15}N dipolar coupling values obtained for residues 6-10. C-terminal analysis was based on both ^1H - ^{15}N dipolar coupling values for residues 13-18 and ^2H quadrupolar splitting values for residues 13, 15 and 17, in which weighting factors of 1 for the deuterium data and 0.5 for the ^1H - ^{15}N dipolar couplings was applied.

Table 5

Best fit results obtained for semi static analysis of the C-terminal section of GWALP23P12 in DLPC and DOPC.

# Data points*		DLPC	DOPC
5	Szz	0.73	0.6
	Tau	22.0	76.3
	Rho	333	218
	RMSD	2.30	0.77
4	Szz	0.68	0.59
	Tau	77.0	75.7
	Rho	87	217
	RMSD	0.31	0.51
3	Szz	0.76	0.37
	Tau	23.7	50.3
	Rho	325	206
	RMSD	0.04	0.05

*Analysis using 5 data points incorporated quadrupolar splitting values corresponding to residues 13, 15, 16, 17 and 21, 4 datapoint analysis reported used data from residues 13,15,16 and 17 and the 3 datapoint analysis used 13,15 and 17.

4.6 Figures

Figure 1

MALDI Mass spectra representative of GWALP23P12 peptides after peptide cleavage.

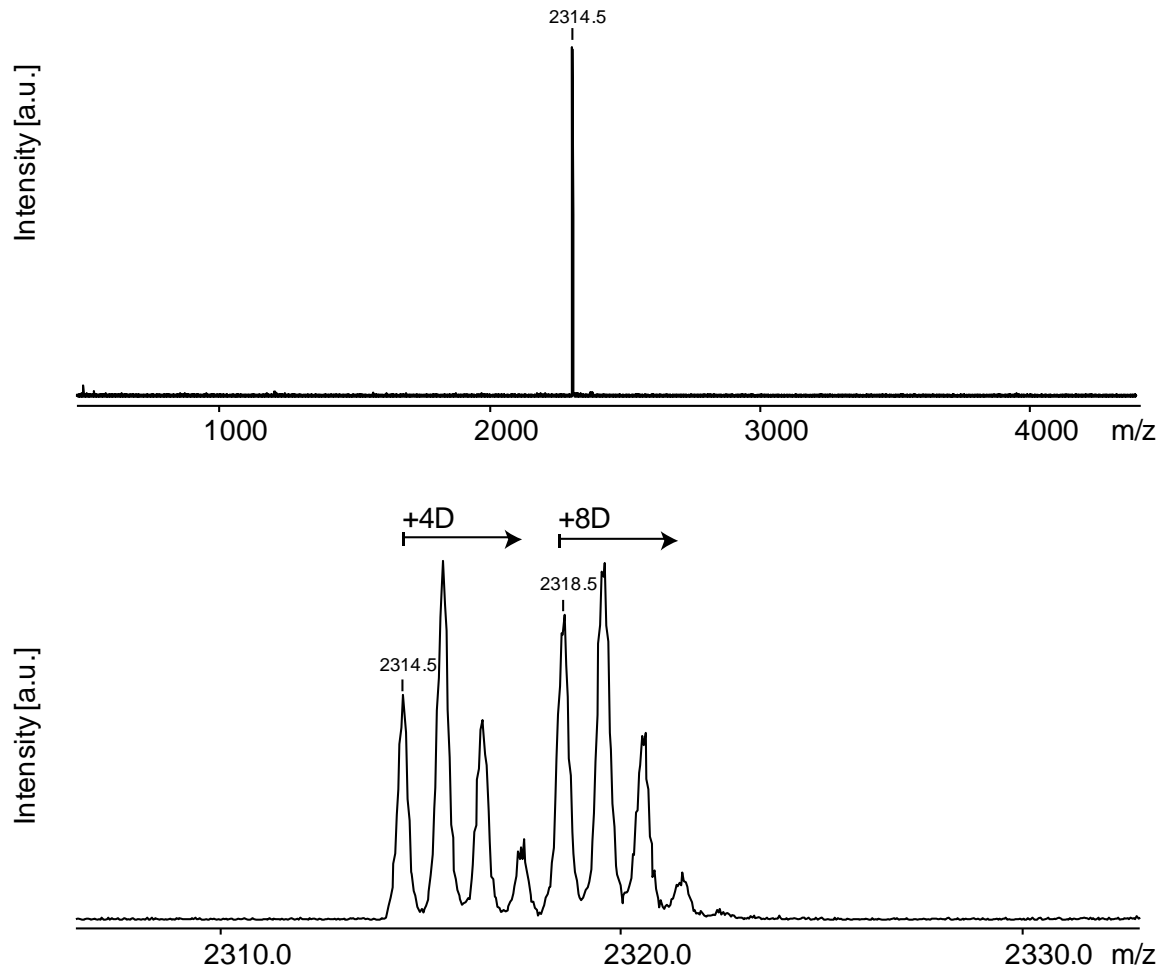


Figure 2

HPLC spectra representative of GWALP23P12 peptides after peptide cleavage.

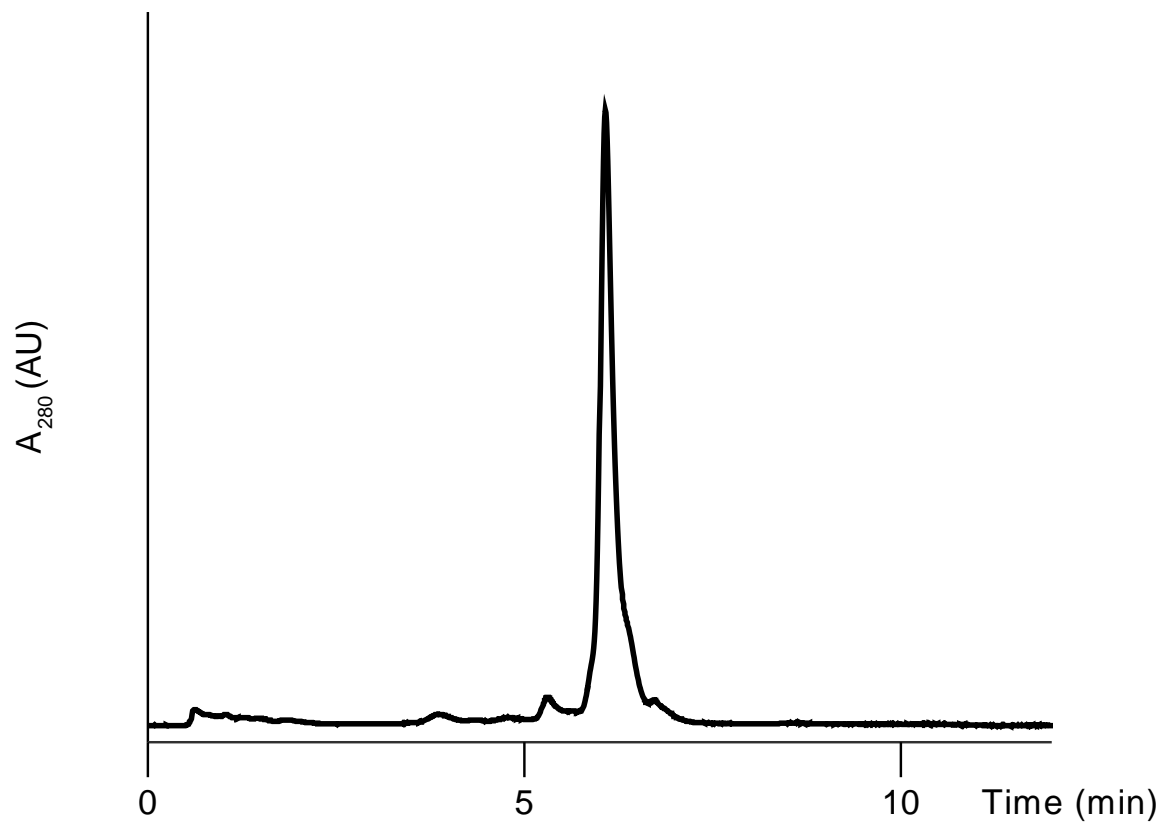


Figure 3

A)

Representative ^{31}P NMR spectra, at $\beta=0^\circ$ (right) and $\beta=90^\circ$ (left) orientation with respect to the magnetic field.

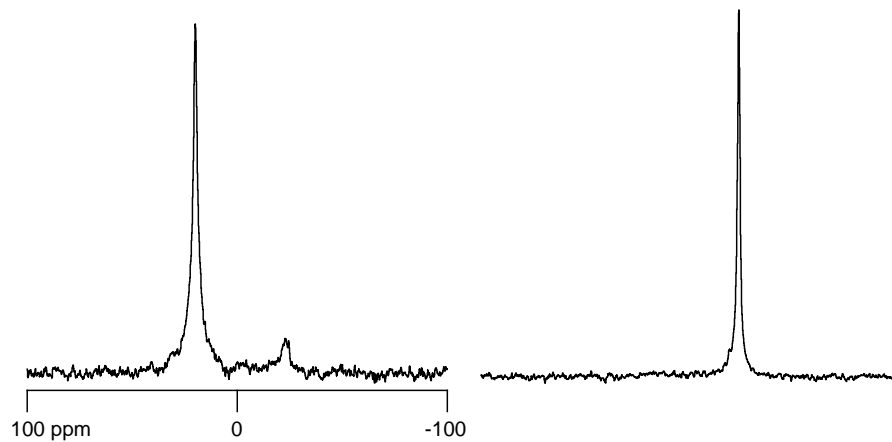
B)

GWALP23P12 ^2H NMR spectra in oriented bilayers of DLPC, DMPC and DOPC at orientation of $\beta 90^\circ$ with respect to the magnetic field. Alanine d_4 labeled residues are indicated on the left.

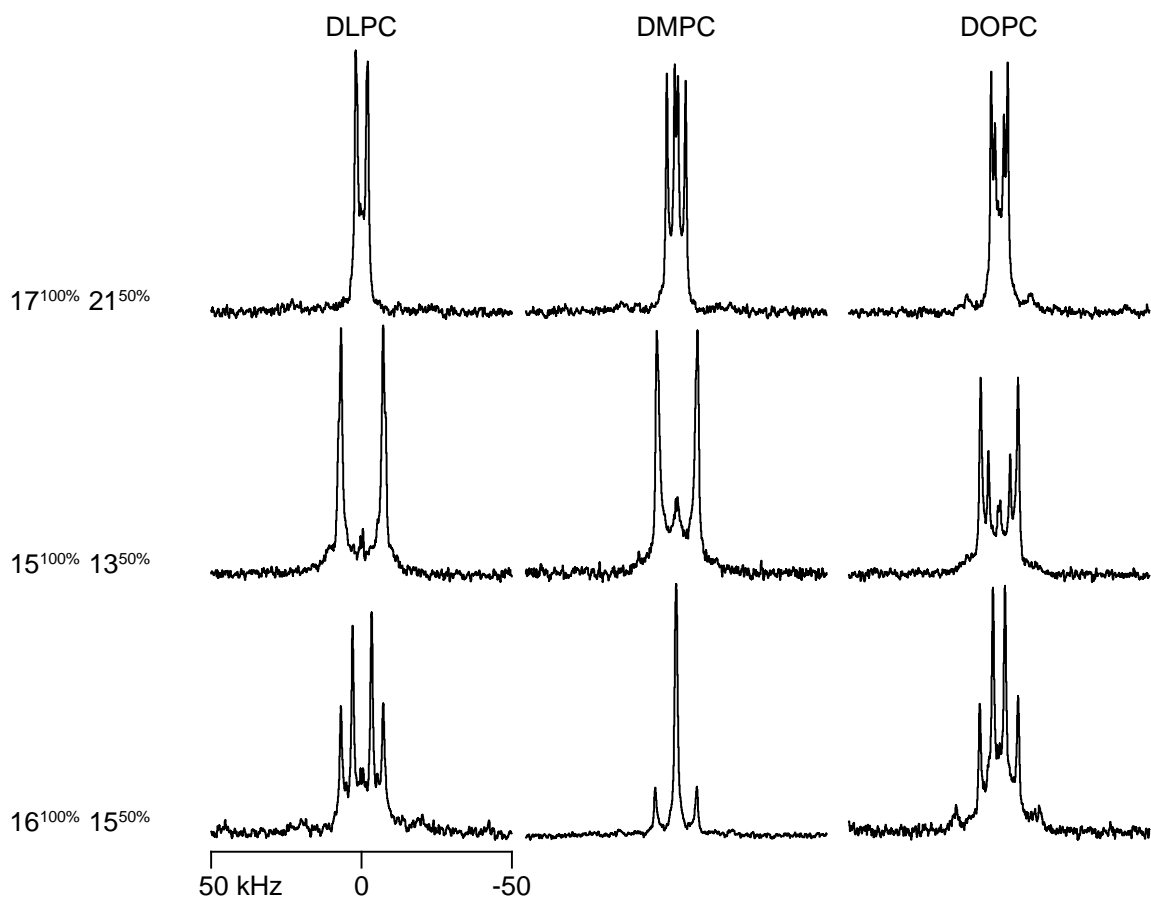
C)

GWALP23P12 ^2H NMR spectra in oriented bilayers of DLPC, DMPC and DOPC at orientation of $\beta 0^\circ$ with respect to the magnetic field. Alanine d_4 labeled residues are indicated on the left.

A



B



C

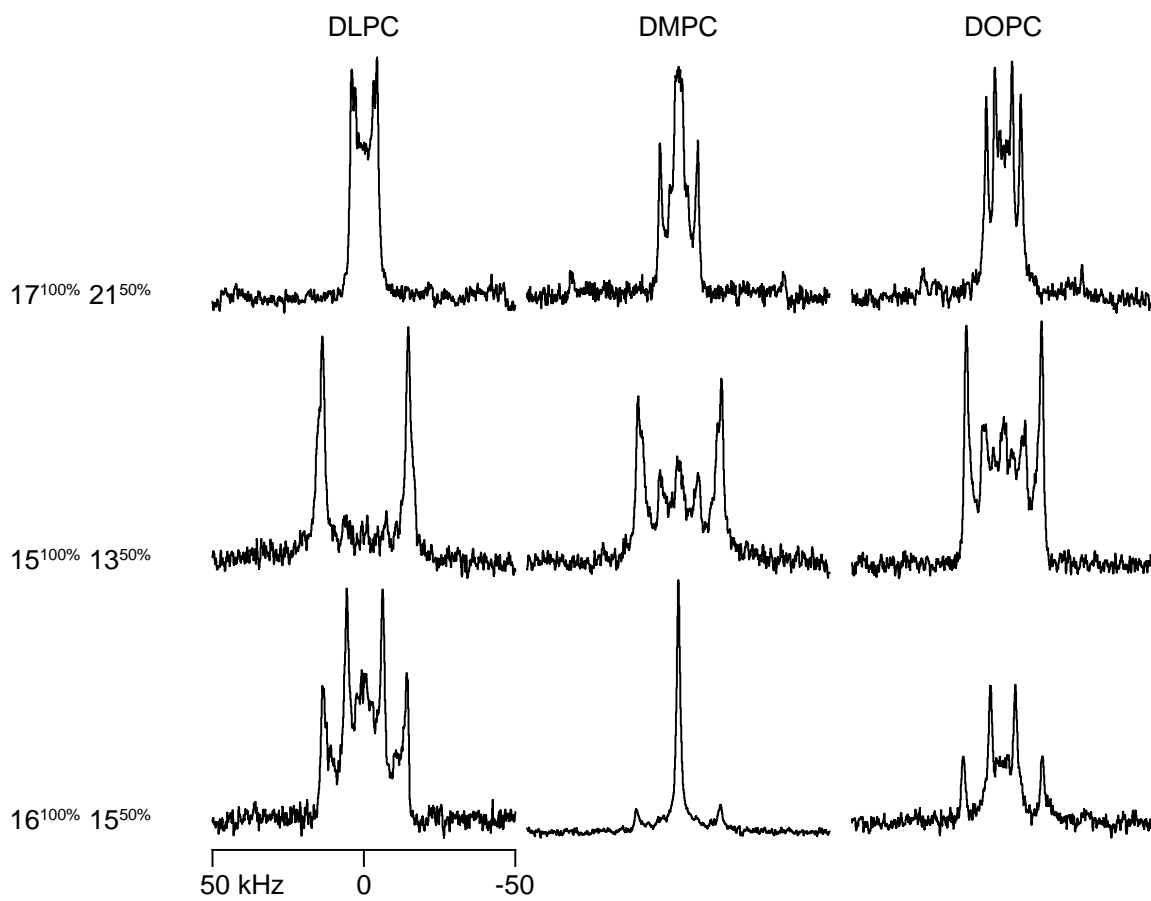


Figure 4

PISEMA spectra of GWALP23P12 peptides in magnetically oriented DM-o-PC/DH-o-PC bicelle bilayers. Resonances corresponding to the labeled residues are indicated in spectra A and B for the different labeling schemes. Helical wheel patterns corresponding to the orientation of the peptide segments, as determined via semi static analysis, are depicted in C and D, representing a N-terminal tilt of 34° with a S_{zz} of 0.63 and a C-terminal tilt of 27° and 0.78.

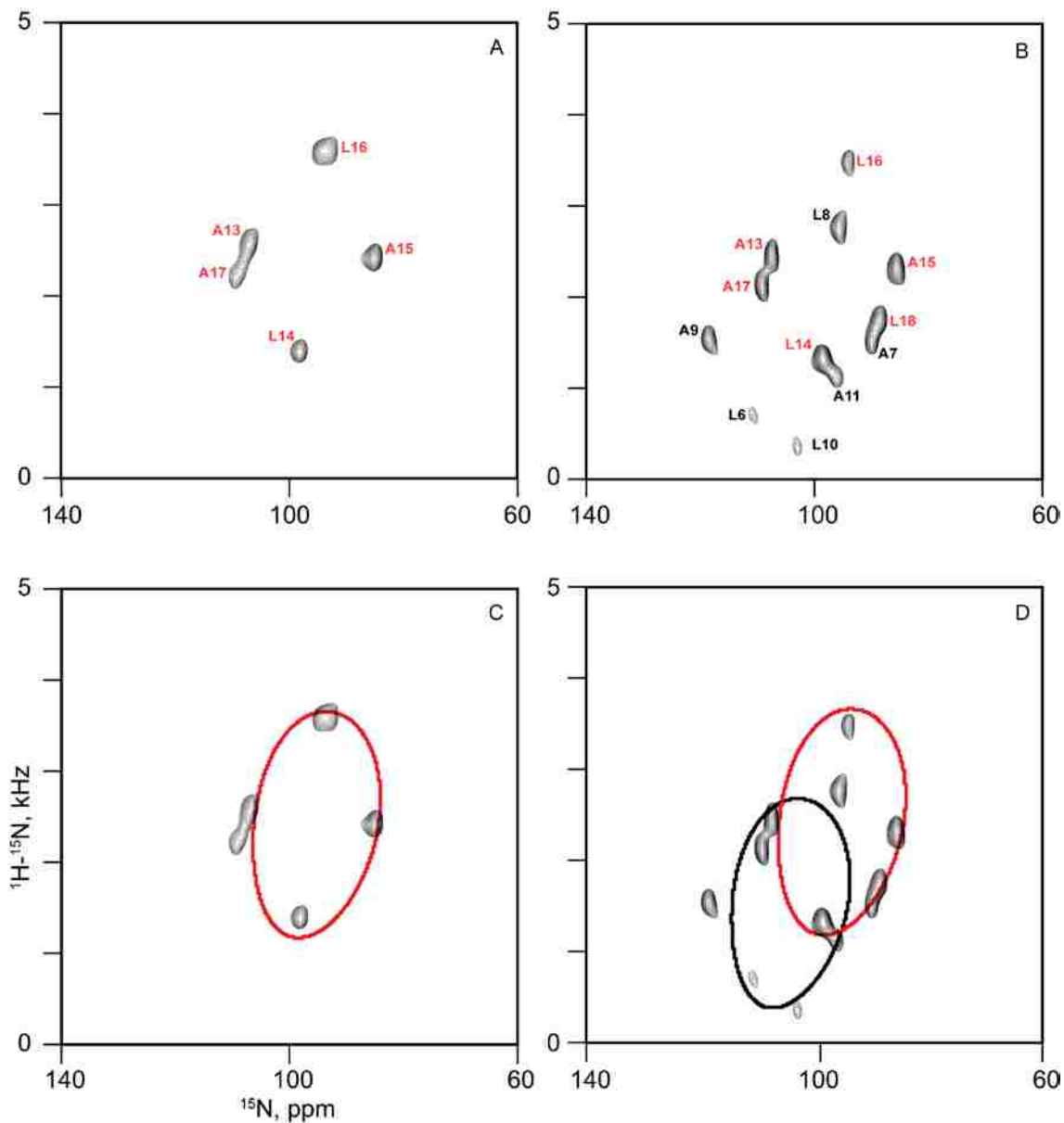


Figure 5

Calculated helical and dipolar wave plots for GWALP23P12 in oriented DLPC (A), DMPC (B, D, E) and DOPC (C) bilayers for the C-terminal (A-D) and N-terminal segment (E). Wave functions based on semi static calculations are represented with a solid line (A-E), wave functions based on Gaussian calculations are represented with a dashed line (B, D, E). Observed quadrupolar splittings indicated by open symbols have been represented in the calculations whereas solid symbols represent data that have been excluded from the calculation.

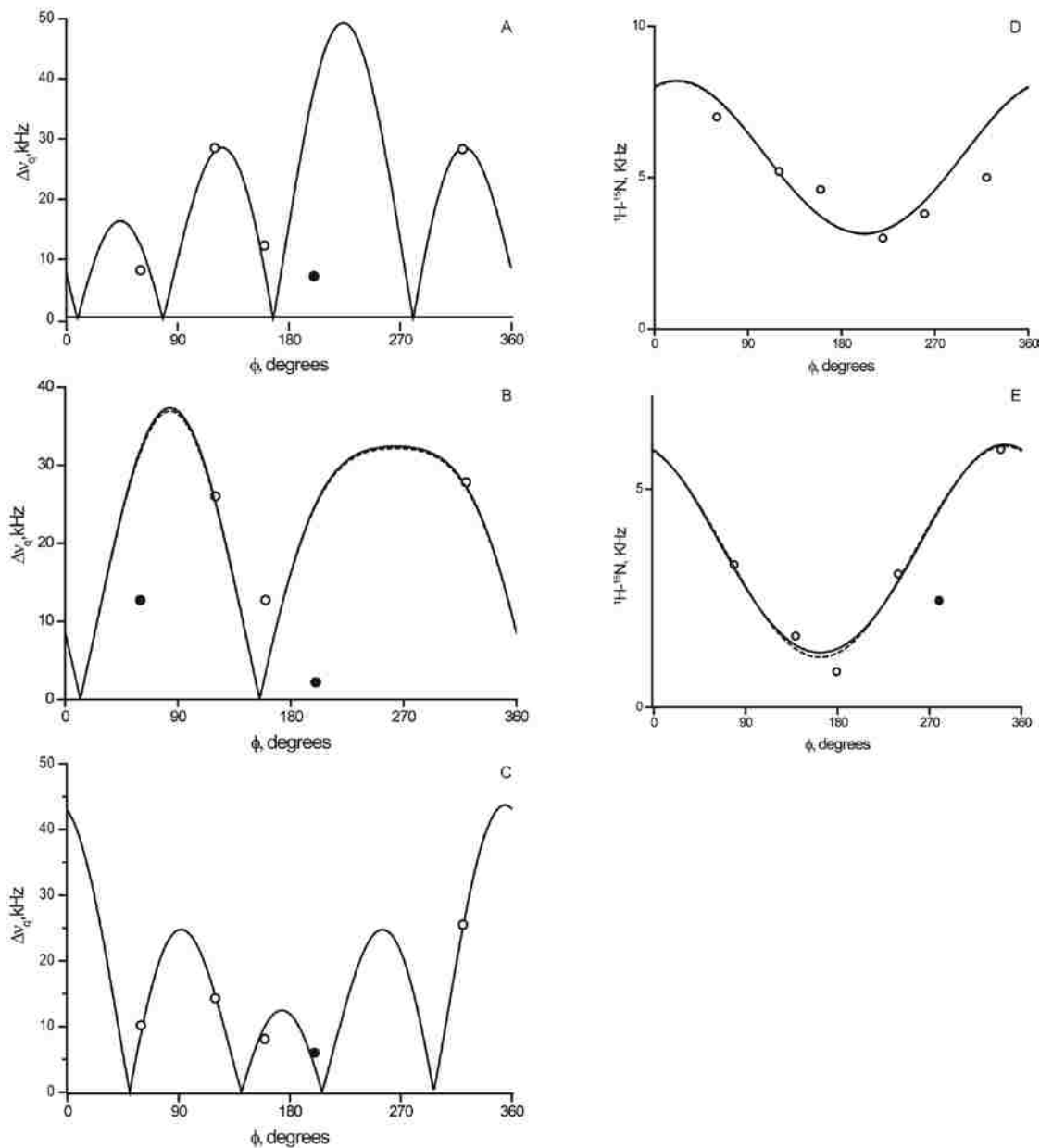
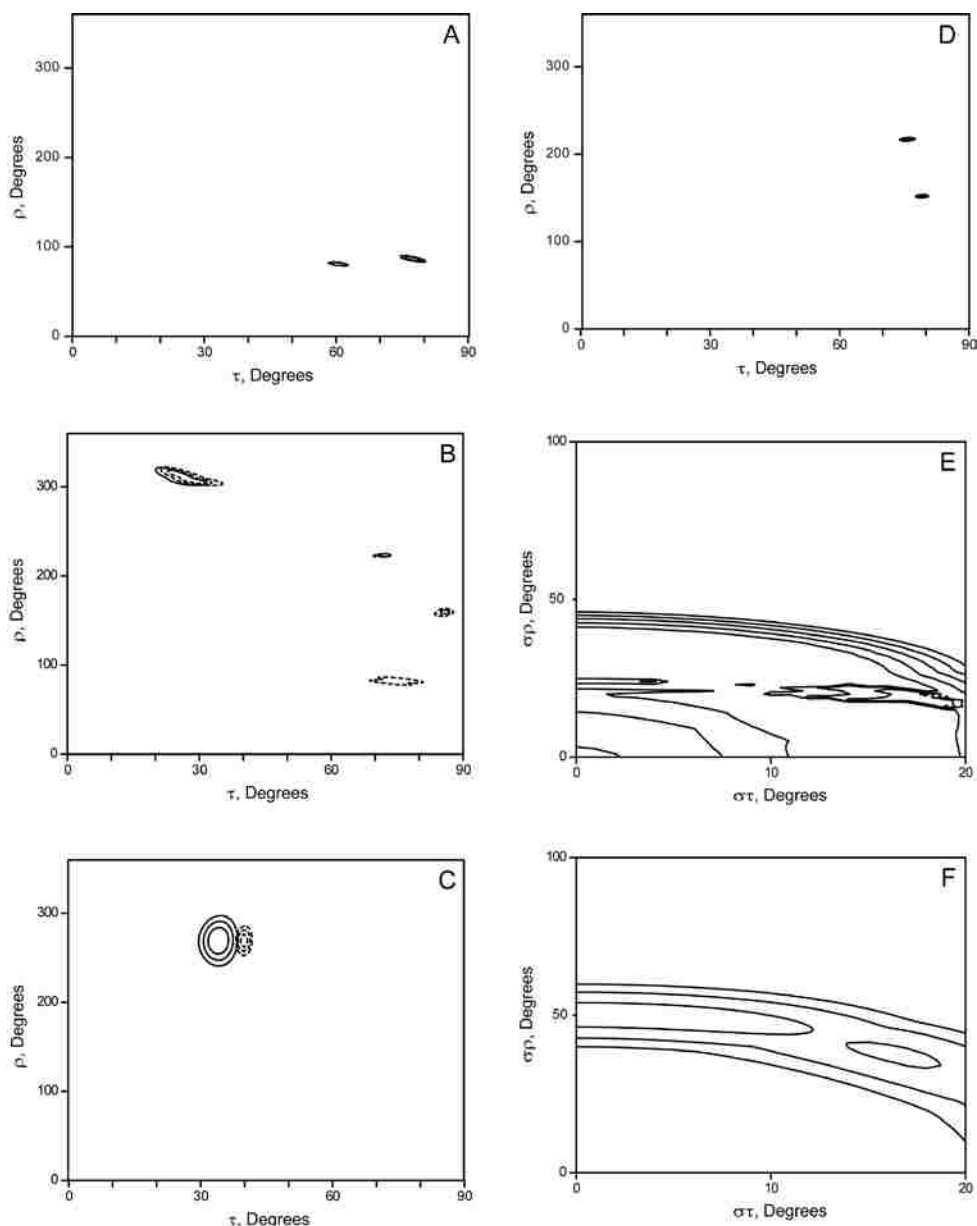


Figure 6

RMSD plots for GWALP23P12 in oriented DLPC (A), DMPC (B, C, E, F) and DOPC (D) bilayers. RMSD plotted as a function of τ and ρ RMSD values representing semi static calculations (A, B, C and D) are represented with a solid line, Gaussian calculations (B, C) are represented with a dashed line. RMSD contour levels depicted are 0.5, 1 and 1.5 for A, B and D and 0.3, 0.4 and 0.5 for C. RMSD plotted as a function of $\sigma\tau$ and $\sigma\rho$ for GWALP23P12 segments in oriented DMPC (E, F). RMSD values obtained from Gaussian calculations for segments C-terminal to proline (E) and N terminal to proline (F) are represented by contour levels 0.5, 0.6, 0.7, 0.8, 0.9 and 1 for E, and 0.25, 0.3 and 0.35 kHz for F.



SUMMARY

In the studies described in this manuscript aspects important for the functioning of biomembranes are addressed. It is imperative to recognize that there is an immense assortment of compounds and processes that play a role in membrane function. Here we address some facets of the large amount of membrane related subject matter still under investigation. In our studies we have employed model systems which enable us to focus on specific variables.

Experiments with carefully chosen model systems have enabled us to increase the fundamental knowledge base concerning protein-lipid interactions and the functioning of biomembranes. Specific aspects of the structural composition of biomembranes, and of peptides/proteins therein, have been linked to the properties and behavior of these membranes.

First, we have addressed the effects of WALP peptides on the phase behavior of lipid mixtures capable of liquid-ordered or “raft” phase formation. In this study we found that WALP peptides under dilute conditions have mild raft stabilizing/promoting effect in some cholesterol-containing ternary lipid mixtures. In related mixtures having a DPhPC instead of DOPC as the fluid lipid component, long but not short WALP peptides promote an isotropic phase. The results provide a motive for further studies to advance the understanding of compositional control of the behavior of biological membranes. Especially important are the potential roles that molecular interactions and domain segregation might play in the regulation of important biological events.

In addition to investigations of the effect that some of our model peptides have on the behavior of lipid mixtures, we have addressed aspects of peptide composition and their subsequent positioning within oriented lipid bilayers of various thickness. In particular, we have further investigated the anchoring properties of tryptophan and the effect that introduction of the helix breaking proline residue into a transmembrane helix has on peptide positioning. These studies are of importance since the correct tethering of peptides to the membrane is crucial to their functioning, and since evolutionarily preserved proline residues are not only found in transmembrane sequences but also have functional importance.

The tryptophan residues that flank the hydrophobic Leu/Ala helix in WALP peptides are a key feature, enabling peptide anchoring within the membrane. Here we report on the orientation and behaviors of peptides flanked by tryptophan on only one side. Using solid-state NMR studies, we find that since these peptides are secured in the bilayer on only one side, they have a quite small average apparent tilt angles. This is likely due to the reduced hydrophobic matching constraint and the increased motional freedom as a consequence of anchoring a peptide on only one side of the membrane. We find remarkable agreement between ^2H and ^{15}N based solid stated NMR techniques.

Although the techniques have different sensitivities toward peptide motions, both methods indicating a small peptide tilt. The small tilt angles for these single anchored peptides are found only for peptides with a sufficient length to span the lipid bilayer.

Shorter single anchored peptides have been found to aggregate, even when incorporated

together with complementary peptides which “could” span the opposing monolayer leaflet and thereby stabilize the peptides in the membrane.

In studies where a third anchor residue is incorporated, approaching a situation similar to the original WALP peptides with two tryptophan residues on each side of the membrane, we have found that the addition of the third anchor indeed does increase the peptide’s apparent tilt. The detailed effects on the magnitude and direction of the tilt depend upon the identity and positioning of the third anchoring residue.

The incorporation of a helix-breaking proline as the central residue in GWALP23 introduces a well defined kink in the peptide. In complementary approaches, I used deuterium and ¹⁵N-based PISEMA solid-state NMR methods to characterize the proline-kinked peptide in DMPC bilayer membranes. The results demonstrated the power of combining these two techniques. The experimental methods and the combined analysis provided a sufficient amount of data to determine well defined orientations for both the N-terminal and C-terminal peptide helical domains. Moreover, the PISEMA analysis provided a striking visual representation in which one can clearly identify two PISA wheels corresponding to the segments on either side of the proline residue. The application of the combined analysis can in principle be extended to other systems, thereby aiding in the elucidation of structural aspects of transmembrane sequences, with or without proline, which might otherwise be hard to uncover.

Bibliography

- Bakht, O., P. Pathak, and E. London, 2007. Effect of the structure of lipids favoring disordered domain formation on the stability of cholesterol-containing ordered domains (lipid rafts): identification of multiple raft-stabilization mechanisms. *Biophys J* 93: 4307-18.
- Cook, G.A., and S.J. Opella, 2010. NMR studies of membrane proteins. *Methods Mol Biol* 637: 263-75.
- Cordes, F.S., J.N. Bright, and M.S. Sansom, 2002. Proline-induced distortions of transmembrane helices. *J Mol Biol* 323: 951-60.
- Daily, A.E., D.V. Greathouse, P.C.A. van der Wel, and R.E. Koeppe, 2008. Helical distortion in tryptophan- and lysine-anchored membrane-spanning alpha-helices as a function of hydrophobic mismatch: A solid-state deuterium NMR investigation using the geometric analysis of labeled alanines method. *Biophys J* 94: 480-491.
- Das, M., and D.K. Das, 2009. Lipid raft in cardiac health and disease. *Curr Cardiol Rev* 5: 105-11.
- Davis, J.H., D.M. Clare, R.S. Hodges, and M. Bloom, 1983. Interaction of a synthetic amphiphilic polypeptide and lipids in a bilayer structure. *Biochemistry* 22: 5298-5305.
- Davis, J.H., K.R. Jeffrey, M. Bloom, M.I. Valic, and T.P. Higgs, 1976. Quadrupolar Echo Deuteron Magnetic-Resonance Spectroscopy in Ordered Hydrocarbon Chains. *Acs Symposium Series*: 70-77.
- de Almeida, R.F., A. Fedorov, and M. Prieto, 2003. Sphingomyelin/phosphatidylcholine/cholesterol phase diagram: boundaries and composition of lipid rafts. *Biophys J* 85: 2406-16.
- de Planque, M.R., and J.A. Killian, 2003. Protein-lipid interactions studied with designed transmembrane peptides: role of hydrophobic matching and interfacial anchoring. *Mol Membr Biol* 20: 271-84.

- de Planque, M.R., D.V. Greathouse, R.E. Koeppe, 2nd, H. Schafer, D. Marsh, and J.A. Killian, 1998. Influence of lipid/peptide hydrophobic mismatch on the thickness of diacylphosphatidylcholine bilayers. A ²H NMR and ESR study using designed transmembrane alpha-helical peptides and gramicidin A. *Biochemistry* 37: 9333-45.
- de Planque, M.R., J.W. Boots, D.T. Rijkers, R.M. Liskamp, D.V. Greathouse, and J.A. Killian, 2002. The effects of hydrophobic mismatch between phosphatidylcholine bilayers and transmembrane alpha-helical peptides depend on the nature of interfacially exposed aromatic and charged residues. *Biochemistry* 41: 8396-404.
- de Planque, M.R., J.A. Kruijtzter, R.M. Liskamp, D. Marsh, D.V. Greathouse, R.E. Koeppe, 2nd, B. de Kruijff, and J.A. Killian, 1999. Different membrane anchoring positions of tryptophan and lysine in synthetic transmembrane alpha-helical peptides. *J Biol Chem* 274: 20839-46.
- de Planque, M.R., E. Goormaghtigh, D.V. Greathouse, R.E. Koeppe, 2nd, J.A. Kruijtzter, R.M. Liskamp, B. de Kruijff, and J.A. Killian, 2001. Sensitivity of single membrane-spanning alpha-helical peptides to hydrophobic mismatch with a lipid bilayer: effects on backbone structure, orientation, and extent of membrane incorporation. *Biochemistry* 40: 5000-10.
- Decaffmeyer, M., Y.V. Shulga, A.O. Dicu, A. Thomas, R. Truant, M.K. Topham, R. Brasseur, and R.M. Epand, 2008. Determination of the topology of the hydrophobic segment of mammalian diacylglycerol kinase epsilon in a cell membrane and its relationship to predictions from modeling. *J Mol Biol* 383: 797-809.
- Doyle, D.A., J. Morais Cabral, R.A. Pfuetzner, A. Kuo, J.M. Gulbis, S.L. Cohen, B.T. Chait, and R. MacKinnon, 1998. The structure of the potassium channel: molecular basis of K⁺ conduction and selectivity. *Science* 280: 69-77.
- Edidin, M., 2003. The state of lipid rafts: from model membranes to cells. *Annu Rev Biophys Biomol Struct* 32: 257-83.
- Epand, R.M., 2004. Do proteins facilitate the formation of cholesterol-rich domains? *Biochim Biophys Acta* 1666: 227-38.

- Epand, R.M., 2008. Proteins and cholesterol-rich domains. *Biochim Biophys Acta* 1778: 1576-82.
- Epand, R.M., B.G. Sayer, and R.F. Epand, 2003. Peptide-induced formation of cholesterol-rich domains. *Biochemistry* 42: 14677-89.
- Esteban-Martin, S., and J. Salgado, 2007. The dynamic orientation of membrane-bound peptides: bridging simulations and experiments. *Biophys J* 93: 4278-88.
- Fastenberg, M.E., H. Shogomori, X. Xu, D.A. Brown, and E. London, 2003. Exclusion of a transmembrane-type peptide from ordered-lipid domains (rafts) detected by fluorescence quenching: extension of quenching analysis to account for the effects of domain size and domain boundaries. *Biochemistry* 42: 12376-90.
- Glukhov, E., Y.V. Shulga, R.F. Epand, A.O. Dicu, M.K. Topham, C.M. Deber, and R.M. Epand, 2007. Membrane interactions of the hydrophobic segment of diacylglycerol kinase epsilon. *Biochim Biophys Acta* 1768: 2549-58.
- Goebel, J., K. Forrest, D. Flynn, R. Rao, and T.L. Roszman, 2002. Lipid rafts, major histocompatibility complex molecules, and immune regulation. *Hum Immunol* 63: 813-20.
- Harzer, U., and B. Bechinger, 2000. Alignment of lysine-anchored membrane peptides under conditions of hydrophobic mismatch: a CD, 15N and 31P solid-state NMR spectroscopy investigation. *Biochemistry* 39: 13106-14.
- Hessa, T., N.M. Meindl-Beinker, A. Bernsel, H. Kim, Y. Sato, M. Lerch-Bader, I. Nilsson, S.H. White, and G. von Heijne, 2007. Molecular code for transmembrane-helix recognition by the Sec61 translocon. *Nature* 450: 1026-30.
- Holt, A., L. Rougier, V. Reat, F. Jolibois, O. Saurel, J. Czaplicki, J.A. Killian, and A. Milon, 2010. Order parameters of a transmembrane helix in a fluid bilayer: case study of a WALP peptide. *Biophys J* 98: 1864-72.
- Jaud, S., M. Fernandez-Vidal, I. Nilsson, N.M. Meindl-Beinker, N.C. Hubner, D.J. Tobias, G. von Heijne, and S.H. White, 2009. Insertion of short transmembrane helices by the Sec61 translocon. *Proc Natl Acad Sci U S A* 106: 11588-93.

- Jensen, M.O., and O.G. Mouritsen, 2004. Lipids do influence protein function-the hydrophobic matching hypothesis revisited. *Biochim Biophys Acta* 1666: 205-26.
- Joh, N.H., A. Min, S. Faham, J.P. Whitelegge, D. Yang, V.L. Woods, and J.U. Bowie, 2008. Modest stabilization by most hydrogen-bonded side-chain interactions in membrane proteins. *Nature* 453: 1266-70.
- Jury, E.C., F. Flores-Borja, and P.S. Kabouridis, 2007. Lipid rafts in T cell signalling and disease. *Semin Cell Dev Biol* 18: 608-15.
- Kabouridis, P.S., and E.C. Jury, 2008. Lipid rafts and T-lymphocyte function: implications for autoimmunity. *FEBS Lett* 582: 3711-8.
- Ketchum, R.R., K.C. Lee, S. Huo, and T.A. Cross, 1996. Macromolecular structural elucidation with solid-state NMR-derived orientational constraints. *J Biomol NMR* 8: 1-14.
- Killian, J.A., I. Salemink, M.R.R. dePlanque, G. Lindblom, R.E. Koeppe, and D.V. Greathouse, 1996. Induction of nonbilayer structures in diacylphosphatidylcholine model membranes by transmembrane alpha-helical peptides: Importance of hydrophobic mismatch and proposed role of tryptophans. *Biochemistry* 35: 1037-1045.
- Lajoie, P., J.G. Goetz, J.W. Dennis, and I.R. Nabi, 2009. Lattices, rafts, and scaffolds: domain regulation of receptor signaling at the plasma membrane. *J Cell Biol* 185: 381-5.
- Lee, J., and W. Im, 2008. Transmembrane helix tilting: insights from calculating the potential of mean force. *Phys Rev Lett* 100: 018103.
- Lewis, R.N., Y.P. Zhang, R.S. Hodges, W.K. Subczynski, A. Kusumi, C.R. Flach, R. Mendelsohn, and R.N. McElhaney, 2001. A polyalanine-based peptide cannot form a stable transmembrane alpha-helix in fully hydrated phospholipid bilayers. *Biochemistry* 40: 12103-11.
- Luo, C., K. Wang, Q. Liu de, Y. Li, and Q.S. Zhao, 2008. The functional roles of lipid rafts in T cell activation, immune diseases and HIV infection and prevention. *Cell Mol Immunol* 5: 1-7.

- MacKinnon, R., 2004. Potassium channels and the atomic basis of selective ion conduction (Nobel Lecture). *Angew Chem Int Ed Engl* 43: 4265-77.
- Marassi, F.M., and S.J. Opella, 2000. A solid-state NMR index of helical membrane protein structure and topology. *J Magn Reson* 144: 150-5.
- Marsh, D., 2010. Liquid-ordered phases induced by cholesterol: a compendium of binary phase diagrams. *Biochim Biophys Acta* 1798: 688-99.
- McIntosh, T.J., A. Vidal, and S.A. Simon, 2003. Sorting of lipids and transmembrane peptides between detergent-soluble bilayers and detergent-resistant rafts. *Biophys J* 85: 1656-66.
- Mouritsen, O.G., and M. Bloom, 1984. Mattress model of lipid-protein interactions in membranes. *Biophys J* 46: 141-53.
- Nevzorov, A.A., and S.J. Opella, 2003. A "magic sandwich" pulse sequence with reduced offset dependence for high-resolution separated local field spectroscopy. *J Magn Reson* 164: 182-6.
- Nevzorov, A.A., M.F. Mesleh, and S.J. Opella, 2004. Structure determination of aligned samples of membrane proteins by NMR spectroscopy. *Magn Reson Chem* 42: 162-71.
- Nilsson, I., and G. von Heijne, 1998. Breaking the camel's back: proline-induced turns in a model transmembrane helix. *J Mol Biol* 284: 1185-9.
- Ozdirekcan, S., D.T. Rijkers, R.M. Liskamp, and J.A. Killian, 2005. Influence of flanking residues on tilt and rotation angles of transmembrane peptides in lipid bilayers. A solid-state ^2H NMR study. *Biochemistry* 44: 1004-12.
- Ozdirekcan, S., C. Etchebest, J.A. Killian, and P.F. Fuchs, 2007. On the orientation of a designed transmembrane peptide: toward the right tilt angle? *J Am Chem Soc* 129: 15174-81.
- Page, R.C., C. Li, J. Hu, F.P. Gao, and T.A. Cross, 2007. Lipid bilayers: an essential environment for the understanding of membrane proteins. *Magn Reson Chem* 45: S2-S11.

- Percot, A., X.X. Zhu, and M. Lafleur, 1999. Design and characterization of anchoring amphiphilic peptides and their interactions with lipid vesicles. *Biopolymers* 50: 647-55.
- Poveda, J.A., A.M. Fernandez, J.A. Encinar, and J.M. Gonzalez-Ros, 2008. Protein-promoted membrane domains. *Biochim Biophys Acta* 1778: 1583-90.
- Raiford, D.S., C.L. Fisk, and E.D. Becker, 1979. Calibration of methanol and ethylene glycol nuclear magnetic resonance thermometers. *Analytical Chemistry* 51: 2050-2051.
- Sanders, C.R., 2nd, and J.P. Schwonek, 1992. Characterization of magnetically orientable bilayers in mixtures of dihexanoylphosphatidylcholine and dimyristoylphosphatidylcholine by solid-state NMR. *Biochemistry* 31: 8898-905.
- Schiffer, M., C.H. Chang, and F.J. Stevens, 1992. The functions of tryptophan residues in membrane proteins. *Protein Eng* 5: 213-4.
- Schmidt, U., G. Guigas, and M. Weiss, 2008. Cluster formation of transmembrane proteins due to hydrophobic mismatching. *Phys Rev Lett* 101: 128104.
- Simons, K., and E. Ikonen, 1997. Functional rafts in cell membranes. *Nature* 387: 569-72.
- Simonsen, A.C., 2008. Activation of phospholipase A2 by ternary model membranes. *Biophys J* 94: 3966-75.
- Singer, S.J., and G.L. Nicolson, 1972. The fluid mosaic model of the structure of cell membranes. *Science* 175: 720-31.
- Sparr, E., W.L. Ash, P.V. Nazarov, D.T. Rijkers, M.A. Hemminga, D.P. Tieleman, and J.A. Killian, 2005. Self-association of transmembrane alpha-helices in model membranes: importance of helix orientation and role of hydrophobic mismatch. *J Biol Chem* 280: 39324-31.
- Strandberg, E., S. Esteban-Martin, J. Salgado, and A.S. Ulrich, 2009. Orientation and dynamics of peptides in membranes calculated from 2H-NMR data. *Biophys J* 96: 3223-32.

- Strandberg, E., S. Morein, D.T. Rijkers, R.M. Liskamp, P.C. van der Wel, and J.A. Killian, 2002. Lipid dependence of membrane anchoring properties and snorkeling behavior of aromatic and charged residues in transmembrane peptides. *Biochemistry* 41: 7190-8.
- Strandberg, E., S. Ozdirekcan, D.T. Rijkers, P.C. van der Wel, R.E. Koeppe, 2nd, R.M. Liskamp, and J.A. Killian, 2004. Tilt angles of transmembrane model peptides in oriented and non-oriented lipid bilayers as determined by ²H solid-state NMR. *Biophys J* 86: 3709-21.
- ten Kortenaar, P.B.W., B.G. Van Dijk, J.M. Peeters, B.J. Raaben, P.J.H.M. Adams, and G.I. Tesser, 1986. Rapid and efficient method for the preparation of Fmoc-amino acids starting from 9-fluorenylmethanol. *Int. J. Peptide Protein Res.* 27: 398-400.
- Thomas, R., V.V. Vostrikov, D.V. Greathouse, and R.E. Koeppe, 2nd, 2009. Influence of proline upon the folding and geometry of the WALP19 transmembrane peptide. *Biochemistry* 48: 11883-91.
- Ulmschneider, M.B., and M.S. Sansom, 2001. Amino acid distributions in integral membrane protein structures. *Biochim Biophys Acta* 1512: 1-14.
- Valiyaveetil, F.I., Y. Zhou, and R. MacKinnon, 2002. Lipids in the structure, folding, and function of the KcsA K⁺ channel. *Biochemistry* 41: 10771-7.
- van der Wel, P.C., E. Strandberg, J.A. Killian, and R.E. Koeppe, 2nd, 2002. Geometry and intrinsic tilt of a tryptophan-anchored transmembrane alpha-helix determined by (²)H NMR. *Biophys J* 83: 1479-88.
- van der Wel, P.C., N.D. Reed, D.V. Greathouse, and R.E. Koeppe, 2nd, 2007. Orientation and motion of tryptophan interfacial anchors in membrane-spanning peptides. *Biochemistry* 46: 7514-24.
- van der Wel, P.C., T. Pott, S. Morein, D.V. Greathouse, R.E. Koeppe, 2nd, and J.A. Killian, 2000. Tryptophan-anchored transmembrane peptides promote formation of nonlamellar phases in phosphatidylethanolamine model membranes in a mismatch-dependent manner. *Biochemistry* 39: 3124-33.

- van Duyl, B.Y., D.T. Rijkers, B. de Kruijff, and J.A. Killian, 2002. Influence of hydrophobic mismatch and palmitoylation on the association of transmembrane alpha-helical peptides with detergent-resistant membranes. *FEBS Lett* 523: 79-84.
- van Meer, G., and H. Sprong, 2004. Membrane lipids and vesicular traffic. *Curr Opin Cell Biol* 16: 373-8.
- Veatch, S.L., K. Gawrisch, and S.L. Keller, 2006. Closed-loop miscibility gap and quantitative tie-lines in ternary membranes containing diphytanoyl PC. *Biophys J* 90: 4428-36.
- Veatch, S.L., I.V. Polozov, K. Gawrisch, and S.L. Keller, 2004. Liquid domains in vesicles investigated by NMR and fluorescence microscopy. *Biophys J* 86: 2910-2922.
- Vetrivel, K.S., and G. Thinakaran, Membrane rafts in Alzheimer's disease beta-amyloid production. *Biochim Biophys Acta*.
- Vidal, A., and T.J. McIntosh, 2005. Transbilayer peptide sorting between raft and nonraft bilayers: comparisons of detergent extraction and confocal microscopy. *Biophys J* 89: 1102-8.
- von Heijne, G., 1991. Proline kinks in transmembrane [alpha]-helices. *Journal of Molecular Biology* 218: 499-503.
- Vostrikov, V.V., A.E. Daily, D.V. Greathouse, and R.E. Koeppe, 2010a. Charged or aromatic anchor residue dependence of transmembrane peptide tilt. *J Biol Chem* 285: 7.
- Vostrikov, V.V., C.V. Grant, A.E. Daily, S.J. Opella, and R.E. Koeppe, 2nd, 2008. Comparison of "Polarization inversion with spin exchange at magic angle" and "geometric analysis of labeled alanines" methods for transmembrane helix alignment. *J Am Chem Soc* 130: 12584-5.
- Vostrikov, V.V., B.A. Hall, D.V. Greathouse, R.E. Koeppe, 2nd, and M.S. Sansom, 2010b. Changes in transmembrane helix alignment by arginine residues revealed by solid-state NMR experiments and coarse-grained MD simulations. *J Am Chem Soc* 132: 5803-11.

Wang, J., J. Denny, C. Tian, S. Kim, Y. Mo, F. Kovacs, Z. Song, K. Nishimura, Z. Gan, R. Fu, J.R. Quine, and T.A. Cross, 2000. Imaging membrane protein helical wheels. *J Magn Reson* 144: 162-7.

White, S.H., and G. von Heijne, 2008. How translocons select transmembrane helices. *Annu Rev Biophys* 37: 23-42.

Yau, W.M., W.C. Wimley, K. Gawrisch, and S.H. White, 1998. The preference of tryptophan for membrane interfaces. *Biochemistry* 37: 14713-8.

APPENDIX I ABBREVIATIONS

CD:	Circular dichroism
CRAC:	Cholesterol Recognition/interaction Amino acid Consensus
DH-o-PC:	06:0 Diether PC; 1,2-di-O-hexyl-sn-glycero-3-phosphocholine
DLPC:	12:0 PC; 1,2-dilauroyl-sn-glycero-3-phosphocholine
DM-o-PC:	14:0 Diether PC; 1,2-di-O-tetradecyl-sn-glycero-3-phosphocholine
DMPC:	14:0 PC; 1,2-dimyristoyl-sn-glycero-3-phosphocholine
DOPC:	18:1 (Δ^9 -Cis) PC; 1,2-dioleoyl-sn-glycero-3-phosphocholine
DPhPC:	4ME 16:0 PC; 1,2-diphytanoyl-sn-glycero-3-phosphocholine
DPPC:	16:0 PC ;1,2-dipalmitoyl-sn-glycero-3-phosphocholine
DRM:	Detergent resistant membrane
DSM:	Detergent soluble membrane
GALA:	Geometric analysis of labelled alanines
HPLC:	High-performance liquid chromatography
L α :	Liquid disordered
Lo:	Liquid ordered
MLV:	Multilamellar vesicles
NMR:	Nuclear magnetic resonance
PISA:	Polarity index slant angle
PISEMA:	Polarisation inversion spin exchange at the magic angle
RMSD:	Root mean square deviation
SM:	Sphingomyelin
SUV:	Small unilamellar vesicles
TFE:	Trifluoroethanol
TM:	Transmembrane
T _m :	Gel / liquid crystalline transition temperature
WALP:	Tryptophan alanine leucine peptide

